UiT The Arctic University of Norway

Molecular Inflammation Research Group

Department of Clinical Medicine

Faculty of Health Science

UiT-The Arctic University of Norway

Exploring the adenosine system by cancer-associated fibroblasts in the context of radiotherapy

Shamima Afroj

Master's thesis in Biomedicine, May 2023

"*If you don’t go after what you want, you’ll never have it. If you don’t ask, the answer is always no. If you don’t step forward, you’re always in the same place."*

- Nora Roberts.

Acknowledgments

Since August 2022, I have conducted the research presented in this thesis as part of my Master's Program in Biomedicine at UiT The Arctic University of Norway.

I am greatly thankful to my thesis supervisor, Dr. Turid Hellevik, from the Department of Radiation Oncology, University Hospital Northern Norway, Tromsø, Norway, who has guided me throughout my thesis with immense patience, and a wealth of knowledge throughout my research. I want to express my appreciation for her support and positive feedback, particularly when the results were not what we expected. I would also like to thank her for introducing me to radiation therapy research.

I will like to express my immense gratitude to my co-supervisor, Professor Iñigo Martínez-Zubiaurre, from Molecular Inflammation Research Group (MIRG), Department of Clinical Medicine, Faculty of Health Science, UiT The Arctic University of Norway, Tromsø, Norway, for giving me the freedom to work independently and make my own decisions, which has contributed to my professional growth.

I would like to take an opportunity to express my utmost gratitude to my co-supervisor, Professor Tor Brynjar Stuge, from the Department of Medical Biology, for introducing me to the interesting field of immunology and for his precious discussions throughout my research journey. From the beginning to the end, his insights were remarkably helpful in shaping my work.

I would like to give special acknowledgment to Dr. Rodrigo Berzaghi for his support and instruction throughout my research. He has been helpful in training me in all the experimental techniques that I have learned and employed during my lab time at MIRG. I am grateful to Indusmita Routray, Vera Susana Maia, and Kristin Lode for their invaluable assistance during my laboratory work.

Finally, I want to express my sincere gratitude to my parents and in-laws for their unconditional love, care, and support throughout my academic journey. I am also grateful to my husband, Ashraful, for his endless love and encouragement. Last but not least, I would like to thank and appreciate my beautiful daughters, Aviyana and Avilynn, for their thoughtful and understanding nature. Their support has been a source of energy and inspiration for me.

Shamima Afroj
Tromsø, May 2023

Summary

Background of the study: Cancer-associated fibroblasts (CAFs) are a heterogeneous population of cells that are mainly found in solid malignancies and play vital roles in tumor progression and metastasis, including important immunoregulatory functions. In this study, our objective was to explore the immunosuppressive adenosine system within the CAFs isolated from non-small cell lung carcinomas (NSCLC) and to examine the impact of radiation on the CD73/adenosine system in CAFs.

Methods: The study was conducted using primary cultures of CAFs isolated from freshly resected NSCLC samples (n=5), as well as Peripheral Blood Mononuclear Cells (PBMCs) isolated from randomly selected healthy volunteers. The effect of different radiation doses (1x6 Gy and 1x18 Gy) on the expression of ectonucleotidases CD73, CD39, and CD38 by CAFs was assessed through various techniques, including flow cytometry, western blotting, and ELISA using both irradiated and non-irradiated CAFs and CAF-conditioned medium (CAF-CM). An adenosine conversion assay was performed to examine cell-associated and extracellular CD73 activity in CAFs lysates and supernatants. Additionally, the immunosuppressive effect of CAF-CM on activated T-cells was investigated by blockade of CAF-derived soluble CD73 with AB630 inhibitor.

Results: Our findings indicate that CAFs may play a more important role in adenosine (ADO)-mediated immunosuppression compared to tumor cells. Following exposure to ionizing radiation (HD-IR), CAFs displayed enhanced CD73 expression, although the changes measured on the surface and in whole-cell expression were not statistically significant. After exposure to ionizing radiation, the surface expression of CD39 and CD38 was enhanced in CAFs, while the total cellular expression of CD39 did not show significant changes and CD38 expression remained undetected. On the other hand, HD-IR was found to have a significant effect on the upregulation of sCD73. Furthermore, the contribution of CAF to ADO generation through sCD73 was increased in cultured supernatants exposed to HD-IR. Soluble factors derived from CAFs exerted strong immune inhibitory effects on Phytohaemagglutinin-L (PHA-L) stimulated T-cells, leading to significant inhibition of their proliferation function ($P<0.001$). Notably, this inhibition was partially restored by targeting CD73 in CAF-CM.

Conclusion: This study demonstrated that CAFs are major contributors to adenosine generation by the CD39/CD73 system *in vitro* and that the expression of ectoenzymes is enhanced upon exposure to radiation, especially after high radiation doses. Importantly, HD-IR triggered the release of sCD73 and the concomitant elevation of adenosine production in the extracellular space. This study also demonstrates that CAF-mediated immunosuppressive effects over activated T-cells can be partially counteracted by blocking ADO-conversion.

Keywords: Cancer-associated fibroblasts, CAFs, Ionizing radiation, Radiotherapy, Tumor microenvironment, TME, CD73, Adenosine

Abbreviations

ADA: Adenosine Deaminase

ADP: Adenosine Diphosphate

AMP: Adenosine Monophosphate

ATP: Adenosine Triphosphate

BMDC: Bone-Marrow-Derived Mesenchymal Cell

CAF: Cancer-Associated Fibroblast

CFSE: Carboxy Fluorescen Succinimidyl Ester

CRT: Calreticulin

DAMP: Damage-Associated Molecular Pattern

DMEM: Dulbecco's Modified Eagle's Medium

CTL: Cytotoxic T lymphocytes

DC: Dendritic Cell

DMSO: Dimethyl Sulfoxide

ECM: Extracellular Matrix

EMT: Epithelial-Mesenchymal Transdifferentiation

EGF: Epidermal Growth Factor

FACS: Fluorescent-Activated Cell Sorting

FAP: Fibroblast-Activation Protein

FBS: Fetal Bovine Serum

HMGB1: High-Mobility Group Box 1

HRP: Horseradish Peroxidase

ICD: Immunogenic Cell Death

IFN-γ: Interferon-γ

MØ: Macrophage

M1-MØ: Classically activated macrophage

M2-MØ: Alternatively activated macrophage

MDSC: Myeloid-Derived Suppressor Cell

NK: Natural Killer Cell

NSCLC: Non-Small Cell Lung Cancer

PBMCs: Peripheral Blood Mononuclear Cell

PBS: Phosphate Buffered Saline

PCD: Programmed Cell Death

PDGF: Platelet-Derived Growth Factor

PHA-L: Phytohemagglutinin-L

PVDF: Polyvinylidene Difluoride

RPMI: Roswell Park Memorial Institute

SBRT: Stereotactic Body Radiotherapy

SDS-PAGE: Sodium Dodecyl Sulfate–Polyacrylamide Gel Electrophoresis

TAM: Tumor-Associated Macrophages

TGF-β: Transforming Growth Factor-β

TMB: Tetramethylbenzidine

Treg: Regulatory T cell

VEGF: Vascular Endothelial Growth Factor

α-SMA: α-Smooth Muscle Actin

Table of Contents

List of Figure

1 Introduction

1.1 Non-Small Cell Lung Cancer

Non-small cell lung cancer (NSCLC) is a heterogeneous class of cancer that includes different varieties (subtypes) of lung cancers. Lung cancer is considered as one of the leading and deadliest cancer types in humans and causes the most common cancer-related death among men and the second most common among women worldwide [1]. The most common type of lung cancer is adenocarcinoma and causes one-half of the lung cancer incidents. Squamous cell carcinoma (SCC) is a type of NSCLC that arises from the squamous cells lining the airways of the lung. There are two types of SCC based on the location of the primary site: central type (C-type) and peripheral type (P-type) [2]. Another subset of NSCLC is large cell carcinoma which is poorly differentiated and difficult to classify further by electron microscopy or immunohistochemistry. NSCLC develops from cells lining the respiratory tract (bronchioles, alveoli, and bronchi), and based on the appearance of the cells under the microscope, it is divided into adenocarcinoma (~40 %), squamous cell carcinoma (25%- 30 %), and Large cell carcinoma (10 %-20%) [3] **(Figure 1.1)**.

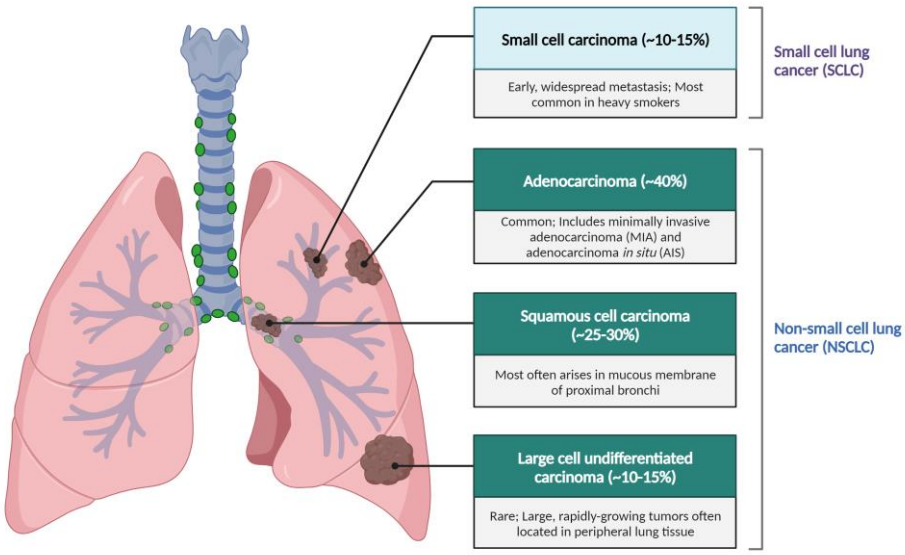

Figure 1.1 Sub-types of non-small cell lung cancer. *Different positions of adenocarcinoma, squamous cell carcinoma, and large cell carcinoma in the lung. Adapted from Ragab et al., European Journal of Medical Research, 27(1):172 (2022).*

1.1.1 NSCLC diagnostic evaluation and treatment

For tissue diagnosis and staging, thoracotomy is the recommended test for patients with early-stage NSCLC, who are also surgical candidates. The other options for tissue diagnosis, when the type and stage of the cancer are less clear, include sputum cytology, flexible bronchoscopy, and transthoracic needle aspiration [4]. Additionally, to detect whether the tumor has spread to the lymph nodes or other parts of the body, patients might need to get a magnetic resonance imaging (MRI) scan. A tissue biopsy is needed for immunohistochemistry and histopathological evaluation for the diagnosis of NSCLC. Once the diagnosis is done, a computerized tomography (CT) scan of the chest and upper abdomen is performed to evaluate the metastasis of the disease. Lately, a novel non-invasive imaging modality called positron emission tomography (PET) is utilized to monitor the tumor landscape [1]. For the staging of NSCLC, the combination of anatomic data from CT and metabolic data (radioactive) flour-18 labelled fluorodeoxyglucose (18F FDG)-PET scan is recommended. This combination allows better accuracy about small lesions and distant metastasis, allowing more accurate diagnosis and treatment planning, with improved patient outcomes [5].

The basis of surgical management for lung cancer is patient-centered treatment, and patients who are medically operable with stage-1 lung cancer being recommended for curative-intent pulmonary resection [6]. However, even after surgery, there is a possible risk of cancer recurrence and metastasis. Furthermore, due to the lack of early detection and adequate screening, most of the tumors during diagnosis state remain in their advanced inoperable stages. Therefore, radiotherapy (RT) has become the most widely used treatment with varying success for patients with NSCLC [7]. Over the last decade, novel therapeutic strategies for the treatment of NSCLC have raised new hopes. Cancer immunotherapy, cancer-targeted therapy, and high-dose radiation regimens have been proved to have highly beneficial treatment outcomes in patients suffering from early-stage lung tumors [8], and have higher rates of overall survival during the last decades. In fact, due to the remarkable outcomes of high-dose radiotherapy (HD-RT) especially stereotactic body radiotherapy (SBRT), this treatment can be considered as an alternative option for operable NSCLC [9]. Previously, medically inoperable patients were typically treated with a standard dose of SBRT with a given dose of 45-66 Gy in fractions of 1.8 to 2 Gy over 6 weeks. However, an institutional trial with stage 1 NSCLC patients has demonstrated promising results by escalating the dose of SBRT from 24 Gy delivered over 3 fractions (8 Gy per fraction) up to 72 Gy in 3 fractions (24 Gy per fraction), showing good patients outcomes in terms of proper efficacy and safety of the treatment [10].

1.2 Tumor microenvironment

In the year 2000, Douglas Hanahan and Robert Weinberg published a landmark review article titled "The Hallmarks of Cancer" in the journal Cell. This article proposed a new paradigm in cancer research by identifying distinctive hallmarks of cancer, that are common features in most types of cancers [11]. Later, in an updated version of their original review article, they also discussed the importance of the tumor microenvironment (TME) in promoting cancer growth and progression [12]. TME is a heterogeneous mixture of cellular and non-cellular elements including cancer cells, stromal cells, endothelial cells, immune cells, extracellular matrix, and soluble factors. Stromal cells in the tumor microenvironment play a crucial role in all stages of tumor development, progression, and metastasis [12, 13]. Based on their functions and contributions to hallmark capabilities in the TME, stromal cells can be grouped into three broad categories: angiogenic vascular cells (AVCs), infiltrating immune cells (IICs), and cancer-associated fibroblastic cells (CAFs) [14]. In a recent review article Hanahan *et al.*, explained about the importance of senescent cells in the TME and the complex interaction between senescent cells and cancer cells [15]. Since we were in the form of a fetus in our mother's womb, cells in our body communicate through a complex system of paracrine factors and cell-cell contact in order to determine whether a cell will remain quiescent, differentiate, proliferate or undergoes apoptosis. These processes are important to maintain homeostasis [16]. Cancer cells gain and accrue genetic mutations, the tissue homeostasis is disrupted and therefore, the tumor-associated stroma become activated and maintains its own homeostasis [17] (**Figure 1.2**).

1.2.1 Different cells located in the tumor microenvironment

A tissue microenvironment of a developing tumor is composed of proliferating tumor cells, infiltrating inflammatory cells, blood vessels, and different kinds of tissue-resident cells. It is a distinctive environment that is ideal for tumor development as a result of interaction with the host. The environment is often dominated by the neoplastic tumor cells, which orchestrate cellular and molecular actions occurring in surrounding tissue [18]. Among the cellular components that can be found in tumors are infiltrated or resident inflammatory cells, bone marrow derived-mesenchymal cells (BMDCs), CAFs, myeloid-derived suppressor cells (MDSCs), effector T-cells and occasional B-cells (**Figure 1.2)**. All these cells are embedded in a fibrous and non-fibrous protein network called extracellular matrix (ECM) that supports the invasive cells for their growth and migration [17, 19].

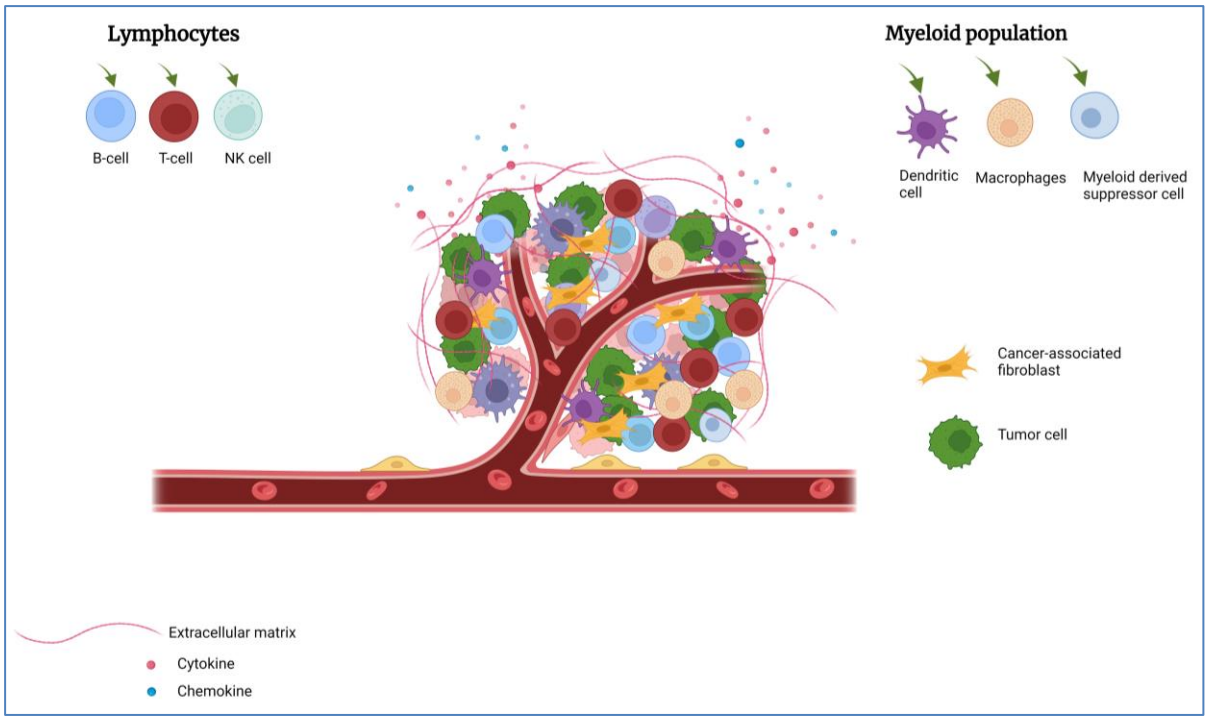

Figure 1.2 Representative image of the main cellular component of the tumor microenvironment. *The TME consists of an extensive diversity of cells and ECM helps with the heterogeneity of tumor stroma. Cells found in the tumor stroma include fibroblasts, MDSCs, BMDCs, and various populations of pro and anti-tumorigenic immune cells. The figure was made with biorender.com and inspired by Zhang et al., Biomark Res. 10(1):5 (2022).*

1.3 Tumor immunology

1.3.1 The immune system

The function of the innate and adaptive immune system is to protect the host from foreign substances, and in general, provide tolerance towards host tissues by differentiating between 'self' and 'non-self' antigens [20]. The innate immune system is the first line defense system of our body against foreign pathogens, responds within a short period and has a variety of defense mechanisms. The innate immune system consists of multiple assorted components including effector cells (macrophages, NK cells, dendritic cells, mast cells, neutrophils, eosinophils, physical barriers (mucosal membranes and skin epithelium), pattern recognition mechanisms (Toll-like receptor) and humoral mechanisms (cytokines and complement proteins) [21] (**Figure 1.3**). Inflammation of tissue is a part of the innate immune response that is responsible to eliminate pathogens along with tissue repair and stimulation of the adaptive immune system through T cells and B cells. However, several evidences have demonstrated that both acute and chronic inflammation can promote genetic abnormalities and cancer development [22, 23].

The adaptive immune system consists primarily of T cells and B cells (**Figure 1.3**). In contrast to the innate immune system which recognizes foreign pathogens based on non-specific molecular patterns, the adaptive immune response is the result of signals mediated by the extraordinarily diverse and highly specific antigen receptors present on T cells and B cells [24]. An effective immune response is generated when T or B cell recognizes antigen in a pro-stimulatory perspective and thereby become activated and proliferate. This process is known as clonal selection and promotes antigen-specific immune responses and the development of memory cells. This phenomenon allows a rapid and vigorous immune response when the body is re-exposed to the same pathogen [25].

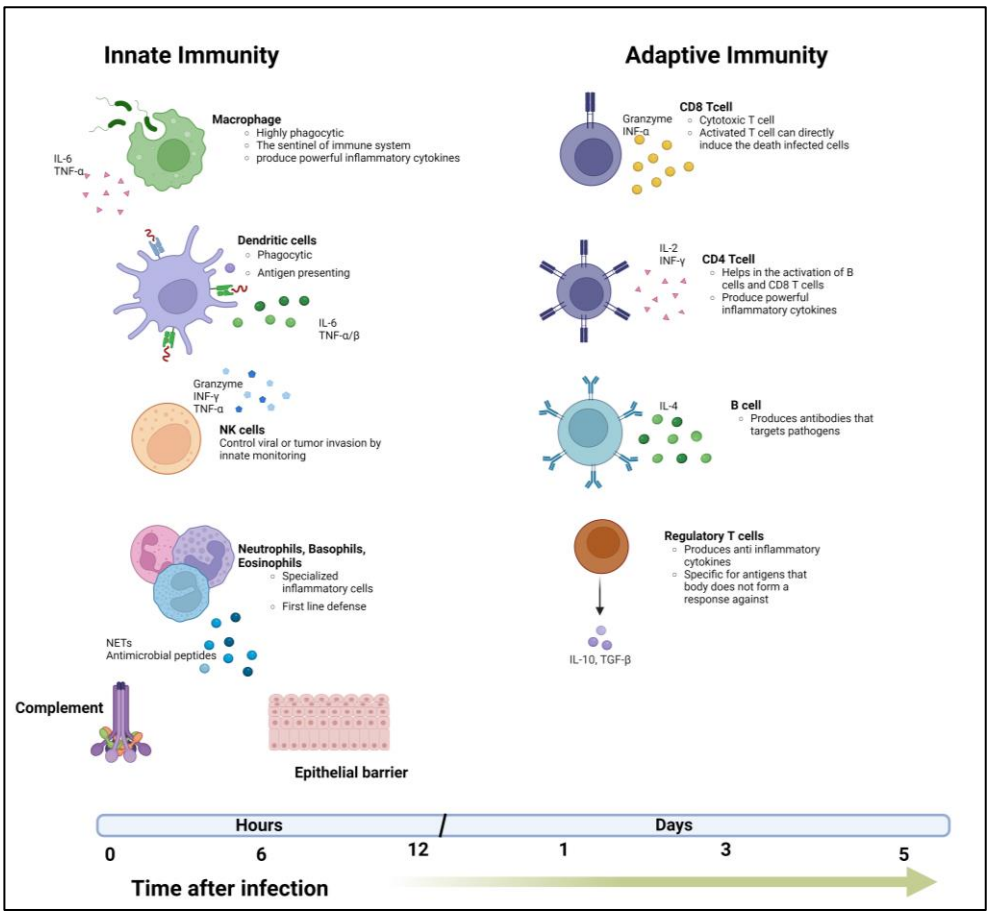

Figure 1.3 Mechanism of Innate and Adaptive immune system*. The innate immune system provides the initial defense against foreign pathogens after a few hours of infection. Adaptive immune responses develop later and are facilitated by the lymphocytes and their corresponding products. The figure was made with Biorander.com*

1.3.2 General principles of tumor immunology

The primary emphasis of tumor immunology is on two crucial concepts that highlight the significant involvement of pre-existing adaptive immune response within the tumor, namely immunosurveillance and immunoediting [26]. As described in section **1.3.1,** both the innate and the adaptive immune system is capable to differentiate between 'self' and 'non-self' antigens, and intriguingly it is thought that the immune system is capable to eliminate certain tumors in their early stage of development. Somatic cells are constantly exposed to factors that can cause mutations and potentially transform them into cancer cells. One of the important mechanisms of the immune system's surveillance is to recognize abnormal cells. The immune system has the ability to recognize and target cells that have undergone genetic alterations or abnormalities that could lead to cancer. The mechanism includes three different ways, (i) control of infection caused by oncogenic pathogens; (ii) resolving the local inflammation to prevent the development of chronic inflammation; and (iii) elimination of potentially transformed tumor cells by interacting with tumor-specific antigens or the molecules induced by cellular stress (immunosurveillance) [27]. However, in the theory of immunosurveillance and immunoediting, it is observed that some tumors are capable of escaping the equilibrium stage, which was previously checked by the immune system and further lead to tumor progression [28].

1.3.3 Tumor immunoediting: from immunosurveillance to immune escape

Tumor immunoediting refers to the relationship between the immune system and cancer cells, where the immune system can both inhibit and promote the growth of tumors. In the early 1900s, Paul Ehrlich first proposed the idea of eliminating cancer cells by using the immune system. Later Frank Macfarlane Burnet and Sir Peter Brian Medawar developed his theory and proposed the theory of immunosurveillance, which suggests that the immune system continuously monitors the body for the presence of abnormal cells, such as cancer cells, and destroys them. This theory is considered to be the basis for many modern cancer immunotherapies, which use the patient's own immune system to fight against cancer [29]. The three phases of immunoediting are elimination, equilibrium, and escape, also known as **3Es** (**Figure 1.4**), describe the various stages of this mechanism [30, 31].

During the phase of **elimination**, both the innate and adaptive immune systems work together to recognize, destroy or eliminate cancer cells, preventing them from establishing themselves and further growing. During the **equilibrium** phase of tumor growth, there is a balance between cell proliferation and cell death. Although the immune system plays a critical role in limiting the growth and spread of tumor cells in this phase, however, sometimes it is unable to completely eliminate the tumor. Tumor cells that can avoid the immune system and survive the elimination phase continue to proliferate and form a constant population of cells. Eventually in the **escape** phase cancer cells are able to evade the immune system by using several mechanisms, including creating an immunosuppressive microenvironment, altering the antigen expression, and inhibiting the activation and function of immune cells. As a result, tumors can grow and spread to other parts of the body, and cause metastasis [30, 32].

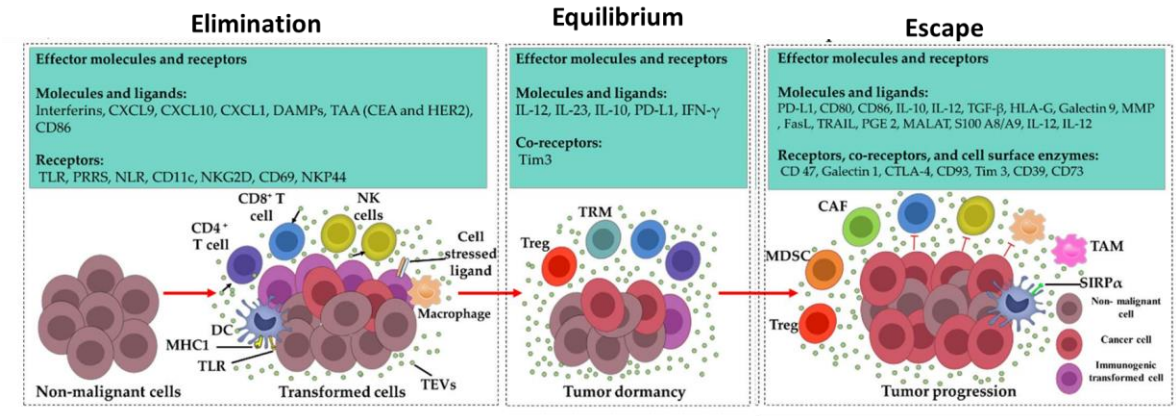

Figure 1.4 The three 'Es' phases of cancer immunoediting and different effective molecules and receptors involved in these phases. *In the elimination phase, the immune system can detect and destroy cancer cells before they form a clinically detectable tumor. If the immune system is not able to eliminate all of the cancer cells, some of them may survive and enter the equilibrium phase, where the immune system and the cancer cells are in a state of balance. However, in the escape phase, the cancer cells are capable of developing mechanisms that allow them to evade the immune system which leads to uncontrolled growth and the formation of a clinically detectable tumor. Adapted from Najaflou et.al., Cancers (Basel) 15(1) (2022).*

In every phase of immunoediting, factors secreted by cancer cells can interact with the immune system in different ways. Some factors, including cytokines and chemokines, can suppress the function of immune cells and allow the cancer cells to escape immune detection and destruction. On the other hand, other factors, such as tumor-associated antigens are capable to stimulate the immune system to respond against cancer by activating immune cells such as T-cells and NK cells [30-32].

1.4 Cancer-Associated Fibroblasts

1.4.1 Heterogenic nature of CAFs

Within the TME, the existence of heterogenous population of mesenchymal cells that are negative for endothelial, epithelial, and leukocyte markers, that have elongated morphology are known as cancer-associated fibroblasts or CAFs [33]. Several studies using human tissue observed that CAFs can be derived from local fibroblasts [33, 34], bone marrow-derived mesenchymal stem cells, pericytes, adipocytes, and endothelial cells [35-37] (**Figure 1.5**).

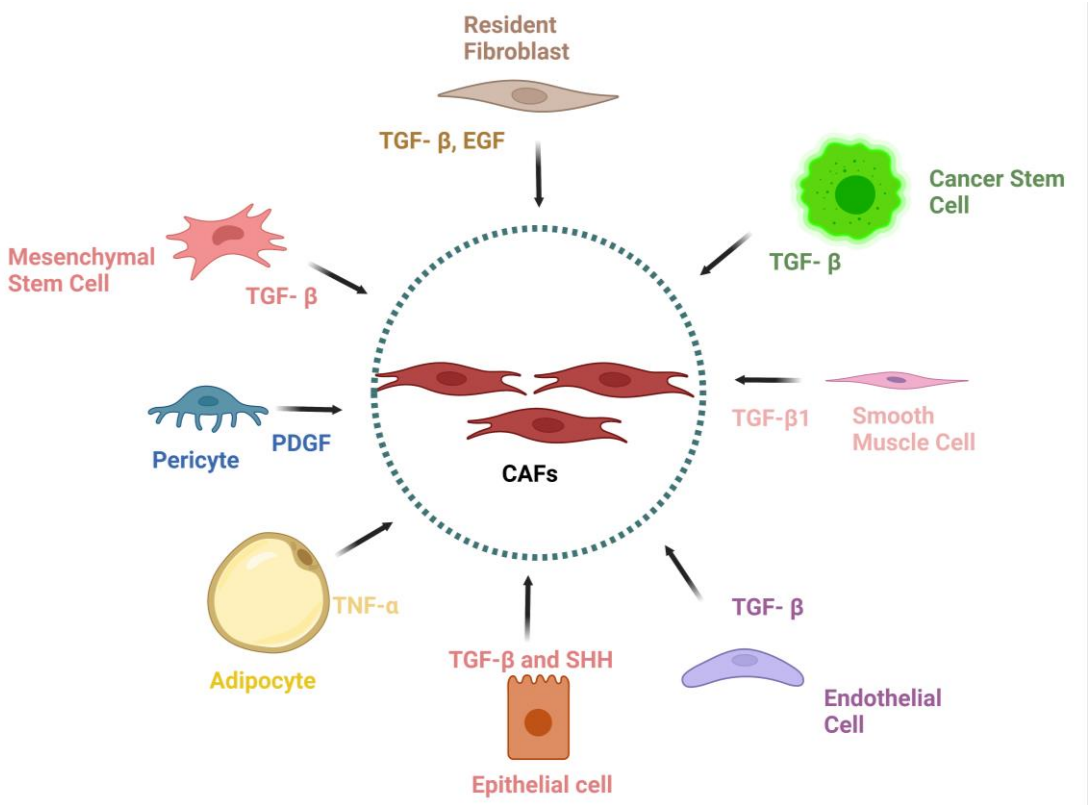

Figure 1.5 The cellular origins of cancer-associated fibroblasts (CAFs). *Different cell types that promote the CAF population and some of the major signaling pathways and factors implicated in the transition toward a CAF phenotype. The figure was made with biorender.com. and inspired by Manoukian et al., Frontiers in Cell and Developmental Biology 9:743907 (2021).*

The different origins of CAFs and their subtypes may explain the heterogenic expression of different cellular markers within the whole CAF population, which includes fibroblasts-activation protein (FAP), α-smooth muscle actin (αSMA), platelet-derived growth factor (PDGF) or receptor (PDGFR) or fibroblast-specific protein-1 (FSP-1). Because of this heterogenic expression of cellular markers, it is difficult to distinguish between activated fibroblasts from other mesenchymal cells expressing similar markers [38].

1.4.2 Difference between CAFs and normal tissue fibroblasts

In normal stroma, fibroblasts maintain epithelial homeostasis and the integrity of the connective tissue in association with the ECM proteins including type 1 collagen and fibrin [39]. Quiescent fibroblasts also secret matrix degradation protein such as matrix metalloproteinase (MMPs) that are essential for ECM remodeling [40]. Usually, fibroblasts interact with their surroundings through integrins and integrins allow fibroblasts to adhere to and communicate with various components of the microenvironment and they are characterized by their cytoskeletal structures consisting of actin fibers and vimentin. For the identification of quiescent fibroblasts in tissues, researchers often use fibroblast-specific protein 1 (FSP-1) and vimentin as cellular markers [41, 42].

A normal fibroblast can obtain an 'activated' characteristic by the induction of various stimuli when tissue injury occurs, including exposure to various growth factors such as transforming growth factor β (TGF-β), PDGF, epidermal growth factor (EGF) and fibroblast growth factor-2 (FGF-2), which are released from the injured epithelial cells [43]. Activated fibroblasts, which are commonly seen during the wound healing process can also be associated with cancer. In the cancer microenvironment, CAFs express α-SMA which is a major mesenchymal marker instead of vimentin expressed in quiescent fibroblasts [39]. After activation, CAFs also express increased levels of several growth factors including hepatocyte growth factor (HGF), insulin-like growth factor (IGF), FGF, and EGF. These growth factors can induce the proliferation signals within the TME and can communicate with neoplastic and non-neoplastic cells in the tumor stroma that leads to the promotion of tumor growth and metastasis [44, 45]. CAFs that become activated and gain proliferation activity also secrets ECM- degrading protease such as MMPs, ECM proteins such as type 1 collagen and tenascin C and fibronectin that contain SPARC (secreted protein acidic and rich in cysteine) [38] (**Figure 1.6**).

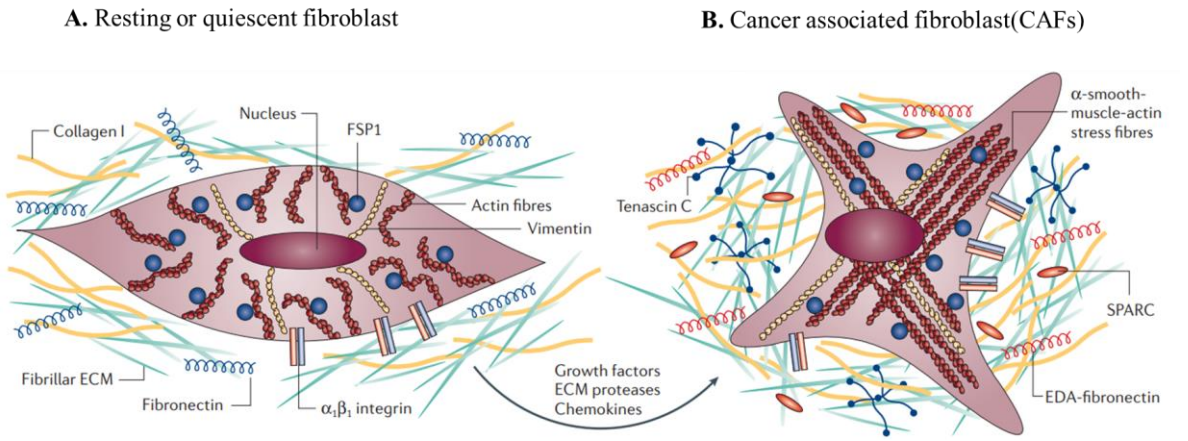

Figure 1.6 Cellular difference between normal fibroblast and cancer-associated fibroblast*. Adapted from Kalluri et al., Nature Review Cancer 6(5):392-401 (2006).*

1.4.3 Role of CAFs in angiogenesis and metastasis

The ability of CAFs to influence tumor growth is comparatively dependent on their ability to induce angiogenesis by CXCL12 and their recruitment of bone marrow-derived endothelial cells [46]. Orimo *et al*., [46] showed that Ras-transformed MCF-7 breast cancer cells grew faster in (mice) xenografts when co-injected with CAFs from an invasive mammary carcinoma compared to control fibroblasts from a non-cancerous area of the same patient. Another study demonstrated that PDGF released by cancer cells usually stimulates the release of proangiogenic factor FGF-2 by CAFs when they bind to the PDGFR in CAFs [47].

Metastasis is a complex process where tumor cells and other factors of primary tumors first prime premetastatic niches (PMNs) in targeted organs, escape from the primary tumor site by travelling through the circulation and finally, effectively seed to the secondary tissue site [48]. For cancer cells to obtain a metastatic phenotype, first they have to gain motile properties through the epithelial-mesenchymal transition (EMT) modification. By this, cancer cells no longer have their cell-to-cell adhesion and gain a mesenchymal phenotype, in a process termed EMT, with an anomalous migratory capability, which enables the cells to invade the surrounding stroma and ultimately intravasate the lymphatic or vascular system. CAFs are proposed to promote cancer cell EMT through the secretion of TGF-β, IL-6, and HGF [49, 50] (**Figure 1.7**). In addition, CAFs may promote the invasion and metastasis process by ECM degradation and remodeling through the secretion of various MMPs. Because of their active nature, CAFs produce an abnormal amount of ECM components that allow the physical space

for the expansion of cancer cells and motility, which leads to the release of matrix-associated growth factors such as VEGF that in turn accelerates tumor angiogenesis [51, 52]. Matricellular protein Tenascin-C secreted by CAFs plays an important role in forming a metastatic niche based on cancer cells by enhancing WNT and NOTCH signaling pathways, which generate cell motility and support cancer cell migration [53]. FSP-1+ CAFs have been found to promote tumor metastasis by promoting an inflammatory environment [54]. All the evidences above illustrate the pro-invasive and pro-metastatic characteristics of CAFs during the progression of cancer.

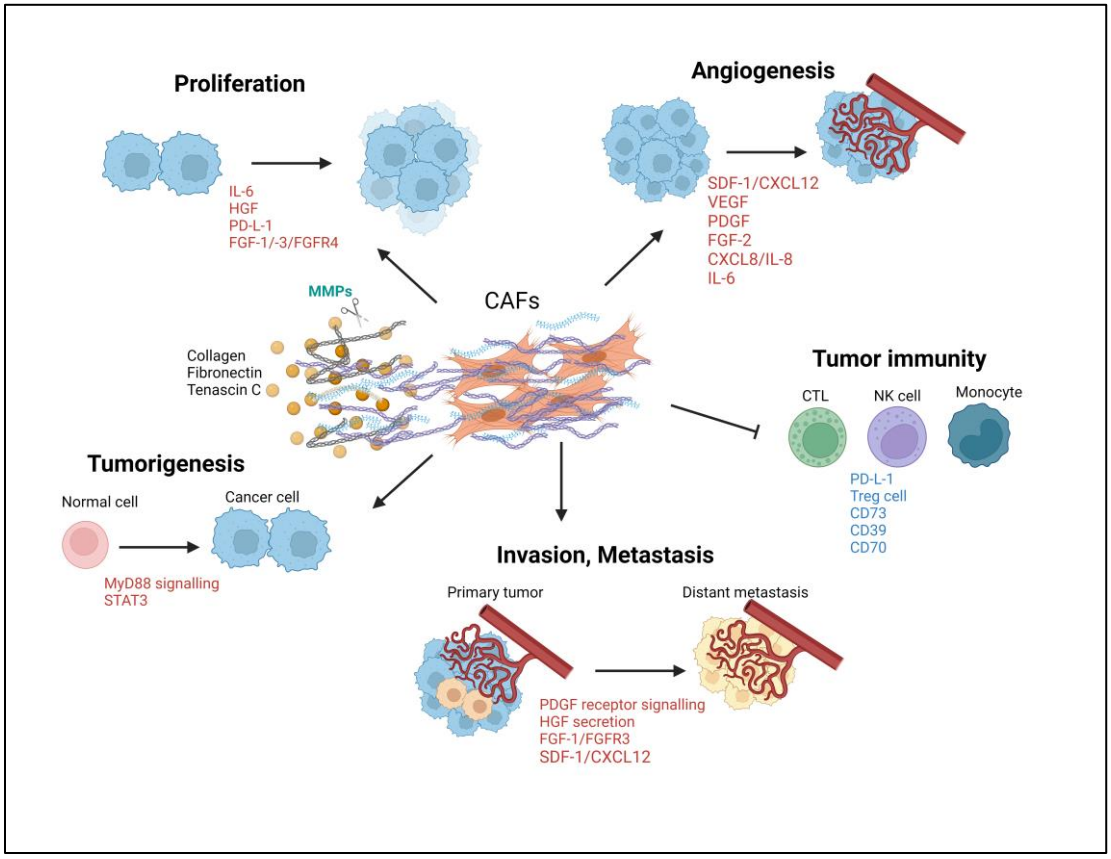

Figure 1.7 Role of CAFs in angiogenesis, invasion, and metastasis*. Factors illustrated in red are positive regulators, whereas factors described in blue are negative regulators controlling CAFs' role in cancer progression. The figure was made with Biorender.com*

1.4.4 Immunoregulatory properties of CAFs

The role of the immune system in cancer progression is dual faced and complicated. Tumors have the capability to alter the immune microenvironment and create an immunosuppressive milieu that allows the cancer cells to evade the immune system and escape from immune surveillance. This can result in the survival and growth of the primary tumor and the

development of distant metastases [12]. CAFs are well known as an important factor in shaping the TME towards an immunosuppressive phenotype [55]. CAFs play a fundamental role in immune escape by producing immunosuppressive cytokines and immune checkpoint ligands, excluding anti-tumor CD8+ T cells from cancer cells, and affecting the functional differentiation of tumor-infiltrating inflammatory cells. This results in tumor survival and growth in TME, and contributes to immune evasion and suppression [56].

It has been demonstrated that CAFs recruit macrophages into the TME in different mouse models, which can contribute to the development and progression of different types of cancers, including squamous cell cancer, prostate, breast carcinoma, and spontaneous lymphoma [57, 58]. Mesenchymal stromal cells (MSCs)-derived CAFs produce chemokine CCL2 and facilitate the recruitment of CD11b+Ly6C+ monocytes, F4/80+ macrophages, and CD11b+Ly6G+ neutrophils to the site of the tumor and leads to the enhanced tumor growth [59]. In breast cancer lung metastasis, TNFα pre-conditioned MSCs play a significant role to promote metastasis. This effect was mediated by CXCR2+ neutrophil recruitment, which was facilitated by the secretion of CXCR2 ligands [60]. Therefore, these findings are evidence of CAFs' role in the regulation of the immune response and cancer progression. When CAFs secret Chitinase-like protein (Chi3L1), they are able to drive M2- like phenotype in recruited macrophages which are associated with reduced CD8+ T lymphocytes infiltration in the TME [57] (**Figure 1.8)**. In liver cancer, a subset of FAP+ fibroblasts showed an inflammatory phenotype directed by STAT3 activation and increased expression of the chemokine CCL2. This resulted in enhanced recruitment of circulating MDSCs that express CCR2 and ultimately led to an increase in tumor growth [61].

When CAFs acquire a senescent phenotype by the expression of senescence-associated secretory phenotype (SASP) gene, they contribute to the recruitment of immunosuppressive cells such as Treg cells and MDSCs in the TME. Also, CAFs' contribution to enhanced ECM deposition create a supportive environment for the recruitment and activation of these immunosuppressive cells [62].

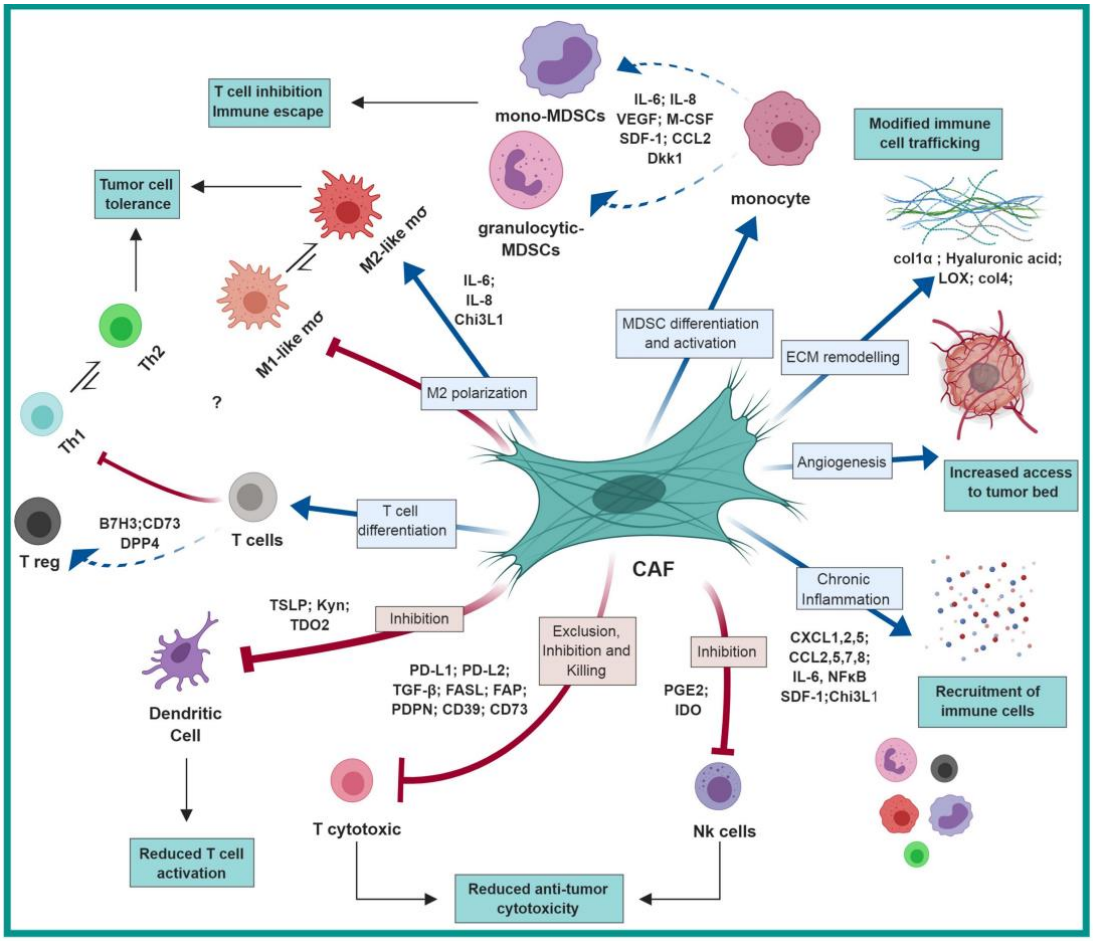

Figure 1.8 CAF-generated immunosuppression: *CAFs play a key role in shaping the immune microenvironment in tumors by influencing the recruitment and function of different innate and adaptive immune cells. Red arrows are indicating negative regulation/inhibition and blue arrows are indicating positive regulation/induction. Adapted from Monteran et al., Frontiers in Immunology 10:1835 (2009).*

CAFs use different mechanisms to directly abrogate the activity of cytotoxic T cells. In melanoma, activated fibroblasts can directly suppress CD8+ T cells proliferation and function, via upregulating their expression of the PD-1 ligand PD-L1, mediated by IL-1α/β [63]. By metabolic effects, CAFs can also suppress the mechanism of T-cells. When compared to normal tissue fibroblasts, the expression of CD39 and CD73 is found to be higher in mesenchymal stem cells (MSCs) obtained from cervical tumors. CD39 and CD73 are enzymes that produce adenosine, a molecule that has potent immunosuppressive effects. CAFs can suppress the proliferation, activation, and functions of cytotoxic T cells and dampen the immune response to cancer by producing significant amounts of adenosine through the hydrolysis of ATP, ADP, and AMP nucleotides [64] (**Figure 1.8**).

1.5 Radiotherapy

1.5.1 General principles

Radiation therapy plays a crucial role in the context of cancer treatment, whether administrated alone or in combination with other systemic therapies. Recent advancements in RT technology have allowed to deliver of high doses of radiation with precision to cancerous tumors, resulting in substantial changes in RT treatment schedules for selective types of cancer [65]. There are several types of RT used to treat cancer including external beam radiation therapy (EBRT), stereotactic body radiotherapy (SBRT), proton and radioimmunotherapy [66]. SBRT is an emerging form of RT that has become popular for the treatment of early-stage NSCLC due to its impressive impact on overall survival. Patients suffering from NSCLCs who have an increased risk of comorbidity from surgery may find SBRT to be an appealing option for treatment as it delivers high doses of radiation in just 1 to 5 treatment sessions (fractions) [10, 67]. The effects of RT are not limited to the destruction of cancerous cells but also affect the tumor and host cells in multiple ways. Over the years, there has been a heightened recognition regarding the significant role of the complex TME in therapy responses [9, 68]. Among various treatment patterns of cancer treatment, radiation therapy is one of the fundamental components and approximately half of the cancer patients receive radiation therapy at some point in their treatment [69]. It is because RT is easily available, cost-effective, and may be co-administered with immunotherapy [65].

1.5.2 Immunomodulatory potential of radiotherapy

Radiation can kill cancer cells by inducing DNA damage, which can lead to cancer cell death through apoptosis, a process of programmed cell death [70]. However, radiation can also cause cellular senescence, a state where cells stop dividing but remain metabolically active, or it can induce mitotic catastrophe, another type of cell death where cells attempt to divide despite having damaged DNA [71, 72]. Radiation therapy can modulate the tumor's immune status in several ways, including tumor antigen generation and the release of various danger signals [73]. It has been believed for many years that radiation therapy exerted exclusively immunosuppressive effects by causing collateral damage to tissue-resident antigen-presenting cells which leads to lymphocytopenia (a reduction in the number of lymphocytes) [74, 75]. However, there are several studies and clinical trials that have shown the regression of distant metastatic tumors outside the radiated field, which is known as the abscopal effect [76-78]. This suggests that radiation therapy can also have a pro-immunogenic effect, rather than exclusively immunosuppressive effects [79].

Radiation can promote cross-priming of anti-tumor T-cells through a process called immunogenic cell death (ICD) [80]. During ICD, dying tumor cells release several danger-associated molecular patterns (DAMPs) or alarmins, which may trigger dendritic cell (DC) activation and maturation by binding to various cell surface receptors, including Toll-like receptors (TLRs). Release of danger signals and/or alarmins from dying tumor cells may also enhance the presentation of tumor antigen-derived peptides to CD8+ and CD4+ tumor-specific T-cells through MHC class I and class II presentation, respectively. This process is known as cross-priming. Once primed, clonally expanded CD8+ T-cells can migrate to the tumor tissue and exert their effector functions in a repeated cycle [81] (**Figure 1.9**). The danger signals that coordinate ICD include the extracellular release of high mobility group box 1 (HMGB1), calreticulin (CRT), secretion of heat shock proteins (HSPs) associated with stressed cells, IFN-β, and release of ATP into the extracellular space [82].

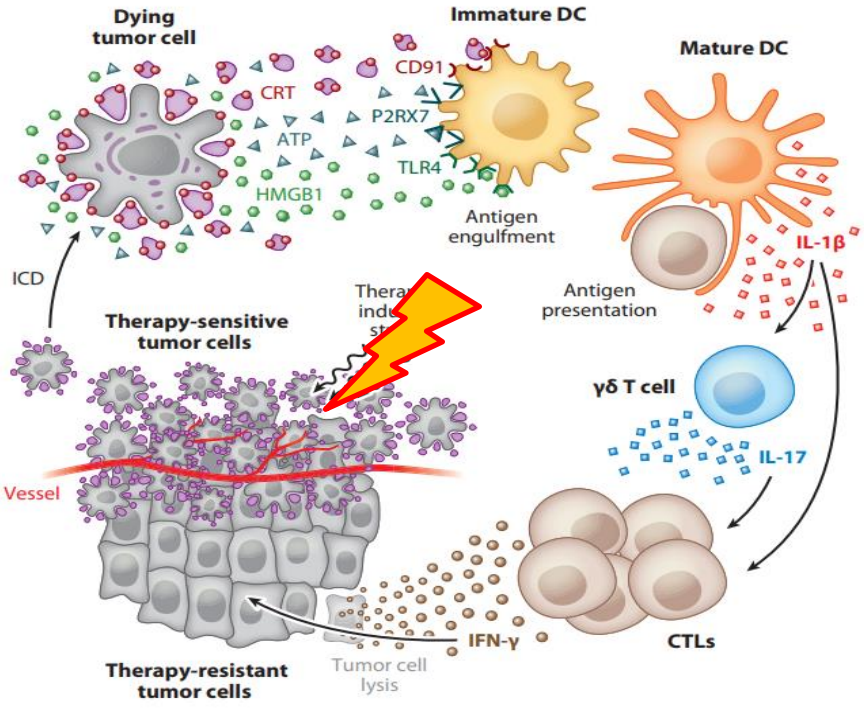

Figure 1.9 Radiation-induced immune regulation. *Release of DAMPs, such as HMGB-1, ATP, and calreticulin leads to immunogenic cell death. DAMPs stimulate an immune response via the maturation of DCs and activation of cytotoxic T lymphocytes (CTL). Adapted from Kroemer et al., Annual Review of Immunology 51-72 (2013).*

In the case of immunotherapy, ICIs have revolutionized the treatment of many types of cancers [83]. The efficiency of ICIs is dependent on the expression of PD-L1 and also on the presence of tumor-infiltrating lymphocytes (TILs) which are capable to recognize and kill tumor cells [84]. Immune-excluded tumors also known as ‘cold tumors’ are characterized by the deficiency of TILs and these cells tend to localize at the invasive margins of the tumor [85]. In cold tumors, immunosuppressive cell populations including Treg cells, TAMs, MDSCs, and CAFs are present [86]. Radiotherapy can be used to enhance the efficacy of immunotherapy by converting "cold" tumors, which are poorly responsive to immunotherapy, into "hot" tumors, which are characterized by increased immune cell infiltration, activation, and higher response ratio to ICIs [87] (**Figure 1.10**).

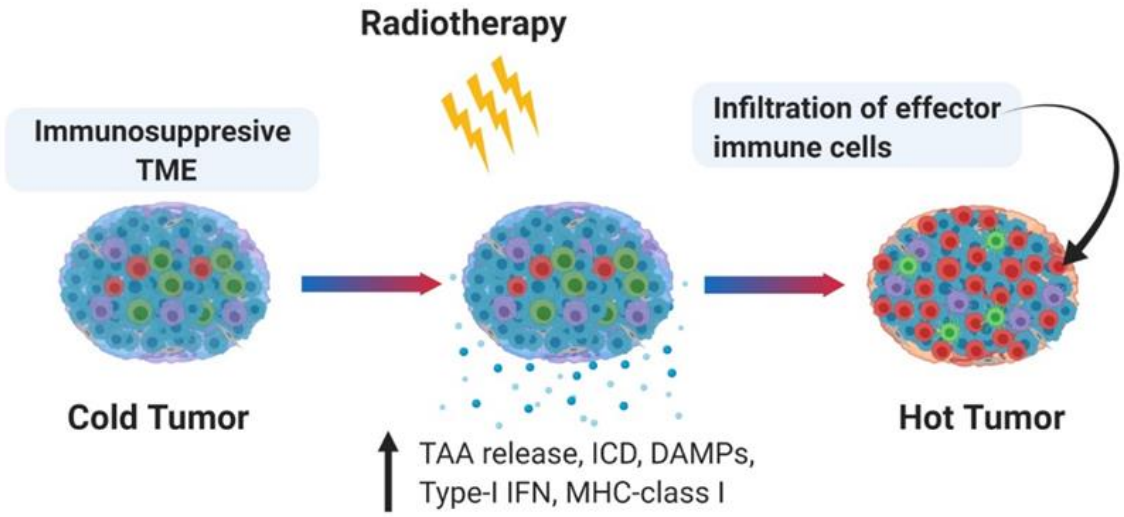

Figure 1.10 Immunomodulatory potential of radiation therapy. *Radiation therapy is a promising tool with a combination of other immunotherapies, and for converting immunologically "cold" tumors into "hot" tumors that are more responsive to immunotherapy. The figure was made with Biorander.com and made by Ashraful Islam.*

1.5.3 Effect of radiation on CAFs

Among all stromal cells present in the TME, CAFs are the most abundant and one of the most active in tumor progression [38]. Radiation therapy has various impacts on TME including cycling hypoxia, inflammation, vascular regeneration, immune modulation, and fibrosis [68]. Radiation has an effect on various cell types within the TME leading to the activation of the TME. Radiation can induce the production of several cytokines and growth factors including EGF, TGF-β, and exposure of fibroblasts to growth factors (TGF-β, PDGF), cytokines (e.g.,

IL-1, IL-6) and ROS can induce the differentiation of fibroblasts into CAFs [88-90]. This activation of CAFs occurs when they achieve a senescence-like phenotype and consequently enhances the secretion of different cytokines and growth factors following the promotion of tissue repair mechanism and remodeling [91-93]. CAFs have been demonstrated to be highly radioresistant, even at a single-high dose of radiation (1x50 Gy) they can avoid cell death and rather enter into a senescence state [94]. When NSCLC-CAFs are exposed to radiation, they do not undergo ICD or switch on IFN type I responses after a single high dose (1×18 Gy) or fractionated (3×6 Gy) radiation [95]. Although cultured NSCLC-CAFs may not directly activate IFN type I responses after radiation therapy, it has been demonstrated that radiation can induce phenotypic changes in CAFs that could impact post-RT immunoregulation. Specifically, IR-induced senescent NSCLC-CAFs display enhanced expression of several cell surface inhibitory ligands, including CD155, HLA-E, CD73, and Fas receptor (**Figure 1.11**). These ligands can inhibit immune cell activation and promote immune suppression [96].

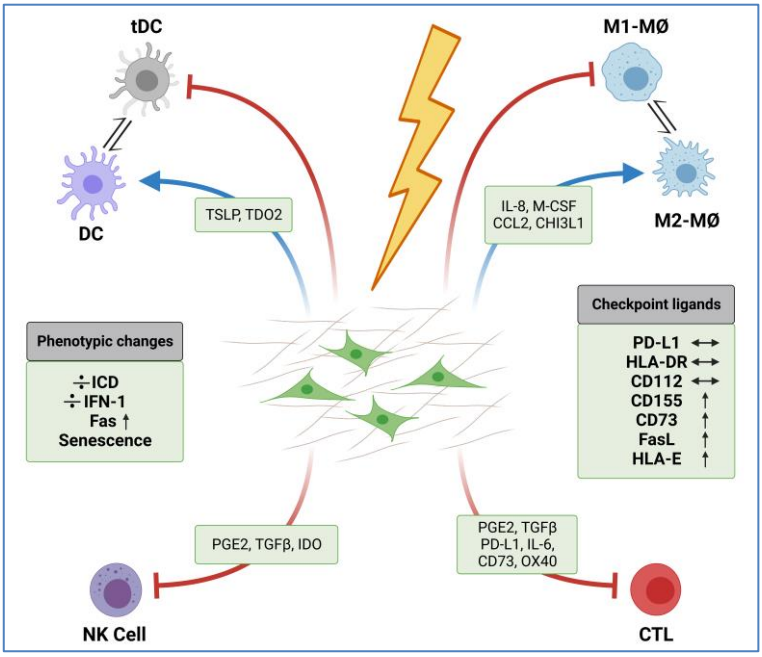

Figure 1.11 Following exposure to IR, CAFs apparently maintain their immunosuppressive phenotype. *Radiation therapy can induce phenotypic changes in CAFs, including upregulation of inhibitory ligands, and the release of key immunoregulators appears to remain constant in radiation-induced senescent CAFs. Adapted from Hellevik et al., Journal of Translational Medicine 437 (2021).*

Several studies in our research group have shown that irradiated CAFs have immunosuppressive effects on both innate and adaptive immune cells [94, 97] (**Figure 1.11**).

Gorchs *et al.*, showed that CAFs-conditioned medium can induce powerful immunosuppressive effects on activated T-cells, and this effect is sustained by senescent CAFs after single doses of IR (2 Gy or 18 Gy) [94]. Another study investigated how IR modulates CAFs-mediated regulatory effects over exogenously polarized monocyte-derived macrophages where non-radiated NSCLC-CAFs were inhibiting the pro-inflammatory features of M1-macrophages and expressed reduced amounts of M1-surface markers [97]. On the other hand, CAFs that received a single high dose (1x18 Gy) or fractioned dose regimens (3x6 Gy) did not alter their immunoregulatory features over macrophages *in vitro* [97]. A study by Berzaghi *et al.*, demonstrated that certain radiation regimens may modify the immunosuppressive effects of CAFs towards DCs in a favorable manner [95].

1.6 The CD73/Adenosine system in immune-oncology

Endogenous adenosine (ADO) is a natural purine nucleoside that is produced both intracellularly and extracellularly by our body cells. Adenosine triphosphate (ATP) breakdown to adenosine which is the primary source of energy for cellular processes [98]. Typically, the concentration of extracellular adenosine under nonpathological conditions remain constant and low (nM range) due to a proper balance between ATP release by cells and the consumption of ATP by membrane enzymes named ectonucleotidases [99]. However, during stress, hypoxia, inflammation, or injury, intracellular nucleotides such as ATP, AMP, and ADP are released into the extracellular space, where through the action of ectonucleotidases such as CD39 and CD73 they are converted to adenosine [100].

ADO can be generated via two main pathways, the canonical and the non-canonical pathway. In the canonical pathway, the initial substrate is ATP which is converted into ADP and AMP by the ectoenzyme CD39, and further catalyzed into ADO by CD73 [101]. In the non-canonical pathway for ADO generation, NAD^+ generates extracellular AMP via the activity of CD38 and CD203a [102] (**Figure 1.12**). The final step of extracellular adenosine production is the dephosphorylation of AMP to adenosine. This reaction is catalyzed by ecto-5'-nucleotidase, also known as CD73. It is expressed on the surface of many cell types, including T and B lymphocytes [103].

Overall, the conversion of ATP to adenosine involves a complex interplay between multiple enzymes, cell types, and receptors and is an important mechanism for regulating cellular processes in response to stress and injury. Dysregulation of the adenosine system has been

implicated in a variety of disease states, including cancer, cardiovascular disease, and inflammatory disorders [104].

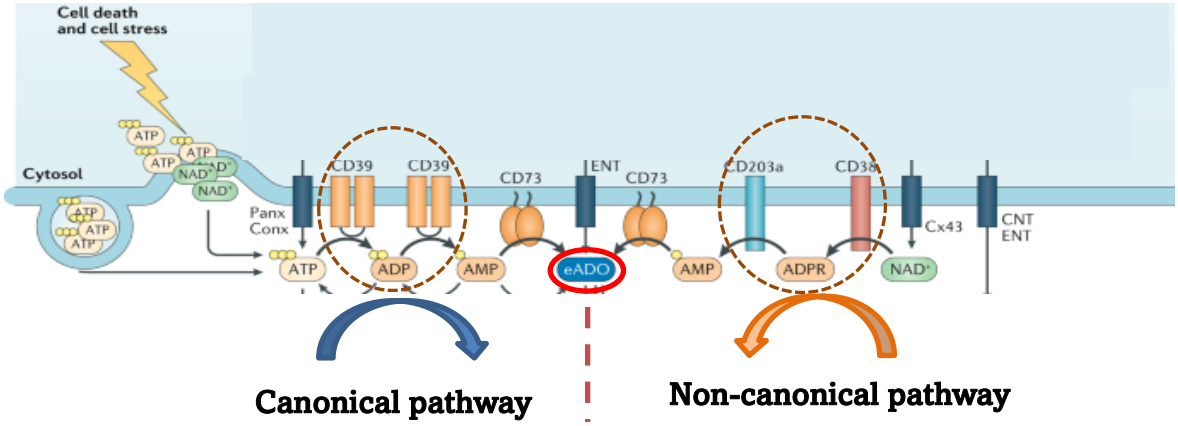

Figure 1.12 Extracellular pathways generating adenosine. *The canonical pathway involves CD39, ATP, ADP, AMP, and CD73. The non-canonical pathway involving NAD+ substrate, AMP via CD38 and CD203a, also via CD73. Adapted from Allard et al., Nature Reviews Clinical Oncology 611-629 (2020). Modified by Turid Hellevik and Shamima Afroj.*

1.6.1 Role of immunomodulatory CD73/adenosine system in the tumor microenvironment

ATP is one of the major energy sources in cells, and its concentration is found to be high in the extracellular milieu of solid tumors. This is due to the passive release of ATP by dying tumor cells, but also due to the active secretion of ATP by tumor cells and other cells in the TME [105, 106]. In addition to its role in energy metabolism, ATP is one of the major biochemical elements in the TME, and the effect of ATP on tumor progression or suppression depends on several factors including its concentration, the specific ectonucleotidases and receptors expressed by cancer cells and immune cells, and the balance between pro-inflammatory and anti-inflammatory signalling pathways [107]. During ICD, cancer cells experiencing apoptosis release several DAMPs including ATP, which act as a "find-me" signal to the immune cells. ATP also acts as a danger signal and activates a series of downstream pathways such as activation of NLRP3 inflammasome that promotes the secretion of pro-inflammatory cytokines [108]. ATP also acts as a signaling molecule in the TME and affects various cellular processes such as immune response and angiogenesis. Thus, the high levels of ATP in the TME can have significant implications for tumor progression and therapeutic response [105]. CD73 can be expressed by various cell types within the TME, including tumor cells themselves and several immune cells such as Treg cells, MDSCs, macrophages, DCs, TH17, endothelial cells,

fibroblasts, and mesenchymal stromal cells. This collection of cells may contribute to the generation of adenosine. Adenosine then acts as an immunosuppressive molecule that promotes the growth of tumors and metastasis by suppressing the function of defensive immune cells and maintaining the function of regulatory immune cells within the TME [109] (**Figure 1.13**).

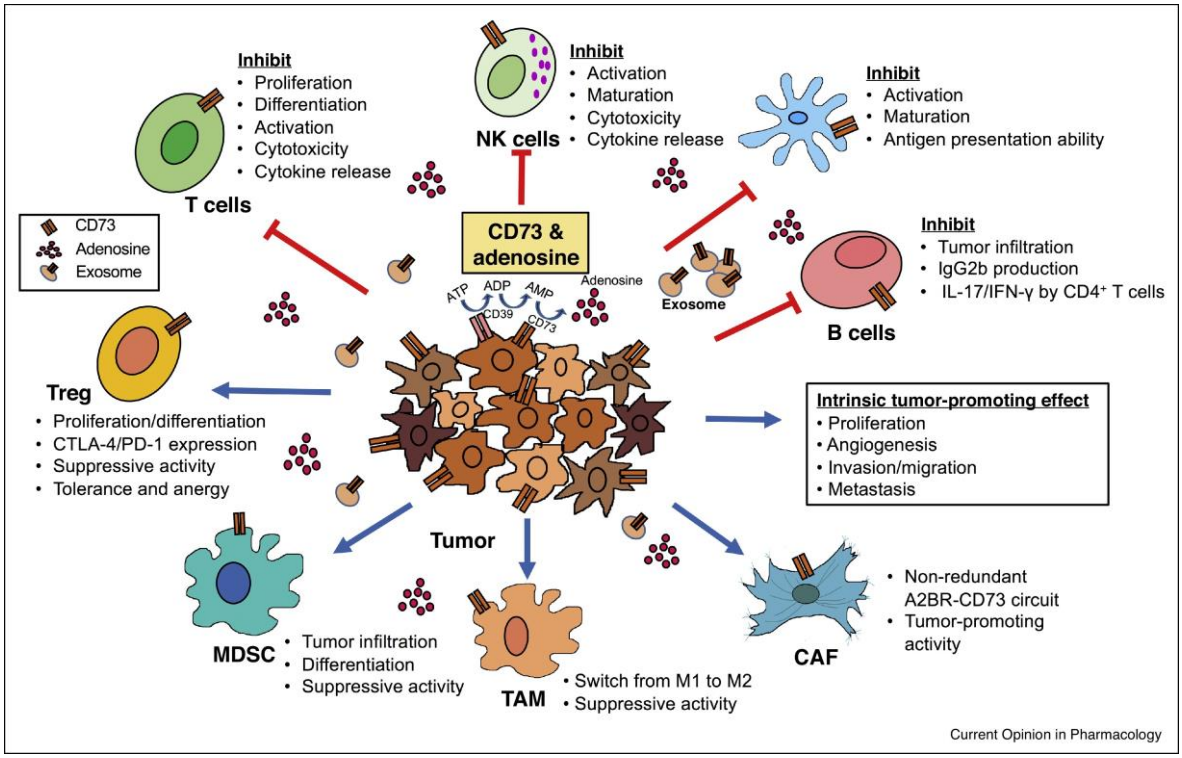

***Figure 1.13 CD73/Adenosine mediated immunosuppression in the TME**. CD73 expression in the TME has been shown to impair anti-tumor immunity by suppressing the function of protective immune cells such as effector T cells, NK cells, DCs, and B cells while maintaining the function of regulatory immune cells such as Tregs, MDSCs, TAMs, and CAFs. The total outcome can create an immunosuppressive microenvironment that promotes tumor growth and metastasis. Adapted from Roh et al., Current Opinion in Pharmacology 66-76 (2020).*

CD73 plays a significant role in tumor cell proliferation and survival through regulating cell cycle, apoptosis, and signaling pathways such as β-catenin/cyclin D1, VEGF, EGFR, and AKT/ERK [110-112]. An elevated level of CD73 is linked to the exhausted T cell phenotype. Th17 cells express CD73 and their enzymatic activity suppresses effector T cell function [113]. In TME, cancerous tissue can avert the action of anti-tumor T cells by activating immunosuppressive signaling through the T cell A_{2A} adenosine receptor pathway. This pathway is activated by the production of extracellular adenosine generated from hypoxic tumors [114]. CD73 is expressed in several subsets of T lymphocytes in mice, but the expression is notably

abundant in Foxp3+ Tregs. CD73 plays a crucial role in Treg-mediated immunosuppression by inhibiting T cell function [115]. The main mechanism of these effects is mediated through the $A_{2A}R$ receptor present on effector T cells. Activation of the $A_{2A}R$ receptor on naïve CD4+ T cells prompts their differentiation into Treg cells [116]. Activation of the $A_{2A}R$ receptor on NK cells also hinders the maturation, activation, and cytotoxic activity of NK cells [117]. Modulation of CD73 activity expressed on resident macrophages can switch the macrophage phenotype from M1 to M2 [118]. In the TME, TAMs expressing CD73 can cause immunosuppression by inhibiting the proliferation and activity of CD4+ T cells through the generation of adenosine [119].

2 Aim of the study

CAFs play a significant role in inducing immunosuppression, and there are different pathways by which they do so. In addition, in the context of radiation therapy, some studies have reported that CAFs exposed to a single high dose of radiation undergo broad and irreversible changes in their phenotype. This suggests that radiation therapy may have an impact on the function of CAFs and their potential role in immunosuppression. However, not much attention has been paid to the contribution of CAFs in adenosine-mediated immunosuppression, particularly in the context of radiation therapy. Therefore, in the present study, we aimed to explore the adenosine system in primary CAFs isolated from NSCLC tumors *in vitro* and to investigate the effects of radiation in the CD73/ADO system in CAFs. The main objective of the study has been subdivided into the following sub-goals,

- To examine the effects of ionizing radiation on surface expression of ectoenzymes (CD73, CD39 & CD38) in CAFs.
- To analyze the effects of radiation on the whole-cell expression of ectoenzymes (CD73, CD39 & CD38) in CAFs.
- To investigate the effects of radiation on the generation of soluble CD73 expression from CAFs.
- To compare CD73 activity via ADO generation in irradiated vs. control CAFs.
- To explore the blocking of CAF-mediated immunosuppressive effects on activated T-lymphocytes by targeting CD73.

3 Materials

3.1 Cell Culture Growth Medium and Supplements

	Catalog #	Supplier	Origin
Classical Medium			
Dulbecco`s Modified Eagle Medium (DMEM)	D5796	Sigma-Aldrich	USA
Roswell Park Memorial Institute (RPMI)	R8758	Sigma-Aldrich	USA
Supplements			
Fetal Bovine Serum (FBS)	S0115	Biochrom	Germany
Penicillin-Streptomycin	P4333	Sigma-Aldrich	USA
L-Ascorbic acid	A92902	Sigma-Aldrich	USA
Complete medium			
Complete DMEM growth medium			
DMEM with 10 % FBS + Penicillin-Streptomycin + L-ascorbic acid			
Complete RPMI growth medium			
RPMI + 10 % FBS + Penicillin-Streptomycin			
Freezing medium for PBMC/Lymphocytes			
FBS + 10 % DMSO			
Freezing medium for CAFs			
DMEM 70%+ FBS 20%+ DMSO 10%			

3.2 Inhibitor

	Catalog #	Supplier	Origin
AB680	HY-125286	MedChemExpress	USA

3.3 Antibodies

	Conjugate	Clonality	Dilution	Catalog #	Supplier	Origin
mAntibodies						
Mouse anti-human CD73	Vio Bright B515	Recombinant (REA804)	1:50	130-112-065	Miltenyi Biotec	Germany
Mouse anti-human CD38	APC	REA572	1:50	130-113-991	Miltenyi Biotec	Germany
Mouse anti-human CD39	APC Vio-770	REA739	1:50	130-110-791	Miltenyi Biotec	Germany
Primary Antibodies						
Anti-CD39 antibody	Rabbit	Monoclonal EPR20627	1:1000	ab223842	Abcam	UK
CD38 (E9F5A) XP®	Rabbit	Monoclonal	1:1000	877-616-CELL	Cell Signalling	USA
NT5E/CD73 (D7F9A) Rabbit mAb	Rabbit	Monoclonal	1:1000	877-678-CELL	Cell Signalling	USA
Secondary Antibody						
Rabbit anti-mouse IgG	HRP		1:2000	Ab97046	Abcam	UK

3.4 Assay kits

3.4.1 Human CD73 Elisa kit

Kit			
	Catalog #	**Supplier**	**Origin**
Human CD73 ELISA Kit	ab213761	Abcam	UK
ELISA reagents			
Anti-Human CD73 coated Microplate(12x8 wells)	TMB Color Developing Agent		
Lyophilized recombinant Human CD73 standard	TMB Stop Solution		
Biotinylated anti- Human CD73 antibody	Adhesive Plate Seal		
Avidin-Biotin-Peroxidase Complex (ABC)			
Sample Diluent Buffer			
Antibody diluent buffer			
ABC Diluent Buffer			

3.4.2 Adenosine Assay Kit

Kit			
	Catalog #	**Supplier**	**Origin**
Adenosine Assay	MET-5090	Cell BioLabs, INC	USA

The KIT included

- **Adenosine Standard** (Concentration 10mM)
- **10X Assay Buffer** (500 mM sodium phosphate ; pH 7.4)
- **Fluorometric Probe**
- **Horseradish peroxidase (HRP**) (100 U/mL solution in glycerol); *Here one unit is specified as the amount of enzyme that will deaminate 1.0 µmole of adenosine to inosine per minute at 25°C.*
- **Adenosine Deaminase** (1000 U/mL) ; *Here one unit is specified as the amount of enzyme that will deaminate 1.0 µmole of adenosine to inosine per minute at 25°C.*
- **Purine Nucleoside Phosphorylase** (18.9 U/mL) ; *One unit is specified as the amount of enzyme that will cause the phosphorolysis of 1.0 µmole of inosine to hypoxanthine and ribose 1-phosphate per minute at a temperature of 25°C.*
- **Xanthine Oxidase** (2.5 U/mL) ; *One unit is described as the amount of enzyme that will convert 1.0 µmole of xanthine to uric acid per minute at 25°C*.

Assay reagents			
Adenosine 5′ - monophosphate (AMP)	01930-5G	Sigma Aldrich	USA

4 Methods

A thorough description of the different methods used in the current project is described in the following diagram. The flowchart from **Figure 4.1** gives an overview of experimental strategies and methods has been used in the present project.

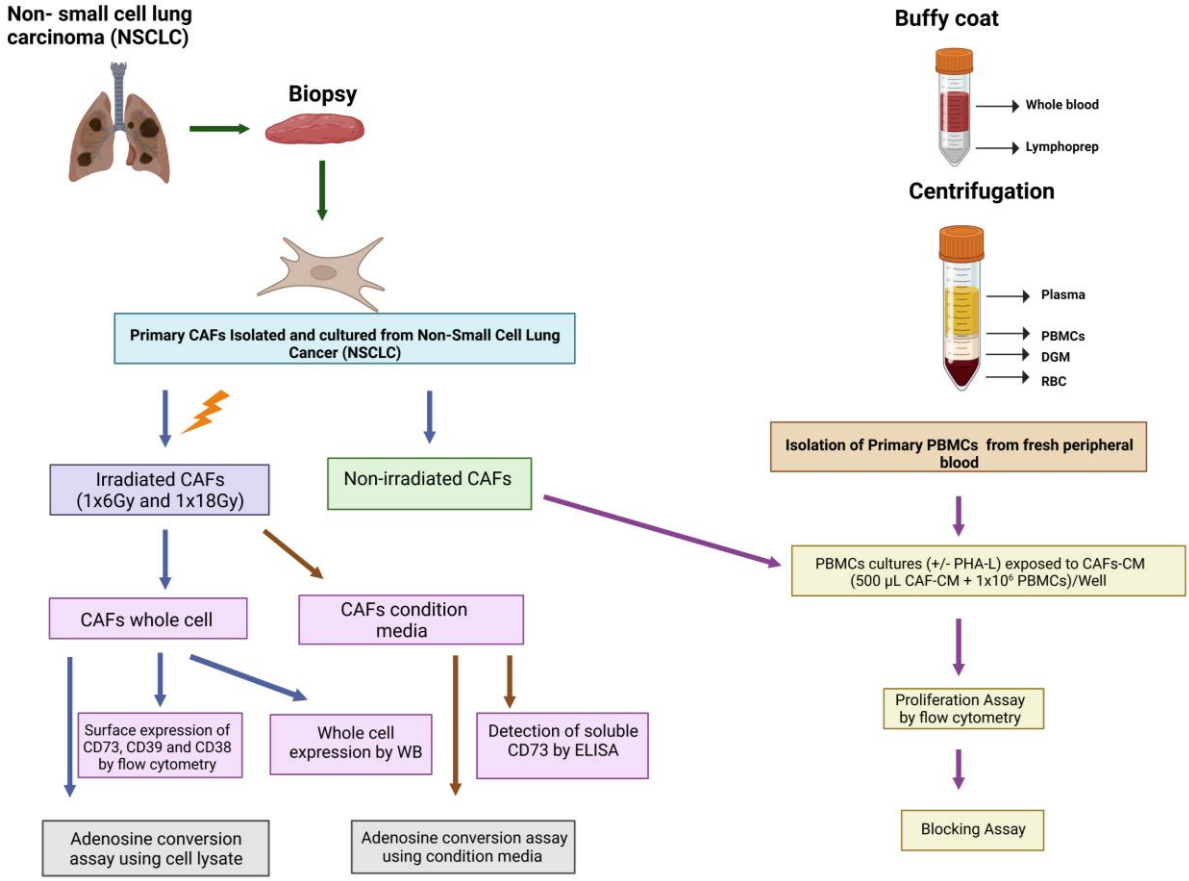

Figure 4.1 Flowchart of different experimental strategies in the current study*. The study was started by isolating and culturing primary CAFs from non-small cell lung carcinoma (NSCLC). Cells were irradiated in two different doses (1x6 Gy & 1x18 Gy). Lymphocyte proliferation assay followed by blocking of adenosine assay was performed by isolating Peripheral Blood Mononuclear Cells (PBMCs) first and Conditioned Medium (CM) from non-irradiated CAFs with or without the mitogenic reagent PHA-L. **Blue** arrow indicates the strategies for irradiated CAFs which leads to examining the surface expression, and whole cell expression of CD73, CD39, and CD38, and goes along with the conversion assay of adenosine. **Brown** arrows show the assays using CM form irradiated CAFs. **Purple** arrows indicate assays carried out using CM from non-irradiated CAFs and freshly isolated PBMCs. The figure was made with Biorender.com*

4.1 Ethical statement

All blood samples from healthy donors and tumor specimens from patients suffering from NSCLC were taken anonymously with written consent from the donors in accordance with the Declaration of Helsinki. The Regional Ethical Committee (REK# 2016/2307, 2016/714, 2014/40) approved the current study. Proper guidelines and regulations were maintained while performing the methods involving human materials in this study.

4.2 Biological samples from patients

Human lung tumor specimens were collected from patients diagnosed with NSCLC at different stages and operated at the University Hospital of Northern Norway (UNN). The average age of patients was 70 years (range 63-80) (**Table 4.1**). Patients included in this study did not get any additional therapy when their tumor biopsy samples were collected. Concentrated leucocyte blood samples (buffy coat) were obtained from healthy, volunteer blood donors who attended the UNN Blood Bank.

Table 4.1: *Donor characteristics related to the source of CAFs used for the experiments in this study*

Number	Age(years)	Sex	Tumor type	T-size(mm)	T-stage and N-stage
Donor 1	80	M	SCC	34	pT2aN0Mx
Donor 2	69	F	ADC	12	pT1bN0Mx
Donor 3	63	M	ADC	64	pT3N2Mx
Donor 4	70	M	SCC	25	pT1cN0Mx
Donor 5	85	M	SCC	46	pT2bN0Mx

F: Female; M: Male

SCC: Squamous Cell Carcinoma; ADC: Adenocarcinoma.

pT2a: Tumor is 5 cm or less; pT1b: Tumor is larger than 2 cm but not larger than 3 cm; pT3N2Mx: Tumor is larger than 5 cm and metastasis cannot be measured; pT1cN0Mx: Tumor is larger than 2 cm but not larger than 3 cm and metastasis cannot be measured.

N0: Cancer has not spread to nearby lymph nodes; N2: Cancer has already spread to lymph nodes within the lung and/or around the area of the lungs.

4.3 Isolation & culturing of cancer-associated fibroblasts from NSCLC

4.3.1 Selection of primary cells:

In our laboratory, we work with human primary cell cultures (cells that are directly isolated from human tissue and cultured *in vitro* using proper media) over cell lines (immortalized cells). The reason behind working with primary cell culture is that they show more similar phenotypic characteristics to the original human tissue than immortalized fibroblasts cell lines [120].

Although cultured human tissue fibroblasts obtained from primary cell cultures have a certain proliferative capacity and can reach the state of replicative senescence (i.e., permanent growth arrest) when they are cultured over longer periods. However, they nearly mimic in vivo fibroblast traits. Therefore, it becomes easy to execute the *in vitro* data to *in vivo* effects in humans.

Besides having advantages, the main disadvantage of working with cells in culture is that the features of tissue-resident cells may change with every passage. Therefore, to get consistent results, enough isolated cells were expanded at once and cryopreserved to ensure that the cells were under the same passage for all experiments.

4.3.2 General cell culture procedure

As already mentioned above about the collection of biological samples from patients, the pathology department of UNN was responsible to collect tissue samples quickly after surgical resection. Tubes used for tumor biopsies were sterile containing Dulbecco`s Modified Eagle`s Medium (DMEM) (Section 3.1). The sample processing method was quick enough to avoid cell death and to obtain the best possible outcome for further studies.

Four different steps were followed for isolating and culturing primary NSCLC CAFs

I. Enzymatic digestion
II. Cell detachment using enzyme-free cell detachment solution
III. Cell passage of fibroblasts
IV. Cryopreservation of primary CAFs

I. Enzymatic digestion

Usually, we receive tissues (around $1cm^3$) in a 50mL falcon tube soaked in DMEM media. The tissues were then minced by two surgical blades into small pieces (1-1.5mm^3) in a petri dish.

The tissues were then transferred to a T-25 tissue culture flask together with 5 mL of 400 IU - Accutase (Dulbecco's PBS (0.2 g/L KCl, 0.2 g/L KH_2PO_4, 8 g/L NaCl, and 1.15 g/L Na_2HPO_4) having 0.5 mM EDTA for enzymatic digestion at 37°C for 90 minutes. Later, the T-25 flask was placed on an orbital shaker in order to unshackle possible cells trapped in the small tissue pieces. Subsequently, the tissue pieces were collected in a 15mL falcon tube and centrifuged (8 minutes, 350 X G) to remove the collagenase. After centrifugation, the supernatant was discarded and the pellet was resuspended in 12mL of complete DMEM CAFs growth medium containing 10 % FBS and 1 % penicillin-streptomycin. The cell suspension was then transferred to a 6-well plate containing 2mL of cell suspension in each well and placed in a cell culture incubator at 37ºC with low oxygen (3% O_2) overnight letting the cells become attached to the solid substrate.

II. Selective cell detachment using enzyme-free cell detachment solution

After enzymatic digestion, each well of the 6 well plate contained primary tumor cells and fibroblasts. Therefore, to get pure fibroblasts, cells were washed with 2mL PBS. Discarding the PBS, 2mL of the enzyme-free solution was added followed by incubation at 37ºC with low oxygen (3% O_2) for 5 minutes To avoid cell clotting and improve cell detachment, a pre-warmed solution of Trypsin-EDTA was added to each well. By using this procedure, it is possible to enrich CAF cultures since only CAFs are detached whereas tumor cell colonies remain adherent to the plastic. The plate was then again placed in an incubator at 37ºC with low oxygen (3% O_2) for 1 minute. Well-detached fibroblasts were then centrifuged at 350 X G for 8 minutes. After centrifugation, cells were resuspended and plated into two T-75 flasks and incubated at 37ºC in a 5 % CO2-humidified atmosphere for further CAFs proliferation.

III. Cell passage of fibroblasts

Cells were observed every 24 hours under a microscope and the growth medium was replaced every 2-3 days until the fibroblasts reached 80-90% confluency. It was important to monitor that the cells do not get over-confluent since CAFs can die without having enough space to grow. It is because fibroblasts have elongated shapes and are anchorage-dependent, meaning that they grow in monolayers while attached to a solid or semi-solid substrate. When the cells became 80-90% confluent, the growth medium was discarded and cells were detached and collected following the same procedure mentioned above.

IV. Cryopreservation of primary CAFs

After the second passage of the CAFs, the cells were either used for planned experiments or cryopreserved for further experiments. For cryopreservation, cells were counted using a Neubauer Hemocytometry and 2 x 10^6 cells per mL per CryoTube were cryopreserved at -80°C in CAFs freezing medium. CAFs freezing medium contains 70% DMEM, 20% FBS, and 10% DMSO. DMSO is the most frequently used cryoprotectant. It has the ability to prevent the formation of ice crystals during the cooling process of living cells which can easily rupture the cell membrane. Nonetheless, DMSO can be highly toxic for the cells if the concentration is high (> 10 %). Therefore, cryopreserved frozen cells were thawed very quickly to avoid possible cell death and to obtain the best survival possible.

4.4 Irradiation and preparation of CAFs and fibroblast-conditioned medium

4.4.1 General principle

Whole cells and CM from both irradiated and non-irradiated CAF cultures were collected for further experiments. The purpose of collecting CM was because they are enriched with many mediator substrates such as different cytokines and growth factors secreted into the medium by CAFs which has significant impact on cellular behavior.

4.4.2 General procedure

After the third passage, CAFs were seeded and incubated for 24 hours for attachment until they reached 60-70% confluency. After another 48 hours, the growth media was changed followed by the irradiation of the cells. Before irradiation, CAFs were seeded in 6 well plates according to the number of cells needed for experiments. Following a period of 24 hours, the cells were deemed suitable for irradiation. The CAFs were irradiated using high-energy produced by megavoltage (MV) beams from a Varian clinical linear accelerator and a single dose of 6 Gy and 18 Gy were applied.

Figure 4.2 Varian clinical linear accelerator. *Six well plate with CAFs were placed on top of tissue-equivalent plates (30 mm depth) with a gantry position below the plate. The figure was taken during cell radiation setting.*

After irradiation, cell culture plates were placed back in incubator at 37ºC in and 5 % CO2-humified atmosphere. After 5 days post-radiation, both CAFs and CAFs-CM were collected and centrifuged at 2000g for 10 minutes. After centrifugation, CM media was then passed through a 0.22 µm filter for elimination of any cell or potential contaminant of cell bodies. Collected CM was frozen down at -80°C for further experimental analysis.

Of importance, cells that were not treated with ionizing radiation were handled carefully so that they don't reach over confluency before harvesting since cells could enter into a senescence state.

4.5 Cell surface marker expression of CD73, CD39 and CD38 by flow cytometry

Cell surface markers represent the proteins solely expressed on or within the cell membrane and capable to sense the surrounding environment of the cells in real-time [121]. To observe the upregulation of ADO conversion enzymes (CD73, CD39, and CD38) on the surface of both non-irradiated and irradiated (1x6 Gy and 1x18 Gy) CAFs, change in the expression of these surface markers were investigated by using flow cytometry.

4.5.1 General principle

Flow cytometry is a sophisticated procedure used to identify, count, and measure the physical and chemical characteristics of a population of cells when the cells flow in suspension through a measuring device. The working of the device depends on the scattering features of the cells which are fluorescently marked by dyes or monoclonal antibodies targeting the molecules located on the surface of the cells [122]. The cells are excited by the laser beam that emitted light at different length ranges. Lights that are transmitted in the forward direction from the passing cells are used to identify the size of the cells. On the other hand, the side scattered light provides detail about the granularity and complexity of the cells. This feature was used in this experiment to identify the expression of ADO conversion enzymes (CD73, CD39, and CD38) on the surface of both non-irradiated and irradiated induced (1x6 Gy and 1x18 Gy) CAFs. The gating methodology for our sample was as follows; Side Scatter -Area (SSC-A) Vs. Forward Scatter- Area (FSC-A) for total cell population, cell doublets, and clumps were eliminated by FSC-H vs. FSC-W. While SSC-A Vs. pacific blue was used to make gates to eliminate dead cells.

4.5.2 Data analysis

Data obtained from flow cytometry experiments were analyzed using FlowJo Office V10 (Additional material A7) installed in another computed connected with UiT server. Data were organized in “workspace” which shows the hierarchical overview of each sample and the analysis. Samples were organized in panels regarding antibodies. The raw data obtained from the FlowJo was transferred to an Excel worksheet to analyze using another software called GraphPad Prism.

4.5.3 General procedure

The surface expression of the cell surface markers (CD73, CD39 and CD38) was observed in two different steps

I. Staining of irradiated and non-irradiated CAFs with dye and antibodies
II. Detection of CAFs expressing CD73, CD39, and CD38

I. Staining of irradiated and non-irradiated CAFs with dye and antibodies

5 days after exposure to IR, CAF preparations were labeled with a panel of specific antibodies (Section 3.2) for each specific protein. The antibody collection included a) Mouse Anti-human CD73 Monoclonal Antibody; b) Alexa Fluor™ 488, Mouse Anti-human CD38 Monoclonal

Antibody; APC, and, c) Mouse Anti-human CD39 Monoclonal antibody; APC-Vio 770 according to manufacturer's protocol. To discriminate dead cells from live cells, CAFs were stained with Viobility 405/452 Fixable dye at a concentration of 0.2 mg/mL.

II. Detection of CAFs expressing CD73, CD39, and CD38

Expression of all three surface markers was detected by Flow Cytometer FACSAria lll after gating the CAFs on the forward and side scatter. Data obtained from the experiment were analyzed following the procedure mentioned in Section 4.5.2.

4.6 Whole-cell expression of CD73, CD39 and CD38 by Western blotting

Western blot analysis was performed to observe the overall expression of proteins CD73, CD39, and CD38 in the whole CAFs lysate of both irradiated and non-irradiated CAFs.

4.6.1 General principle

Western blot is a technique used to separate proteins based on their molecular weight [123]. The proteins are first boiled at 100°C for 5 minutes together with detergent Lithium dodecyl sulfate (LDS) and the reducing reagent, DTT. The heat was used to disrupt the quaternary and non-covalent bonds in the tertiary structures of the proteins. LDS coats the proteins to maintain the uniformity of the negative charges in proportion to the protein's molecular weight that masks the intrinsic charges of the protein. Therefore, when an electric field is applied to the SDS-PAGE, the negatively charged proteins are then migrated towards the positive pole at various rates depending on their molecular weight (polypeptide length). Sample-reducing reagent DTT was used to avoid protein refolding. After running the SDS page, proteins are then transferred to a polyvinylidene difluoride (PVDF) membrane to detect the protein of interest by using specific antibodies. A successful western blot is dependent on the selection of antibodies that explicitly reacts with the protein of interest and has very little or non-crossed interactions with other proteins.

4.6.2 General procedure

The overall process of western blotting can be divided into the following steps. The same process was followed to check the overall expression of all three markers, CD73, CD39 and CD38 in different CAF donors with two different radiation time points.

I. Sample preparation
II. Protein quantification and Western blots
III. Quantification of the protein bands using the software ImageJ (Additional material A7)

I. Sample preparation

For performing western blots, the strategy of plating and radiation of the cells was the same as for flow cytometry. After collecting the CAFs CM, cells were washed 5 times using sterile PBS. A mixture of Radio-Immunoprecipitation Assay (RIPA) lysis buffer, distilled water, and protease and phosphatase inhibitor at a dilution of 10:1:100 was used to lyse the cells. RIPA buffer was used for rapid and efficient cell lysis and it solubilizes proteins from adherent and suspension of cultures mammalian cells. Protease and phosphatase inhibitor was used for the protection of proteins so that the proteins do not get degraded and obtain the best possible protein yield and activity during cell lysis. The volume of lysis buffer was used depending on the confluency of the cells. Cell scraper was used for the gentle removal of cells from the surface of the well plate minimizing the damage to the cells. Cells were then collected in Eppendorf tubes and frozen down at -20°C since the SDS page was run on the next day.

II. Protein quantification and Western blots

To measure the total concentration of proteins in samples, the Bradford assay was used. Bradford reagent is used in this assay that contains Coomassie Blue which produces a distinctive bluish color upon binding to proteins in the sample [124]. Samples were diluted 10 times and the final concentration of Bovine Serum Albumin (BSA) was 10mg/mL. The protein concentration (expressed as µg/µL) of each sample was estimated at an absorbance of 595 nm, using a calibration curve with BSA.

III. Run SDS-PAGE

After determining the protein concentration of each sample, a Master mix containing samples, 1:2 final volume of 4x NuPAGE LDS Sample buffer, and 1:10 final volume of 10x NuPAGE Sample Reducing Agent in Milli-Q water was made and heated at 100°C for 5 minutes. Denatured samples (15µL) were then loaded on a SDS-PAGE gel (NuPAGE®Novex 10% Bis-Tris Gel 1.5 mm 15 well) and transferred onto a PVDF membrane. The membrane was blocked with a solution containing 1% BSA in tris buffered saline, 0.05% Tween 20 (TBS-T) for 1 hour at room temperature. The membrane was then incubated at 4°C overnight with the primary

antibodies (CD73 rabbit-monoclonal antibody, CD39 rabbit-monoclonal antibody and CD38 rabbit-monoclonal antibody) (Section 3.2) at a dilution of 1:1000 (in 0.05% PBS-Tween with 0.1% BSA) and placed in a laboratory vertical rotator. Subsequently, the membrane was washed 5 times using 0.05% PBS-T and incubated with secondary antibody (anti-rabbit HRP-conjugated) at a dilution of 1:2000 (in 0.05% PBS-T with 0.1% BSA) for 1 hour at room temperature. Before incubation of the membrane in the blocking buffer, the membrane was again washed 3 times in 0.05% PBS-T. The membrane was then incubated with Super Signal West Pico Chemiluminescent Substrate and the protein transfer was visualized immediately at ImageQuant LAS 4000 CCD (Additional material A8).

VIII. Quantification of protein bands using the software ImageJ

Each band of the protein was analyzed using the software ImageJ. The values obtained from ImageJ were later plotted and analyzed using another software called GraphPad Prism V10 to observe the overall expression of CD73, CD39, and CD38 in irradiated and non-irradiated CAFs.

4.7 Isolation and culturing of human PBMCs

PBMCs from healthy volunteers were collected from UNN and isolated using a density gradient media called Lymphoprep™ (Additional material A1).

4.7.1 General principle

Lymphoprep™ is a density gradient medium that was used for the isolation of (mononuclear) cells from peripheral blood by utilizing differences in cell density. Cells having higher densities than this medium (1.077 g/mL), including red blood cells and polymorphonuclear leukocytes, can sediment through the medium, while cells having lower densities 1.077 g/mL, such as mononuclear cells (myeloid cells and lymphocytes), are kept at the interface by centrifugation.

4.7.2 General procedure

The buffy coat was diluted (1:1) in sterile PBS and carefully layered on the Lymphoprep-™ gradient, followed by centrifugation for 1 hour at 800 x g at 20°C temperature without any break to make sure good separation of different blood cells. To remove platelets from peripheral blood, PBMCs from the interface were collected very carefully using a Pasteur pipette. Red blood cells in the PBMCs pool were removed using red blood cells lysis buffer, followed by

incubation of cells on ice for 5 minutes. Cells were then centrifuged again at 350 x g for 10 minutes at room temperature. Isolated PBMCs can be used freshly for experiments or can be frozen down for later use. Cells were then frozen down at -80°C using freezing media containing 10% DMSO and 90% FBS to protect cells from damage related to freezing/thawing.

For experiments performed using freshly isolated PBMCs, it was necessary to dilute the cells since there was a huge number of cells. Cells were diluted using sterile PBS at a dilution ratio of 1:100. Cells were then counted using Neubauer Hemocytometry.

4.8 Lymphocyte proliferation and adenosine blocking assay

T-cell proliferation assays containing PHA-L -activated lymphocytes and nonirradiated CAF-CM were carried out. PHA-L are plant-based lectins and carbohydrate-binding proteins that can bind to the T-cell surface receptors, triggering the activation and proliferation of T-lymphocytes in an antigen-independent manner [125]. The T-cell proliferation and adenosine blocking assay rate was measured by flow cytometry using the 5-(and 6)-Carboxyfluorescein diacetate succinimidyl ester (CFSE) dye.

4.8.1 General principle

CFSE is widely used to monitor the rate of T-cell proliferation. CFSE is a membrane-permanent dye that easily crosses intact cell membranes. Successful incorporation of CFSE into the cells gives a powerful tool to observe cell migration, proliferation and quality of cell division by observing the consequent decrease in fluorescent labeling/intensity in daughter cells [126] **(Figure 4.3)**. The progressive decrease of fluorescence intensity in the daughter cells can be observed by flow cytometry, using a BD LSRFortessa™ Cell Analyzer. The BD LSRFortessa™ Cell Analyzer can count and identify single cells by their physical characteristics when the cells are passing one by one through a light source. The machine is also capable to identify single cell surface molecules or their inherent molecules bound to either fluorescent dyes like CFSE, or fluorescent-labelled antibodies. Therefore, the light source of the machine, which is a laser beam, excites the fluorescent molecule to a higher energy state and emits light at a different wavelength. When the CFSE dye is used, CFSE-labelled intracellular molecules exposed to blue (488nm) laser light emits green laser light. The intensity of the emitted light is proportional to the amount of dye present in the cells. The fluorescent

detector can detect the fluorescent light while FSC-A which corresponds to the cell size and Side Scatter SSC-A which corresponds to the cell density can detect scattered light [127].

4.8.2 General procedure

The assay was performed in three different steps

I. CFSE–labelling of PBMCs
II. T-cell proliferation and adenosine blocking assay
III. Analysis by flow cytometry

I. CFSE–labelling of PBMCs

After isolation of PBMCs, cells were washed with pre-warmed sterile PBS followed by centrifugation at 300 x g for 5 minutes at room temperature. The resulting pellets were then resuspended in pre-warmed sterile PBS that contained CFSE at a concentration of 2.5 µg/mL. To allow the cellular uptake of CFSE, cell pellets were incubated with the CFSE solution for 15 minutes at 37°C, with tubes placed in a water bath. Tubes were inverted occasionally to make sure even uptake of CFSE to all cells. Cells were washed 3 times with RPMI (10% FBS) at 300 x g for 5 minutes at room temperature.

II. T-cell proliferation and adenosine blocking assay

For the assay, thawed CAF-CM previously collected from cultured CAFs was mixed with fresh, pre-warmed complete RPMI medium and co-cultured with 1 x 10^6 PBMCs in a 24-well plate. AB680 was added to the desired wells at a concentration of 200 nM/L in a final DMSO concentration of 0.1% and incubated at 37ºC for 1 hour. After incubation, cells were exposed to the mitogenic reagent PHA-L having a final concentration of 1µg/mL. There was both negative and positive control in duplicates using PBMCs. Except for the negative control, PHA-L was added in all the wells. The plate was then incubated at 37ºC, at 7.5 % CO2 for 5 days. Half of the media (500µL) on day three was changed with fresh RPMI medium with PHA-L (1µg/mL) and AB680 (200 nM/L).

III. Analysis by flow cytometry

Following incubation, PBMCs were transferred to Eppendorf tubes and centrifuged at 1500 rpm for 5 minutes. In a separate 15mL Falcon tube, 5mL of MACS buffer containing propidium iodide (PI) solution was added to a final (PI) concentration of 1µg/mL. PI is a fluorescent dye that can penetrate the cell membrane of dying or dead cells, excluding the viable cells. After

centrifugation, supernatant was discarded and 500µL of MACS buffer with PI was added to the Eppendorf tubes. Following resuspending of the palates, cells were transferred to flow cytometry tubes to analyze the CFSE fluorescence by BD LSRFortessa™ after gating the lymphocytes on the forward and side scatter. Data obtained from the flow cytometer was analyzed using the software FlowJo V10.

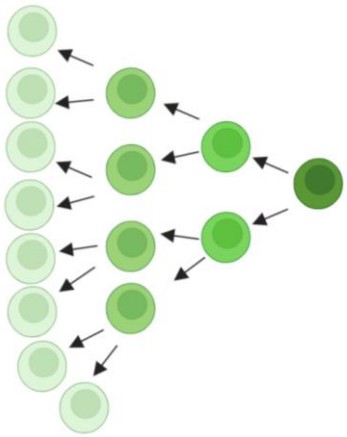

Figure 4.3 Visualization of cell divisions using CFSE dye*. CFSE is internalized by the cell and binds with the intracellular amines and is diluted by cell divisions. The figure was made with Biorender.com and inspired by Thermofisher.com*

4.9 Enzyme-linked immunosorbent assays (ELISA)

To measure the presence of soluble CD73 in cell culture supernatants, 'sandwich ELISA' was performed using a human CD73 ELISA kit.

4.9.1 General principle

A sandwich ELISA uses two antibodies, a capture antibody and a detection antibody, to quantify an antigenic protein in a sample. The capture antibody was immobilized on the surface of a 96-well plate and binds specifically to the target antigen in the sample. The detection antibody, which was conjugated to an enzyme like HRP, was added to the well and binds to a different epitope on the antigen.

After washing away any unbound components, tetramethylbenzidine (TMB) was added, and the enzyme catalyzed a reaction that generates a colored product. The intensity of the color is proportional to the amount of antigen present in the sample, and the concentration of the antigen can be determined by comparing the color intensity of the sample to that of a standard curve.

4.9.2 General procedure

The present ELISA experiment was carried out to measure and quantify the level of CD73 in the conditioned media (CM) from cultures of CAFs that were either irradiated or non-irradiated. The human CD73 ELISA kit (Section 3.3.1) and samples were used in duplicates according to

the manufacturer's instructions (Additional file B1) and the plate was read in a CLARIOstar Plus multi-mode plate reader at a wavelength of 450 nm. The Mars Software® was used for constructing standard curve and determining protein concentrations in unknown samples. The negative control used for all the kits was complete DMEM medium with sample dilution buffer at a dilution of 2:1.

The ELISAs used a four-parameter logistic algorithm for curve fitting according to the manufacturer's instructions. The solutions and reagents were provided in the kits or purchased separately and reconstituted as indicated in the protocol manual.

4.10 Adenosine conversion assay

CD73 activity was analyzed as the capacity of the cell lysate and culture supernatants to generate adenosine. Adenosine conversion capacity was measured in whole-cell lysate from irradiated and control CAFs, as well as CAF-CM after exogenous administration of AMP using an adenosine assay kit (Section 3.3.2) and later the conversion of AMP to ADO was observed with a fluorescence microplate reader equipped for excitation in the 530-570 nm range and for emission in the 590-600 nm range.

4.10.1 General principle

An adenosine assay kit is used to measure the total amount of adenosine within any biological sample. Non-irradiated and irradiated CAFs along with CAF-CM were used as biological samples to determine the generation of adenosine within 2 hours after the addition of 200µM AMP.

4.10.2 General procedure

The adenosine conversion assay was performed by the following steps

I. Preparation of non-irradiated and irradiated CAFs and CAFs CM
II. Preparation of reagents
III. Generation of the standard curve

I. Preparation of non-irradiated and irradiated CAFs and CAFs CM

CAFs were seeded in 24 well plate at a number of 10,000 cells per well. After 24 hours of seeding, cells were irradiated at a radiation dose of 1x6 Gy or 1x18 Gy. Five days post-radiation, both cells and CM were ready to perform the adenosine conversion assay.

Before performing the assay, adenosine monophosphate (AMP) was added to the media at a final concentration of 1.5mg/mL to define capacity for ADO generation within 2 hours of incubation of every sample at 37°C, 5% CO_2. To make the final solution from AMP solute, DMEM media was used containing only penicillin streptomycin and ascorbic acid but without any serum. After 2 hours of incubation, CM was collected in 15 mL Falcon tubes and centrifuged at 2000g for 10 minutes. Following centrifugation, CM was collected and passed through 0.2µm sterile syringe filter, using 10mL syringe for transferring solution to other 15mL Falcon tubes.

To perform the experiment with CAF cell lysate, the same procedure was followed as CAFs CM.

II. Preparation of reagents

The first step of the experiment consisted in preparing the adenosine standard according to the manufacturer's instruction (section 3.3.2). Next, the reaction mix and the control mix were prepared following the manufacturer's protocol (Additional file B2) provided with the assay kit. Each sample including the standard was assayed in duplicates. For the experiment black microtiter plate suitable for fluorescence plate reader was used. The plate was read in a CLARIOstar Plus multi-mode plate reader at the wavelength stated above. The Mars Software® was used for constructing standard curves and determining the conversion of adenosine in the samples. The standard reagents were diluted by a two-fold serial dilution and run in duplicates for all assays.

III. Generation of standard curve

The assay used a four-parameter logistic algorithm for curve fitting according to the manufacturer's instructions. The solutions and reagents were provided in the kits or purchased separately and reconstituted as indicated in the protocol manual.

4.11 Statistical analysis of all assays

The results in general represent the average measurements from all donors (median), with standard deviations (S.D), and displayed as a fold of CAFs control. For experiments with ELISA and Adenosine assay, only readings above the detection limit of the assays are included in the results. Comparison of the data from two or more groups were analyzed using one- way ANOVA test followed by Dunnett post hoc corrections for multiple comparisons. Student's t-test was used to compare the means of two groups of data. In all cases, P values < 0.05 were considered to be statistically significant. The statistical analysis was performed using GraphPad Prism 9.4.1, and the graphs were made using Microsoft 365 Excel and GraphPad Prism version 9.5.1.4. Results were presented in graphs where each dot on graph corresponds to a single donor, and the position of the dot on the graph corresponds to the value of a particular variable for that donor.

5 Results

5.1 Characterization of cancer-associated fibroblasts

To check for the identity and purity of CAFs isolated from human NSCLC patients' biopsy following the procedure described in section 4.3, CAF positive markers α-SMA and CD90 (**Figure 5.1**) were used. To ensure that the isolated cells are indeed CAFs, they should be negative for markers that are commonly expressed by epithelial cells (such as CD326/EpCAM), endothelial cells (such as CD31), and macrophages (such as CD68) (**Figure 5.1A**). This helps to exclude contamination from other cell types that may be present in the biopsy sample. During conducting the experiment, CAFs with early passages were used to ensure that they retain their original characteristics and behavior.

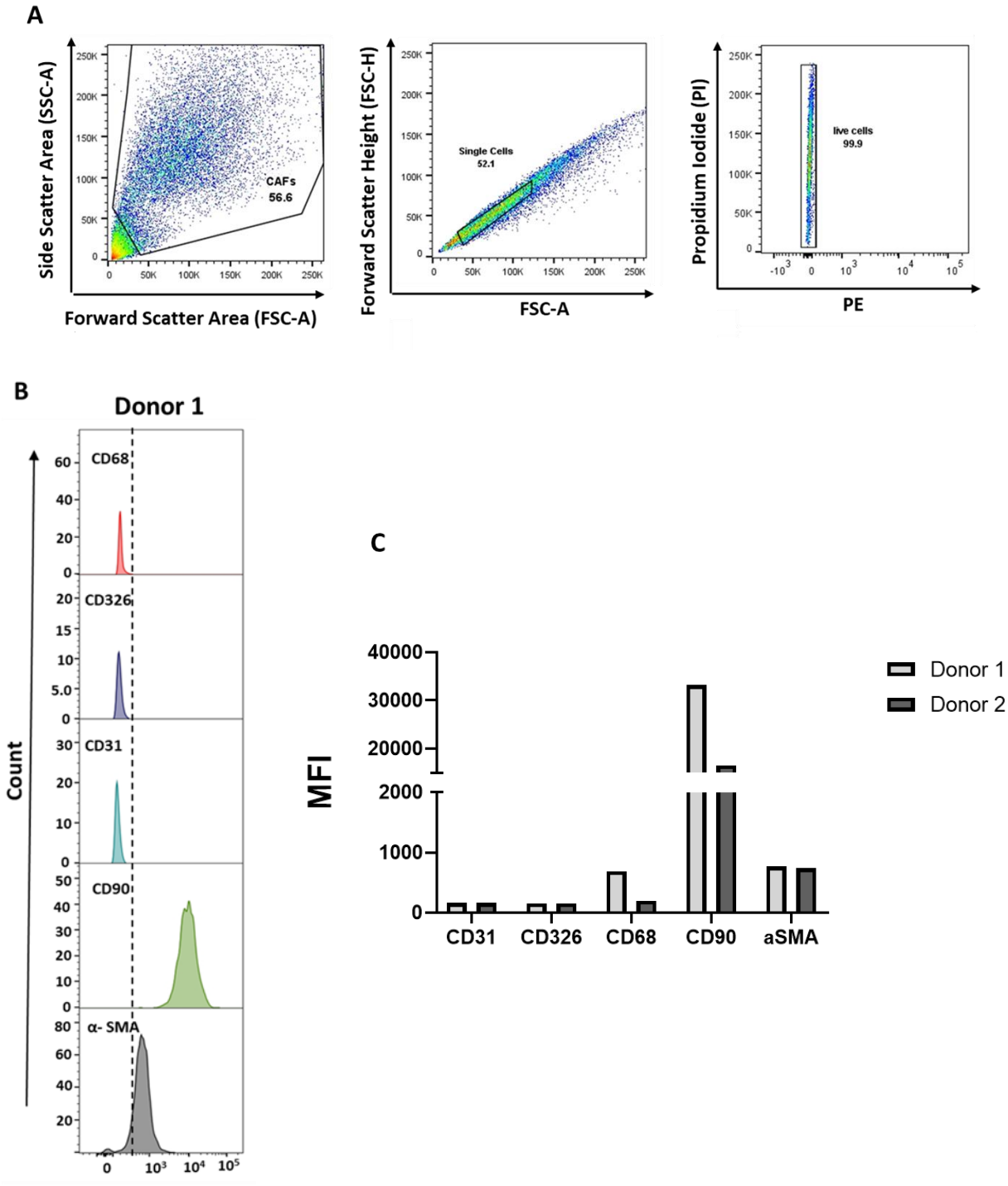

Figure 5.1 CAFs culture characterization. A) *Gating strategy of forward and side scattered population of CAFs and histogram for CAFs positive markers (CD90, α-SMA) and negative marker (CD68).* ***B)*** *Flow cytometry-based phenotyping of established CAFs showing positive staining of α-SMA and CD90, and negative for CD68, CD326, and CD31 expression.* ***C)*** *Flow cytometry analysis of CAFs (n=2) positive for αSMA and CD90 and negative for CD68, CD326, and CD31. Data are expressed as median fluorescence intensity (MFI) obtained from two different donors in duplicates.*

CAF markers CD90 and α- SMA expression levels were determined in two different CAF donors and compared with non-CAF markers (CD68, CD326, and CD31) (**Figure 5.1B**). The markers CD90 and α- SMA typically showed elevated expression in CAFs compared to other cell markers (**Figure 5.1C**). Based on analyses for cell lineage-specific markers, the results confirm the correct identity of CAFs and reveal high purity of cultures.

5.2 Radiation-induced morphological changes in primary cultured CAFs

Taking into consideration the fact that different radiation schemes can lead to different responses in biological systems, in this thesis we have included two different experimental groups of irradiated CAFs; one exposed to single medium-dose (1x6 Gy) and a second group exposed to a single high-dose radiation (1x18 Gy), in addition to untreated (control) CAFs, sometimes referred as 0 Gy group. By including both experimental groups, it was possible to compare and contrast the effects of different radiation doses on CAFs. The radiation doses used in this study are corresponding to radiation doses used in the clinics for lung cancer patients in the context of SBRT.

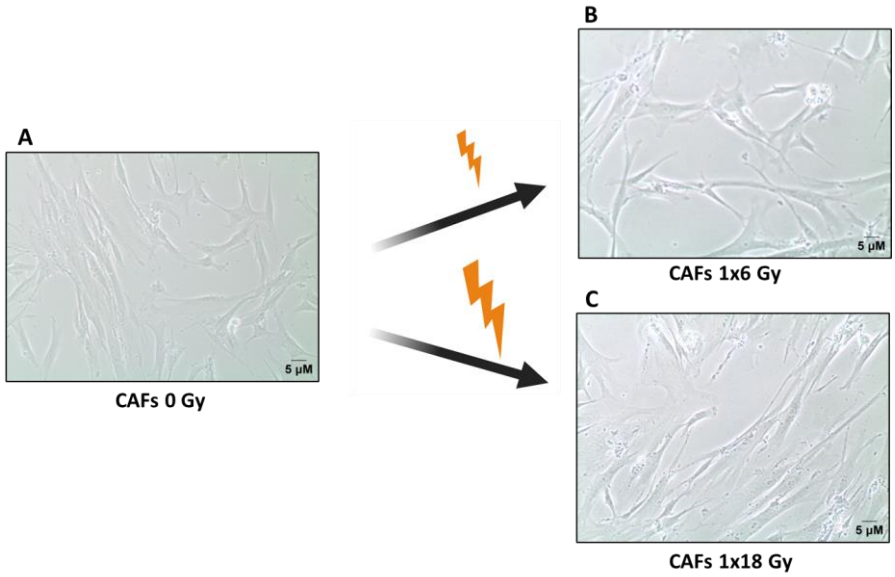

Figure 5.2 Morphological changes occurring in CAFs after being exposure to different radiation doses. A) *Representative culture of spindle-shaped, non-treated with radiation NSCLC CAFs at passage three.* ***B)*** *Representative image of CAFs obtained 5 days after exposure to single dose of ionizing radiation (1x6 Gy).* ***C)*** *Image of irradiated CAFs in culture, acquired 5 days after receiving a single dose of high-energy ionizing radiation (1x18 Gy).*

The morphological changes that occurred in cultures of human lung cancer CAFs upon radiation exposure were visualized by phase-contrast microscopy. Non-irradiated CAFs were observed as elongated, with flattened, and spindle-shaped morphology, which is a typical morphological characteristic of tumor fibroblasts in culture **(Figure 5.2A).** In contrast, irradiated CAFs exposed to single medium-dose radiation (1x6 Gy) showed enlarged and significantly flat and spindle-shaped morphology **(Figure 5.2B)**. CAFs receiving high-dose radiation showed similar flattened and more senescence-like morphology **(Figure 5.2C)**.

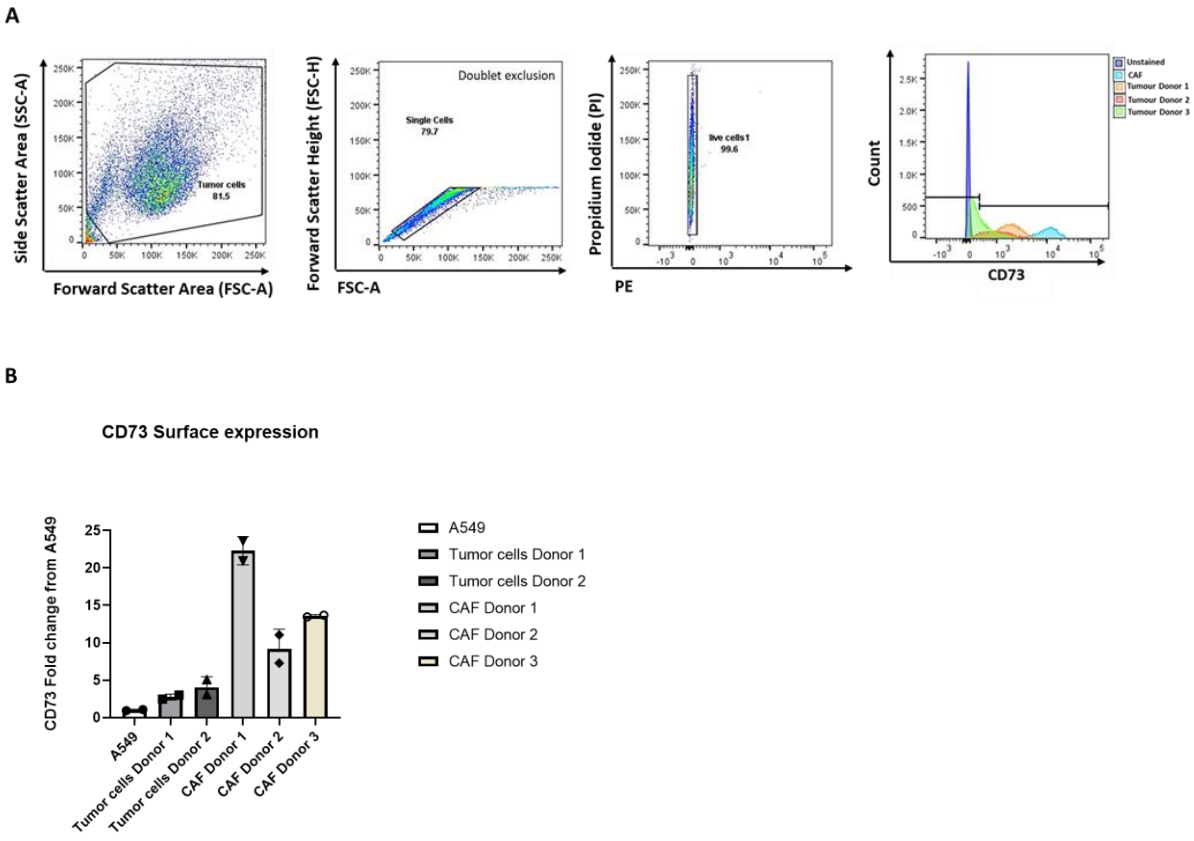

Figure 5.3 Surface expression of CD73 on CAFs and tumor cells. A) *Gating strategy of cells by flow cytometry and expression of CD73 on CAFs (n=3) and tumor cells (n=3) presented in a histogram.* ***B)*** *Quantitative surface expression of CD73 presented as fold changes in Median Fluorescence Intensity (MFI) calculated for three CAFs donors, tumor cells isolated from two lung cancer patients and tumor cell line A549. Bars represent the mean (± SD) value from duplicates of each donor.*

5.3 CD73 is highly expressed in CAFs compared to tumor cells

To ascertain which cell type in the TME plays a bigger role in the CD73/ADO system, in this study we compared the surface expression of CD73 on CAFs as well as patient-derived tumor cells from two lung cancer patient donors, and one commercial tumor cell line (A549). To determine the actual expression of CD73 on different cell populations, correct gating was crucial when using flow cytometry. The gating strategy can be observed in **Figure 5.3A**.

Upon (flow cytometry) analysis of CAFs and tumor cells *in vitro*, we found that CAFs showed a significantly higher surface expression of CD73 compared to both patient-derived tumor cells and the commonly used (human lung) tumor cell line A549. The expression level of this ectonucleotidase on the surface of these cells was calculated as a difference in median fluorescence intensity (MFI) and the value differed greatly between cell types (**Figure 5.3B**).

5.4 Radiation enhances surface expression of ectonucleotidases CD73, CD39 and, CD38 in CAFs

To investigate for potential changes induced by radiation on the surface expression of CD73 on CAFs, we treated cultured CAFs with different radiation doses and analyzed the surface expression of CD73, CD39, and CD38 with flow cytometry (**Figure 5.4A**). Five days post-radiation, CAFs treated with both intermediate (1x6 Gy) and high (1x18 Gy) radiation doses showed a tendency of elevated CD73 expression compared to non-irradiated CAFs. However, due to existing inter-donor variabilities, the outcomes were not statistically significant (**Figure 5.4B**).

On the other hand, CD38 and CD39 surface expression levels were significantly enhanced in all CAFs donors compared with non-irradiated controls (**Figure 5.4B**). The upregulation of these ectoenzymes by irradiated CAFs was confirmed when the data were statistically significant and passed all the normality tests.

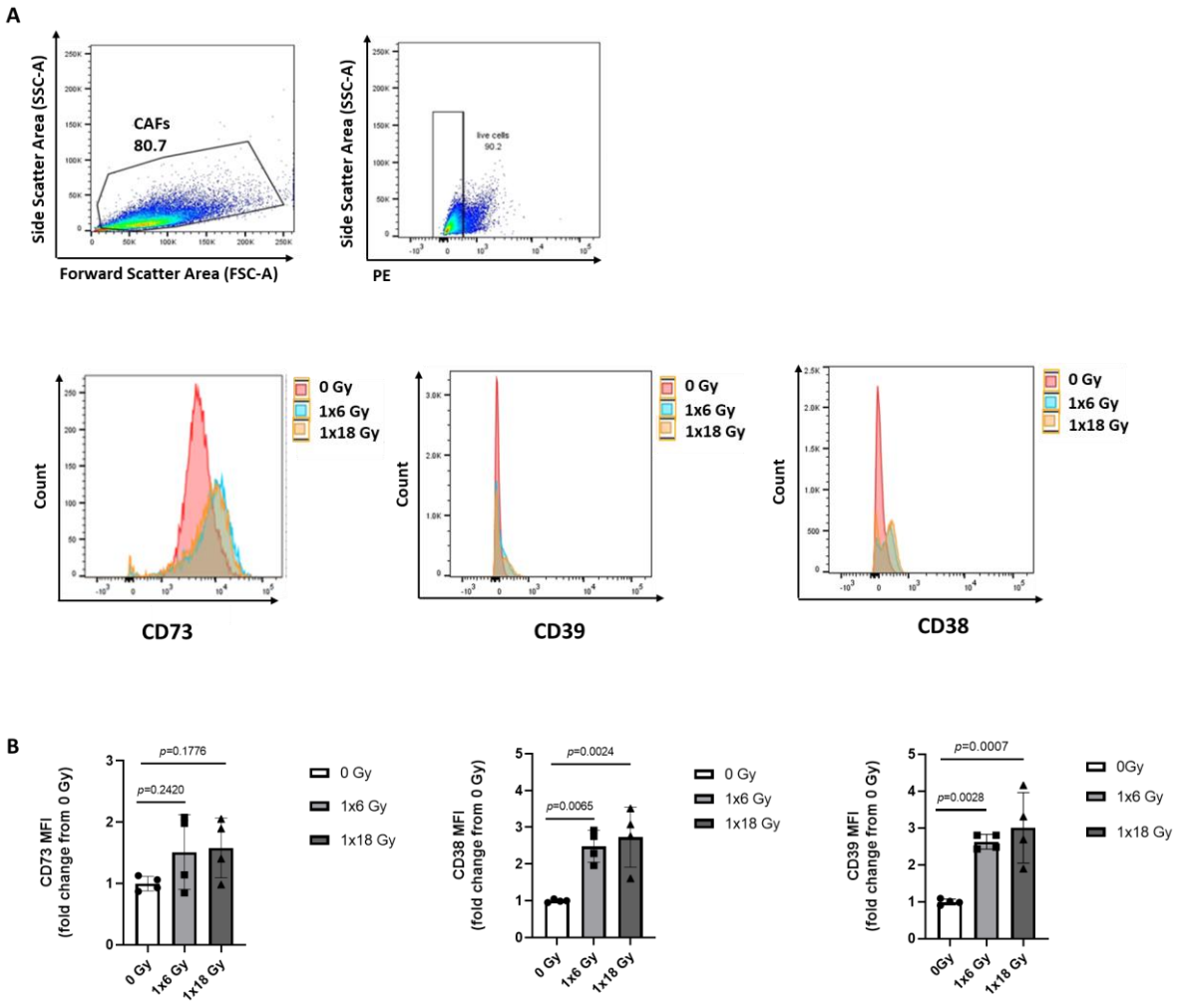

Figure 5.4 Radiation effects on surface expression of ectoenzymes CD38, CD39, and CD73 on CAFs. A) *Gating strategy and expression of CD73 on control and irradiated CAFs from one donor.* ***B)*** *Fold changes in MFI of CD73 surface expression, comparing non-treated CAFs (0 Gy) with CAFs exposed to different radiation doses. Analyses were performed 5 days post-irradiation. All data shown in (± SD) and one-way ANOVA was used to compare changes in MFI crosswise treatment groups followed by Dunnett's multiple comparison test.*

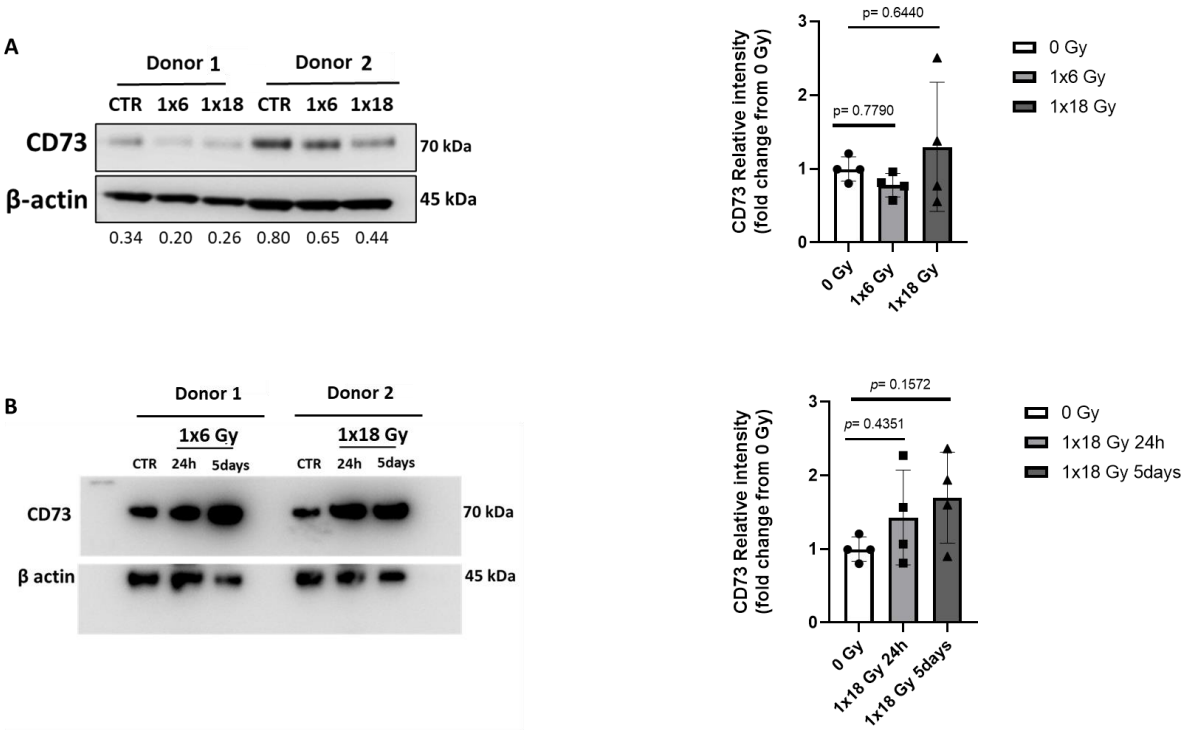

Figure 5.5 Effects of radiation on whole cell CD73 expression by Western blot. A*) Overall cell-associated (whole cell) expression of CD73 was determined by Western blotting. β actin was used as loading controls. Results show expression levels measured 5 days post-irradiation with 1x6 Gy and 1x18 Gy. The panel to the right shows quantitative bands densitometry analyses from 4 different donors.* ***B)*** *Overall expression of CD73 by CAFs (n=4) at two different time points (post-IR) was also determined by Western blotting, and results were normalized against β actin expression. Data represent mean (± SD) values from four different CAF donors. For experiment* ***A,*** *the one-way ANOVA test was used to compare changes in relative intensity crosswise treatment groups followed by Dunnett's multiple comparison test. For experiment* ***B,*** *a One-way ANOVA test was performed and P-values were determined between non-irradiated vs irradiated cells with HD-RT at different time points, followed by Dunnett's multiple comparison test.*

5.5 Radiation effects on whole cell expression levels of CD73, in CAFs

To ascertain if radiation was affecting the expression levels of CD73 in CAFs globally or specifically at the surface, we analyzed the overall expression of the enzymes by western blot. The result from the Western Blotting analysis from four different CAF donors suggests that exposure to high dose of ionizing radiation showed a tendency to a modest increase in CD73 protein expression level in whole-cell lysates (**Figure 5.5A**). However, the result was not statistically significant, meaning that the observed increase in expression of CD73 with higher radiation dose was not large enough to confidently conclude that radiation affected the

upregulation of CD73 in whole cell lysate. To investigate whether time can affect the expression of CD73 in CAFs cell lysate after the cells were exposed to higher dose of radiation, we modified the experimental design by adjusting the radiation dose to only higher dose (1x18 Gy) and checked the CD73 protein expression in two different time points, 24 hours and 5 days. There was a trend towards increased CD73 expression at 5 days post-radiation than 24 hours (**Figure 5.5B**), but the difference was not sufficient between the control and the treated groups to detect a significant difference.

5.6 Radiation effects on whole cell expression levels of ectonucleotidases CD38 and CD39

Similarly, we checked if the observed effects of radiation on the expression of CD38 and CD39 were global or surface-specific. Whole-cell lysates from CAF cultures collected 5 days post-irradiation showed detectable bands for CD39 (**Figure 5.6A)**, however, we could not observe any bands in western blots for CD38 (**supplementary figure D1**). After quantitative measurements of relative band intensities, the results showed enhanced expression of CD39 in CAFs exposed to 1x18 Gy radiation dose (**Figure 5.6B**) as compared to the intermediate and non-treated CAFs. However, according to the statistics, the difference was not significant enough.

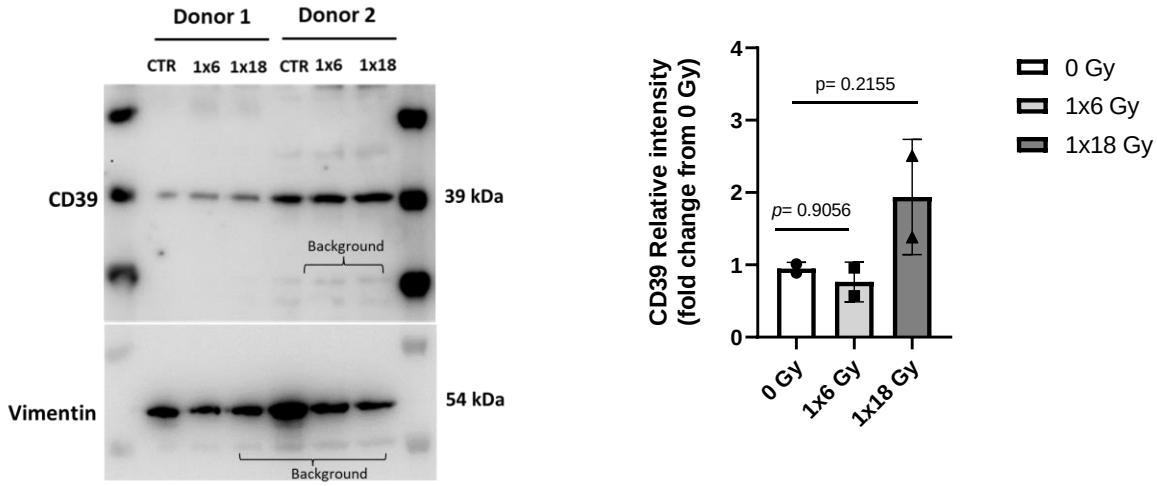

Figure 5.6 Effect of radiation on CD39 expression by non-radiated and irradiated CAFs (n=2) whole cell*. Cells were irradiated with a single dose of 6 Gy and 18 Gy. Overall expression of CD39 was determined by Western blotting and results were normalized against vimentin expression. Relative intensity of the bands corresponding to fold change is shown as bar graph. One-way ANOVA test was used to compare changes in relative intensity crosswise treatment groups followed by Dunnett's multiple comparison test.*

5.7 Radiation-mediated upregulation of soluble CD73 in CAF-CM

As opposed to CD38 and CD39, CD73 is the only ectonucleotidase that can be cleaved off from the plasma membrane and function extracellularly as soluble CD73 (sCD73). We, therefore, sought to analyze the effects of radiation on the production of soluble CD73 amounts in CAFs-CM from four different CAF donors. After 5 days post-radiation with two different radiation doses it was observed that the concentration of sCD73 was significantly increased from baseline in the high radiation dose group. The results indicate that CAFs secrete considerably higher level of sCD73 (2,2 folds) when radiated with a high dose (18 Gy) of radiation compared to non-radiated CAFs. On the other hand, 1x6 Gy radiation was able to induce a modest elevation of sCD73 compared to non-irradiated CAFs, but the values did not reach statistical significance (**Figure 5.7**).

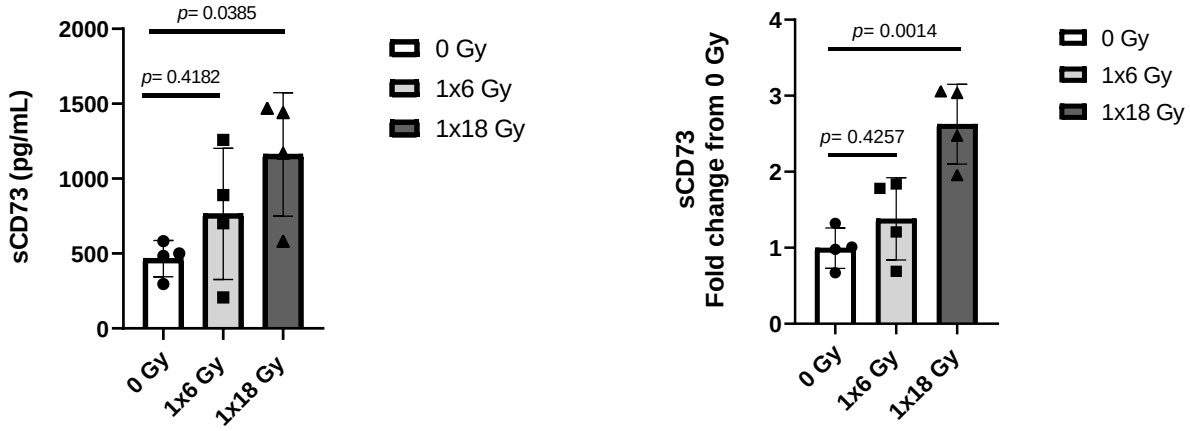

Figure 5.7 Soluble CD73 (sCD73) in supernatant from CAFs treated with a single dose of 6 Gy or 18 Gy radiation. *Cell supernatants were harvested 5 days post-irradiation and the concentration of sCD73 was quantified by ELISA. The panel to the left shows results expressed in pg/mL, whereas the panel to the right show results as fold change from untreated controls. Data represent mean (± SD) values from four different CAF donors measured in duplicates. One-way ANOVA test and P-values were determined between non-irradiated vs irradiated cells, followed by Dunnett's multiple comparison test.*

5.8 Radiation-mediated AMP-ADO conversion by CAF-CM and CAF lysates

In our next experiment, we investigated the effect of different radiation doses on the capacity of CAFs for ADO generation in CAF-CM from two different CAF donors. After 5 days post-radiation with two different radiation doses, CAF-CM was collected and 200µM AMP was added to the CAFs culture to observe the concentration of ADO which was significantly increased from baseline to higher radiation dose. The result signifies that CAF-CM generates higher level of ADO when radiated with a higher dose (18 Gy) of radiation compared to non-radiated CAFs. In contrast, exposure to 1x6 Gy radiation resulted in a modest generation of ADO to non-irradiated CAFs, but the observed differences did not reach statistical significance (**Figure 5.8A**). In order to define the ADO generation potential by CAF lysate, the same experimental protocol was employed. The result showed that radiation did not affect the ADO generation when CAFs were exposed to different radiation doses. Non- irradiated CAFs which are referred as control here, generated more ADO compared to irradiated CAFs and the differences in ADO generation were not statistically significant (**Figure 5.8B**).

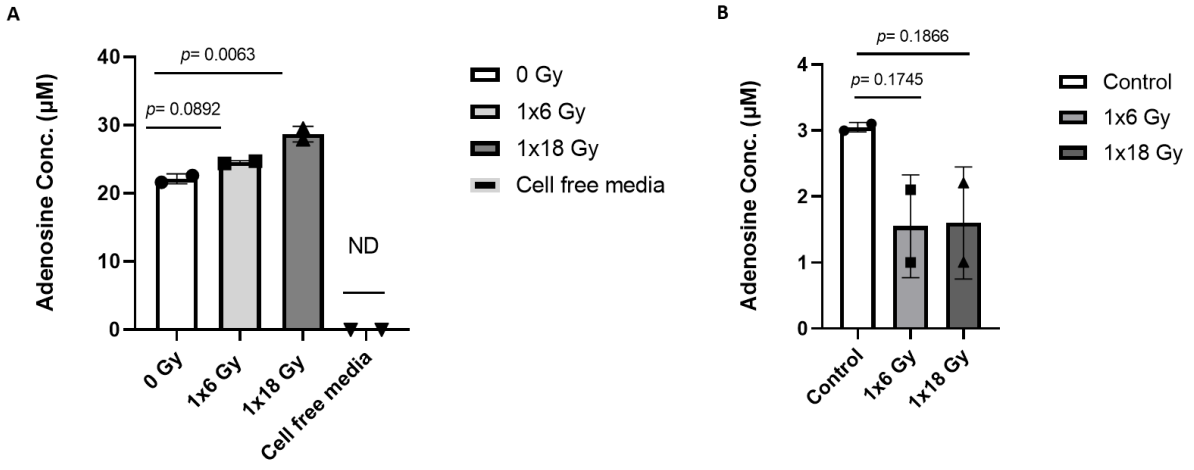

***Figure 5.8 Radiation-mediated effects in AMP-ADO conversion by CAFs-CM and CAFs**. **A)** The capacity of ADO generation by CM from non-radiated and irradiated CAFs (1x6 Gy and 1x18 Gy) (n=2) within 2 h in the presence of 200µM AMP was compared. **B)** ADO generation capacity by non-irradiated and irradiated CAFs (n=2) (1x6 Gy and 1x18 Gy) was also compared. Error bars illustrate mean ± SD. P-values were determined via One-way ANOVA test followed by Dunnett's multiple comparison test.*

5.9 Inhibition of sCD73 activity reverts the immunosuppressive effects of CAF-CM on activated T-cells

We conducted an *in vitro* functional assay to investigate if soluble CD73 in CAF-CM and the subsequent generation of adenosine was responsible for the immunosuppressive effects observed when PHA-activated T cells are exposed to conditioned medium from CAFs. AB680 is a novel small-molecule inhibitor of CD73 that has the potential to hinder the enzymatic activity of both membrane-bound and sCD73 on tumor cells, human and mouse $CD8^+$T cells [128]. Results depicted in **Figure 5.9** demonstrated a powerful immunosuppressive effect of CAF-CM over T-lymphocytes in comparison to the positive control where PHA-stimulated T-lymphocytes were cultured in regular growth medium. In the test group, treatment with AB680 restored partially the proliferation of T-cells, indicating that sCD73 and the subsequent generation of adenosine is responsible for some of the T-cell inhibitory effects exerted by CAF supernatants.

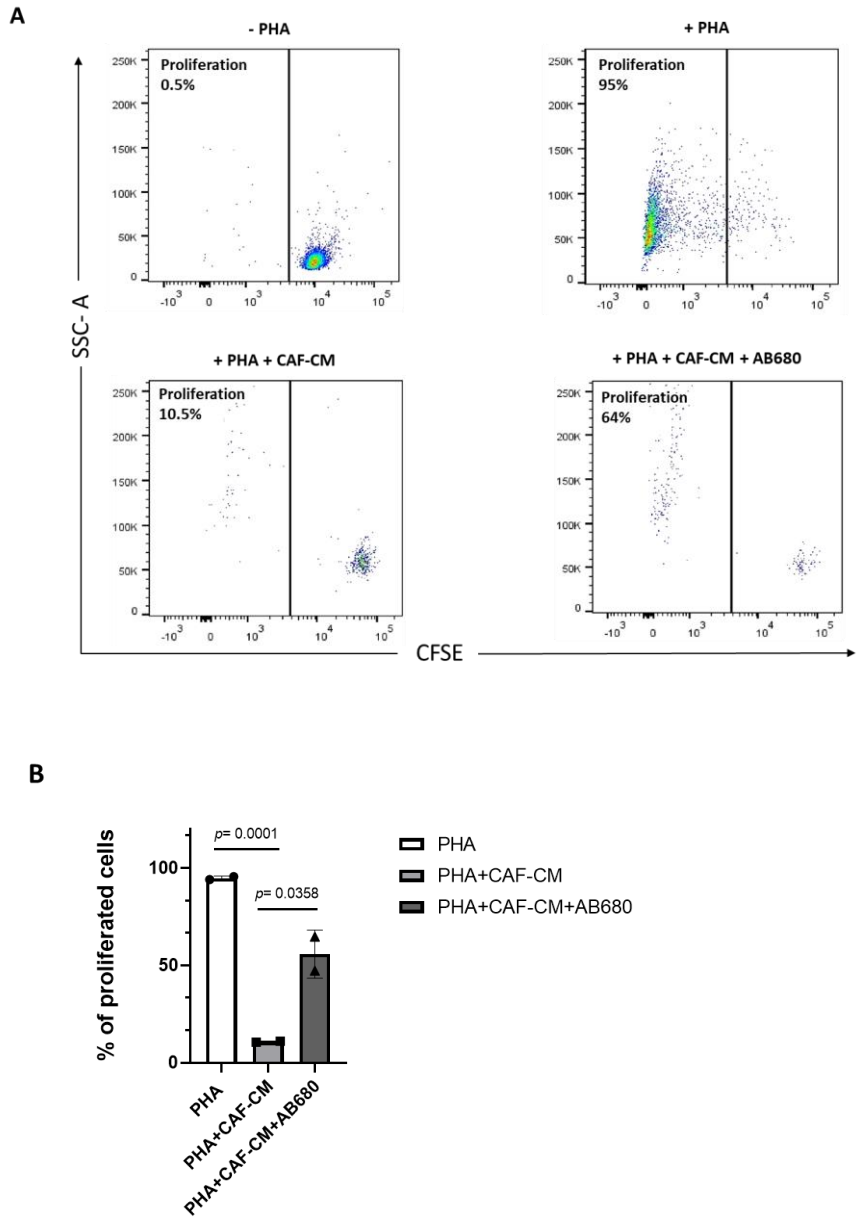

Figure 5.9 The inhibitory effect of adenosine generation by CAFs on T-cell proliferation was rescued by treatment with the CD73 inhibitor AB680. *T-cell proliferation assay was performed using CellTrace™ CFSE labeled human PBMCs activated with 1µg/mL PHA. PBMCs were co-cultured with non-irradiated CAFs-CM and a combination treatment of PBMCs, CAFs-CM, and AB680 and allowed to proliferate for 5 days. T-cell proliferation was assessed by measuring the decrease in CFSE fluorescence intensity after gating the lymphocytes population based on the forward scatter (FSC-A) and side scatter (SSC-A).* ***A)*** *Representative flow cytometry dot plots illustrate the percentage of low CFSE-labeled T-cells.* ***B)*** *The quantification of T-cells proliferation rates, where outcomes using duplicates of each sample are represented. P-values were determined by performing a Student's T-test.*

6 Discussion

CAFs are a diverse group of stromal cells in the TME [129] and they exhibit distinct phenotypic and epigenetic characteristics that set them apart from normal fibroblasts [42, 130]. CAFs differ from normal tissue-resident fibroblasts in that they are constantly activated [131] and influence biological processes by modulating the extracellular matrix and producing soluble factors such as cytokines and growth factors [132]. The presence of CAFs within the TME is related to elevated angiogenesis, invasion, and metastasis, and consequently, a detrimental prognosis in various types of cancer, including colorectal, pancreatic, and esophageal cancer. Despite ongoing efforts to investigate the role of CAFs in causing therapeutic resistance [133], because of CAFs' heterogeneous and adaptable nature the progress in this field is being obstructed [134]. Functional subsets of CAFs have been shown to have either pro-tumorigenic/immunosuppressive or anti-tumorigenic/immunogenic effects within TME [135, 136]. Because of CAFs' diverse functions within the TME, in the current research, we elected CAFs to work with. In our present study, cell lineage characterization was performed to demonstrate that the CAF cultures we were working with were pure, and also expressing the expected fibroblast markers including α-SMA and but not expressing non-fibroblast markers. Data obtained from flow cytometry analysis showed that the cells we have isolated from tumor biopsies were indeed CAF cells. The NSCLC biopsy-derived cells were subjected to analysis by staining with markers specific to CAFs, namely α-SMA and CD90, as well as non-CAFs markers including CD68, CD31, and CD326. Several studies have explored the correlation between the higher expression of α-SMA and CD90 by CAFs in the stroma and poor prognosis, as well as the significance of CAFs in the stroma of different cancer types [137, 138]. In one of the CAF donors, we observed some expression of CD68 which is a specific marker for macrophages. Although studies are limited, however, one study has provided evidence that CAFs can express CD68 and CD68-positive CAFs can facilitate the growth of tumors by inducing the infiltration of Tregs through CCL17 and CCL22 and contributes to poor clinical outcomes in patients suffering from oral squamous cell carcinoma (OSCC) [139].

Within TME, stromal and immune cells communicate with each other in a two-way exchange mechanism that includes both the secretion of soluble signaling molecules and physical interactions. This means that tumor-infiltrated immune cells can release pro-inflammatory cytokines such as TNF-α and IL-1β that facilitate the recruitment and activation of mesenchymal progenitor cells into the tumor. Furthermore, activated CAFs can exacerbate the

inflammatory response by the release of a multitude of chemokines, cytokines that attract other immune cells, such as regulatory T-cells and myeloid-derived suppressor cells. These cells can suppress the anti-tumor immune response within TME [62, 140, 141]. Apart from the direct effect of CAFs on innate and adaptive immune cells, CAFs also have indirect effect on TME which includes CAF-mediated tumor vasculature and hypoxia. Hypoxia can trigger CD73 and CD39 ectonucleotidase and can facilitate the generation of immunosuppressive adenosine [142, 143]. CAFs are commonly found in solid tumors, closely intertwined with cancer cells, frequently occupying the connective tissue bundles surrounding clusters of tumor cells [144]. During radiotherapy, both tumor cells and CAFs in the stromal tissue of tumors receive the same radiation dosages. Research exploring the cytotoxic effects of IR have revealed that fibroblasts represent a highly radio-resistant cell type [145, 146]. Our preliminary experiment demonstrated that radiation provoke a decline in the proliferative capacity and induces morphological changes in CAFs, which was probably due to the significant number of CAFs that underwent senescence following exposure to radiation. A study on NSCLC revealed that CAFs displayed a response to DNA damage that was contingent on the administered radiation doses. CAFs were exposed to a single radiation dose that varied from 2 to 18 Gy, and the level of radiation-induced permanent senescence in CAFs was found to increase proportionally with the amount of radiation delivered [147]. Radiation exposure to cells provokes immediate cell damage, however, some of the effects provoked by radiation are late effects, occurring several days or even weeks after the radiation exposure. Stress-induced cellular senescence is a process that may take several days. It is because of this reason that we have performed most of the analyses at day 5 post-radiation when the senescence phenotype is fully established.

Although the diverse immunoregulatory roles of CAFs have been extensively examined and well-documented [62, 141], there is a lack of thorough investigation into their ability to regulate the immune system in the context of radiation. Earlier studies performed on cultured CAFs from NSCLC showed that CAFs do not release immunogenic cell death signals following radiation, and thus CAFs are not involved in anti-tumor adjuvanticity [94]. Nevertheless, radiation can trigger phenotypic alterations in CAFs that may have an impact post-RT immunoregulation. Following ionizing radiation, senescent NSCLC-CAFs shows an elevated expression of various cell surface immunoregulatory receptors, including CD155, CD73, and Fas receptor. This phenotypic changes in CAFs can have an effect on T cell-mediated immune response [96].

Therefore, to observe CAFs' contribution to expressing immunoregulatory CD73 compared to tumor cells, our next experiment was performed. The result demonstrates that the surface expression of CD73 is more pronounced in NSCLC-isolated CAFs compared to NSCLC-derived tumor cells and tumor cell line A549. Several factors can cause an upregulation of CD73 expression in the TME which include tissue hypoxia, epithelial-to-mesenchymal transition [148], inflammation, and/or cytotoxic stress (such as radiotherapy, chemotherapy) [149, 150]. CD73 expression has been exhibited in different cell types, including tumor cells, endothelial cells, CAFs, lymphocytes, and myeloid cells, and depending on the specific cell type, their effect and its impact on anti-tumor immunity varies [151]. It has been widely acknowledged for several decades that the purine nucleoside adenosine has suppressive effects on the migration and cytotoxic activity of T-cells and NK-cells. Tumor cells that express CD73 have the potential to impede lymphocytes proliferation capacity and carry out their function, allowing them to evade immune system detection and promote their survival [152]. It is therefore not unexpected that CD73 is frequently overexpressed in different types of cancers and often associated with negative prognosis for patients [153, 154]. In addition to tumor cells, several studies have suggested that human CAFs also express high levels of CD73 in various cancer types [151, 155-157]. CD73+ CAFs in triple-negative breast cancer (TNBC) have been found to exhibit strong immunosuppressive functions and promote the recruitment, survival, and differentiation of Tregs. The immunosuppressive ability of CD73+ CAFs is partially mediated by the production of adenosine [156]. The expression of CD73 by both tumor cells and CAFs in lung cancer has been demonstrated [158]. However, few studies have compared the surface expression of CD73 between tumor cells and CAFs. One study evaluated the expression of CD73 in both lung cancer cells and CAFs and found that CD73 was expressed by both cancer cells and CAFs. However, cancer cells played a role in the generation of adenosine through CD73 activity in cases when CAFs fail to upregulate CD73 expression. This up-regulation of CD73 involved in adenosine production in lung cancer has an association with the lactate dehydrogenase LDH5 and hypoxia-inducible factor HIF1α expression by cancer cells [159].

On the bases of our previous experiment, it became evident that CAFs are major contributors to the generation of extracellular adenosine in the TME by the concerted action of the ectoenzyme CD73 also known as 5′ ectonucleotidase. However, the complex mechanism of producing extracellular adenosine relies on enzymes and transporters, which play a crucial role in regulating the biological functions of purine metabolites [160]. The complex system involves

two different pathways, which has been previously discussed. The first pathway, known as the canonical pathway, breaks down extracellular ATP into ADP and AMP, through the action of CD39 [101] and AMP is converted into ADO with the aid of CD73 enzyme [161]. Alternatively, the non-canonical pathway uses NAD+ as a substrate to create extracellular AMP through the activity of CD38, which is then hydrolyzed by CD73 to generate adenosine [102, 162]. Under normal physiological conditions, levels of both extracellular ATP and ADO are maintained in nanomolar range. Nevertheless, under stressed conditions or following death, cells can release higher amounts of ATP and ADO reaching micromolar level [105, 163]. Exposing tumor cells to ionizing radiation can lead to immunogenic cell death, which involves the amplification or release of DAMPs including ATP, which act as a signal to alert the immune system of a potential danger [164, 165]. However, most of the studies in radiobiology mainly focused on tumor cells, overlooking the complex cellular interaction within the TME [68, 166]. The precise function of CAFs in regulating the immune response during radiation therapy has not been thoroughly examined. In addition to its direct effect on killing tumor cells, research has indicated that radiotherapy has a negative impact on CAFs by causing growth arrest and inducing a senescence-like phenotype [167, 168]. Radiation-exposed senescent CAFs cause permanent DNA damage, resulting in the CAFs becoming more pro-tumorigenic. This, in turn, can promote tumor development by releasing paracrine signals [169].

As previously described, there are several factors involved in immune deviation that can be induced by tumors or radiation and targeting these factors may present appealing opportunities for improving the outcome of radiation. This approach could be beneficial by modulating the radiation response of tumors. However, the complexity of the changes that occurred in the TME by radiation and the immunostimulatory and immunosuppressive ‘dual face’ of radiation that are time and tissue-dependent, highlighted the importance of identifying strategies that can balance the dual face of radiation [170]. Purinergic CD73/ adenosine is one of the important endogenous regulators that is expressed by several cell types within the TME and has documented impact on tumor immune evasion, as well as the adverse late effects of radiotherapy [171, 172]. However, radiation-induced CD73/adenosine upregulation by CAFs and their adenosine-mediated immunosuppression within the TME has not been investigated. Therefore, in our current study, we tried to demonstrate the effect of radiation on the surface expression of CD38, CD39, and CD73 by CAFs. We discovered that there was a trend of elevated surface expression of CD73 when CAFs were exposed to single doses of radiation (6 Gy and 18 Gy) compared to non-treated CAFs. Furthermore, the same radiation doses showed

significant increase in the surface expression of CD38 and CD39 by CAFs compared to control CAFs. In our experiments, we administered SBRT in a single dose of 6 Gy and 18 Gy. Previous studies have shown that these radiation doses do not cause cell death but rather induce DNA damage in CAFs in a dose-dependent manner (18 Gy > 6 Gy) [147]. According to Hellevik *et al.,* CAFs showed a more profound senescence response to single dose of RT than fractionated treatment. CAFs obtained from lung tumors maintain their immunosuppressive abilities and continue to secret several immunosuppressive molecules after exposure to high dose of radiation [94]. In one study Wennerberg *et al.,* found that exposure to different radiation doses causes an increased CD73 expression on mouse and human breast cancer cells [173]. Other studies found evidence of CAFs expressing higher levels of CD73 which has an association with poor prognosis for many tumor types [157, 174, 175]. However, all these studies were conducted on non-irradiated CAFs. In an attempt to examine the influence of radiation on CD39 expression in mouse breast cancer cells, Wennerberg *et al.,* did not observe any surface expression of CD39 on tumor cells [173]. In NSCLC patients, MDSCs present in both the peripheral blood and tumor tissues expressed surface ectonucleotidase CD39 [176]. One recent study demonstrated that under hypoxic stress, CAFs can enhance the surface expression of CD39 much like other immunosuppressive factors including TGF-β, IDO, and PD-L1 [177]. Based on a previous study that was conducted both *in vivo* and *in vitro* settings, it was observed that CD73 exhibited high expressed in metastatic clone and radiation exposure further enhanced this expression [178], our finding suggest that radiation may induce the CD73 expression on CAFs and the upregulation might be due to the DNA damage and cellular stress of CAFs caused by radiation. RT was observed to induce the surface expression of CD38 in both mouse and human breast cancer cells, suggesting that the noncanonical pathway may be involved in the generation of adenosine [173]. CD38 has been found to generate adenosine in melanoma, and its increased expression on tumor cells has been associated with resistance against anti-PD-1/PD-L1 therapy [179]. In combination with the known role of radiation to disrupt NAD^+ metabolism [180], our findings suggest that NAD^+ may act as a source of adenosine production in irradiate CAFs.

The CD73 protein is anchored to the plasma membrane via a GPI anchor, which is a complex molecule consisting of a phospholipid and several sugars [181]. CD73 is held in place on the cell surface by the anchor, facilitating its efficient conversion of extracellular ATP into adenosine. When extracellular AMP is present, CD73 cleaves the molecule, releases a phosphate group and generates adenosine [182]. Our findings reflect the fact that radiation is

affecting the whole cell expression levels of CD39 and CD73, although the expression level was not statistically significant. CD73 is not only expressed on the cell surface but may also be present in the intracellular compartment where it is being processed and modified being transported to the plasma membrane, opening up the potential for the nucleoside to function as a danger signal [183]. In one study, an elevated level of CD73 expression was observed in whole gastric cancer cell line compared to non-malignant cells [184]. However, there is a lack of evidence to support the correlation between the expression of CD39 and CD73 in the cancer whole cell lysate and the effect of RT. This means that while the roles of CD39 and CD73 in adenosine generation and their role in cancer progression has been extensively studied, there has been no clear correlation established between their overall expression levels in a cell and the response of that cell to radiation. The whole CAFs expression of CD38 was also investigated in our study, however, no bands for the specific protein were detected. Possible reasons for not detecting any bands corresponding to CD38 could be a bad performance of the antibody, or that the protein is not expressed in CAFs.

As mentioned earlier, CD73 can be cleaved from the cell surface by proteolytic enzymes and released into the extracellular fluid as an enzymatically active soluble form. These active soluble CD73 continue to catalyze the conversion of AMP to adenosine [182]. This rate-limiting final step of adenosine generation is an important negative-feedback mechanism that helps to prevent excessive immune responses and maintain immune homeostasis [185]. In our study, the observed increase of sCD73 after radiation in CAFs with NSCLC, supports the finding of a previous study where RT-mediated upregulation of sCD73 in patients with metastatic breast cancer was observed [173]. Our experiment was conducted using CAFs-CM from fibroblasts treated with single dose (6 Gy and 18 Gy) of radiation. CAFs-CM from irradiated CAFs (4 Gy and 8 Gy) are capable to enhance the invasiveness of cancer cells when treated together [186]. High expression of sCD73 enzyme activity has been observed in patients with metastatic melanoma stage IV. Patients who exhibited a high level of sCD73 enzyme activity in their serum were found to have a greater risk of both disease progression and death, compared to those with low level sCD73 enzyme activity [187]. The observed increase in sCD73 level in CAFs-CM after RT supports the concept that this pathway can be a target in clinics to improve treatment responses. It is also important to investigate whether sCD73 expression could serve as a predictive biomarker to predict the response of NSCLC patients to RT.

The study also investigated irradiated and non-irradiated CAF contribution to ADO- production by CD73 activity in supernatants and cell lysate. The result of the study suggested that radiation can enhance the conversion of extracellular ATP to extracellular adenosine and therefore activating the ADO-CD73 pathways. Upon radiation, the presence of enzymatically active CD73 in irradiated CAFs-CM indicates that this enzyme is involved in the generation of adenosine. Whether radiation can influence the conversion of CAFs- contribution to adenosine generation by the cell lysate, a similar experiment was done and our finding indicates that radiation does not have any effect on CD73-mediated adenosine generation by NSCLS-CAFs. Nevertheless, the concentration of adenosine in the CAFs-CM was higher than the whole cell lysate. This is because radiation-induced elevated expression of CD73 in CAFs ultimately ends as a soluble enzyme in the supernatant and can be found on the surface of cells and as a soluble protein form in extracellular fluid. Because of the cleavage of membrane-anchored CD73, the activity of CD73 in cell lysate is reduced. Therefore, highly elevated CD73 in CAFs by converting ATP to adenosine through the CD73-ADO pathway in the CAF network can be a promising immune checkpoint. It has been already demonstrated that blocking both the A_{2A} and A_{2B}-dependent CD73-ADO immune checkpoint pathway simultaneously in tumor cells is highly effective approach for antitumor immunity [157].

To gain more insights into the effect of CAFs on T-cell proliferation and to evaluate the potential of CD73 inhibitor AB680 in reversing the immunosuppressive effect of CAFs, experiments were conducted using CAFs and T-cells with and without AB680 treatment to block the conversion of ATP to adenosine. Our result demonstrated that CAF-CM exhibits a constant suppressive effect ($P<0.0001$) on human PHA-L-activated T-cells derived from healthy volunteers' peripheral blood. At the same time, our result revealed that CD73 inhibition was able to restore the proliferative activity of T-cells ($P<0.05$). One study has demonstrated that the co-regulatory membrane molecules, PD-L1 and PD-L2, expressed by CAFs maybe contribute to their immunosuppressive functions [188], whereas another study found that the inhibitory effects of CAFs on T-lymphocytes are mediated by paracrine signals rather than contact-dependent signals [94]. However, based on our experiment we hypothesized that CD73 expressed by CAFs might have contribution to ADO-mediated immunosuppression by inhibiting T-cell proliferation and by blocking CAF-mediated conversion of ATP to adenosine can improve T-cell proliferation. In clinics, commercially available small molecule AB680 CD73 inhibitor is currently being tested to block CD73 in pancreatic ductal adenocarcinoma (PDA) [189]. An *in vivo* study conducted on pancreatic PDA has shown that a combination

therapy involving radiofrequency ablation and inhibition of the adenosine pathway results in a decrease in tumor size and enhance anti-tumor immune responses in preclinical models [128].

7 Methodological considerations and limitations of the study

To ensure the relevance of our study to clinical settings, we utilized a single dose of ionizing radiation, specifically 1x6 Gy and 1x18 Gy, to treat CAFs consistently throughout all experiments. Golden *et al.,* demonstrated that ICD signals for each component can be effectively induced by clinically relevant doses of IR in a dose-dependent manner ranging from 2-20 Gy [190]. When comparing the radiation doses, it is important to take into account the concept of "biological effective dose" (BED), which considers the dose per fraction and the overall treatment time. This is because the biological effects of radiation depend not only on the radiation doses but also on the fraction schedule and repair mechanism of the body [191]. In clinical settings, it is difficult to compare the effective outcome of 18 Gy compared to 6 Gy without considering the specifics of the clinical situations, such as the type of cancer being treated and the size and location of the tumor. In our *in vitro* study, we used single dose of 6 Gy and 18 Gy because such doses are clinically relevant in the context of SBRT [147]. One study performed by Hellevik *et al*., showed that proliferation rates of CAFs were reduced after 18 Gy compared to 6 daily fractions of 6 Gy [147]. However, other studies performed in our lab observed that 18 Gy or in conventional fractions (4x 2 Gy) were not effective enough to overcome CAFs immunosuppressive effects and the level of immunosuppressive molecules produced by irradiated CAFS compared to non-irradiated CAFs remained the same and radiation did not appear to affect the immunoregulatory features of CAFs over immune cells [94, 97]. To the end, some authors have suggested that a high single dose of RT, also known as hypo-fractionated radiation therapy, may be more effective than intermediate or low doses for certain types of cancer [192, 193]. Therefore, in combination with the previous studies and studies performed in our lab and to observe the radiation-induced upregulation of immunosuppressive adenosine, we decided to treat NSCLC-CAFs with 6 Gy and 18 Gy radiation doses where the higher RT dose showed more effective results than medium dose.

In every experimental plan, we waited five days post-radiation to observe the biological effects of radiation. RT demonstrates substantial DNA damage and growth delay in CAFs in long-term cultures. Five days after radiation was enough to observe the effect on CAFs because, within this approximate time frame, majority of the cells undergo apoptosis or senescence [194]. Five days post-radiation, senescence CAFs undergo phenotypic changes and influenced post-RT

immunoregulation by displaying enhanced expression of several cell surface markers including CD73 [96].

As a rule of thumb, statistical analysis was carried out to identify if the differences between control and different treatment groups were statistically significant. Throughout this thesis, we repeated experiments several times with multiple biological replicates. This was done to minimize random biological variations and technical errors and to make sure that the results are consistent and reliable. During determining the significance of the treatment effect, consideration is given to the SD of each means, ensuring the significance of the treatment. We ensured that the data set meets the prerequisites of the selected statistical analysis when determining the statistical significance between treatment groups. Typically, ordinary one-way ANOVA with Dunnett's post hoc test is used to determine the significance between treatment groups and control [195]. Therefore, one-way ANOVA was used to identify which specific treatment group (1x6 Gy or 1x18 Gy) was different from the control group.

The extensive impact of RT on CAFs and the cross-talk between CAFs and CAF-mediated immunoregulation has not been thoroughly investigated. Several *in vitro* studies have demonstrated increased expression of immunoregulatory cytokines and growth factors, the results are distinct when the attention is shifted to CAFs instead of non-active fibroblasts. Also, the impact of radiotherapy on CAFs varies in different studies, potentially resulting from the use of diverse radiation regimens involving doses and fractions. Many of the studies including our study have focused on the short-term effects of RT on CAFs, with investigations lasting only a few days. However, radiation can have prolonged effects on the tissue that persist for several years. In our study, we have used primary cultures CAFs from NSCLC tumor specimens. This *in vitro* model is limited in its ability to fully replicate the physiological environment where other immune cells and cancer cells interact with CAFs through physical contact or paracrine signaling. During our study, we employed flow cytometry for several experiments. However, in one particular study, we encountered issues with a low cell count, resulting in varying numbers of viable cells in different samples. This could be attributed to the high pressure and fluidic forces utilized during sample acquisition, leading to the loss of samples. Due to time limitations, this particular study was not possible to repeat. However, in the future, to obtain more apparent and conspicuous result, this specific experiment will be performed further.

It should be noted that CAFs are heterogeneous population of cells and the proportion of different subtypes can vary based on organ, anatomical location, tumor types, or stage. Therefore, CAFs-derived immunosuppressive molecules and soluble factors may differ significantly. The study population in this study was small, therefore, it was difficult to get significant results because with a small sample size, the statistical power of the study is reduced, and the likelihood of detecting significant differences between treatment groups decreases.

8 Concluding remarks and future prospectives

A few notable observations can be highlighted from this study: i) CAFs derived from NSCLC are more significant contributors to the immunosuppressive adenosine than the tumor cells, ii) The surface expression of CD73, CD38, and CD39 is slightly upregulated on CAFs when treated with high-dose radiation, iii) CD73 and CD39 expression in whole cell lysate is elevated by high dose RT, iv) High-dose radiation has an effect on the upregulation of sCD73, v) Radiation- mediated adenosine generation is more pronounced in CAF-CM compared to CAFs itself and single high-dose radiation has more effect on adenosine generation than single medium- dose, vi) Blocking CD73 activity in CAF supernatants reverts partly the suppressive effects of CAF-CM over T-cells.

The administration of small molecules or mAbs to inhibit adenosine signaling, by either decreasing its production or blocking of receptor bindings, has shown significant efficacy in controlling tumors in the pre-clinical trial. As adenosine signaling blockade and using $A_{2A}R/A_{2B}R$ antagonist are being tested in clinical trials as standalone therapies, more and more trials are also exploring combinations of adenosine-signaling blockade with classic treatment approaches like radiotherapy. Therefore, in the future, we can complete our study by working in different directions: i) By using inhibitory agents to target $A_{2A}R/A_{2B}R$ pathways and combining the effect with radiation; ii) Exploring and targeting the adenosine system in CAFs to improve radiation-induced immunosuppression *in vivo*.

Works Cited

1. Clark, S.B. and S. Alsubait, *Non Small Cell Lung Cancer*, in *StatPearls*. 2022: Treasure Island (FL).
2. Funai, K., et al., *Clinicopathologic characteristics of peripheral squamous cell carcinoma of the lung.* Am J Surg Pathol, 2003. **27**(7): p. 978-84.
3. Ragab, E.M., et al., *Therapeutic potential of chrysin nanoparticle-mediation inhibition of succinate dehydrogenase and ubiquinone oxidoreductase in pancreatic and lung adenocarcinoma.* European Journal of Medical Research, 2022. **27**(1): p. 172.
4. Collins, L.G., et al., *Lung cancer: diagnosis and management.* Am Fam Physician, 2007. **75**(1): p. 56-63.
5. Kaseda, K., *Recent and current advances in FDG-PET imaging within the field of clinical oncology in NSCLC: a review of the literature.* Diagnostics, 2020. **10**(8): p. 561.
6. Deboever, N., et al., *Current Surgical Indications for Non-Small-Cell Lung Cancer.* Cancers (Basel), 2022. **14**(5).
7. Provencio, M., et al., *Inoperable stage III non-small cell lung cancer: Current treatment and role of vinorelbine.* J Thorac Dis, 2011. **3**(3): p. 197-204.
8. Palma, D. and S. Senan, *Stereotactic radiation therapy: changing treatment paradigms for stage I nonsmall cell lung cancer.* Curr Opin Oncol, 2011. **23**(2): p. 133-9.
9. Hellevik, T. and I. Martinez-Zubiaurre, *Radiotherapy and the tumor stroma: the importance of dose and fractionation.* Front Oncol, 2014. **4**: p. 1.
10. Heinzerling, J.H., B. Kavanagh, and R.D. Timmerman, *Stereotactic ablative radiation therapy for primary lung tumors.* Cancer J, 2011. **17**(1): p. 28-32.
11. Hanahan, D. and R.A. Weinberg, *The hallmarks of cancer.* Cell, 2000. **100**(1): p. 57-70.
12. Hanahan, D. and R.A. Weinberg, *Hallmarks of cancer: the next generation.* Cell, 2011. **144**(5): p. 646-74.
13. Pietras, K. and A. Ostman, *Hallmarks of cancer: interactions with the tumor stroma.* Exp Cell Res, 2010. **316**(8): p. 1324-31.
14. Hanahan, D. and L.M. Coussens, *Accessories to the crime: functions of cells recruited to the tumor microenvironment.* Cancer Cell, 2012. **21**(3): p. 309-22.
15. Hanahan, D., *Hallmarks of Cancer: New Dimensions.* Cancer Discov, 2022. **12**(1): p. 31-46.
16. Streuli, C., *Extracellular matrix remodelling and cellular differentiation.* Curr Opin Cell Biol, 1999. **11**(5): p. 634-40.
17. Mueller, M.M. and N.E. Fusenig, *Friends or foes - bipolar effects of the tumour stroma in cancer.* Nat Rev Cancer, 2004. **4**(11): p. 839-49.
18. Whiteside, T.L., *The tumor microenvironment and its role in promoting tumor growth.* Oncogene, 2008. **27**(45): p. 5904-12.
19. Henke, E., R. Nandigama, and S. Ergün, *Extracellular Matrix in the Tumor Microenvironment and Its Impact on Cancer Therapy.* Front Mol Biosci, 2019. **6**: p. 160.
20. Muromoto, R., K. Oritani, and T. Matsuda, *Current understanding of the role of tyrosine kinase 2 signaling in immune responses.* World J Biol Chem, 2022. **13**(1): p. 1-14.
21. McComb, S., et al., *Introduction to the Immune System.* Methods Mol Biol, 2019. **2024**: p. 1-24.

22. Multhoff, G., M. Molls, and J. Radons, *Chronic inflammation in cancer development.* Front Immunol, 2011. **2**: p. 98.
23. Zhao, H., et al., *Inflammation and tumor progression: signaling pathways and targeted intervention.* Signal Transduct Target Ther, 2021. **6**(1): p. 263.
24. Cooper, M.D. and M.N. Alder, *The evolution of adaptive immune systems.* Cell, 2006. **124**(4): p. 815-22.
25. Raval, R.R., et al., *Tumor immunology and cancer immunotherapy: summary of the 2013 SITC primer.* J Immunother Cancer, 2014. **2**: p. 14.
26. Schreiber, R.D., L.J. Old, and M.J. Smyth, *Cancer immunoediting: integrating immunity's roles in cancer suppression and promotion.* Science, 2011. **331**(6024): p. 1565-70.
27. Chimal-Ramirez, G.K., N.A. Espinoza-Sanchez, and E.M. Fuentes-Panana, *Protumor activities of the immune response: insights in the mechanisms of immunological shift, oncotraining, and oncopromotion.* J Oncol, 2013. **2013**: p. 835956.
28. Vinay, D.S., et al., *Immune evasion in cancer: Mechanistic basis and therapeutic strategies.* Semin Cancer Biol, 2015. **35 Suppl**: p. S185-s198.
29. Hato, T. and P.C. Dagher, *How the Innate Immune System Senses Trouble and Causes Trouble.* Clin J Am Soc Nephrol, 2015. **10**(8): p. 1459-69.
30. O'Donnell, J.S., M.W.L. Teng, and M.J. Smyth, *Cancer immunoediting and resistance to T cell-based immunotherapy.* Nat Rev Clin Oncol, 2019. **16**(3): p. 151-167.
31. von Locquenghien, M., C. Rozalen, and T. Celia-Terrassa, *Interferons in cancer immunoediting: sculpting metastasis and immunotherapy response.* J Clin Invest, 2021. **131**(1).
32. Dunn, G.P., et al., *Cancer immunoediting: from immunosurveillance to tumor escape.* Nat Immunol, 2002. **3**(11): p. 991-8.
33. Sahai, E., et al., *A framework for advancing our understanding of cancer-associated fibroblasts.* Nat Rev Cancer, 2020. **20**(3): p. 174-186.
34. Nair, N., et al., *A cancer stem cell model as the point of origin of cancer-associated fibroblasts in tumor microenvironment.* Sci Rep, 2017. **7**(1): p. 6838.
35. Quante, M., et al., *Bone marrow-derived myofibroblasts contribute to the mesenchymal stem cell niche and promote tumor growth.* Cancer Cell, 2011. **19**(2): p. 257-72.
36. Miyazaki, Y., et al., *Adipose-derived mesenchymal stem cells differentiate into pancreatic cancer-associated fibroblasts in vitro.* FEBS Open Bio, 2020. **10**(11): p. 2268-2281.
37. Kim, K., et al., *Cancer-Associated Fibroblasts Differentiated by Exosomes Isolated from Cancer Cells Promote Cancer Cell Invasion.* Int J Mol Sci, 2020. **21**(21).
38. Kalluri, R. and M. Zeisberg, *Fibroblasts in cancer.* Nat Rev Cancer, 2006. **6**(5): p. 392-401.
39. Kalluri, R., *The biology and function of fibroblasts in cancer.* Nat Rev Cancer, 2016. **16**(9): p. 582-98.
40. Xing, F., J. Saidou, and K. Watabe, *Cancer associated fibroblasts (CAFs) in tumor microenvironment.* Front Biosci (Landmark Ed), 2010. **15**(1): p. 166-79.
41. Saraswati, S., et al., *Identification of a pro-angiogenic functional role for FSP1-positive fibroblast subtype in wound healing.* Nature communications, 2019. **10**(1): p. 3027.
42. Sahai, E., et al., *A framework for advancing our understanding of cancer-associated fibroblasts.* Nat Rev Cancer, 2020. **20**(3): p. 174-186.
43. Zeisberg, M., F. Strutz, and G.A. Muller, *Role of fibroblast activation in inducing interstitial fibrosis.* J Nephrol, 2000. **13 Suppl 3**: p. S111-20.

44. Bhowmick, N.A., E.G. Neilson, and H.L. Moses, *Stromal fibroblasts in cancer initiation and progression.* Nature, 2004. **432**(7015): p. 332-7.
45. Augsten, M., *Cancer-associated fibroblasts as another polarized cell type of the tumor microenvironment.* Front Oncol, 2014. **4**: p. 62.
46. Orimo, A., et al., *Stromal fibroblasts present in invasive human breast carcinomas promote tumor growth and angiogenesis through elevated SDF-1/CXCL12 secretion.* Cell, 2005. **121**(3): p. 335-48.
47. Pietras, K., et al., *Functions of paracrine PDGF signaling in the proangiogenic tumor stroma revealed by pharmacological targeting.* PLoS Med, 2008. **5**(1): p. e19.
48. Follain, G., et al., *Fluids and their mechanics in tumour transit: shaping metastasis.* Nat Rev Cancer, 2020. **20**(2): p. 107-124.
49. Huang, L., et al., *Cancer-associated fibroblasts in digestive tumors.* World J Gastroenterol, 2014. **20**(47): p. 17804-18.
50. Ding, X., et al., *HGF-mediated crosstalk between cancer-associated fibroblasts and MET-unamplified gastric cancer cells activates coordinated tumorigenesis and metastasis.* Cell Death Dis, 2018. **9**(9): p. 867.
51. Bremnes, R.M., et al., *The role of tumor stroma in cancer progression and prognosis: emphasis on carcinoma-associated fibroblasts and non-small cell lung cancer.* J Thorac Oncol, 2011. **6**(1): p. 209-17.
52. Miles, F.L. and R.A. Sikes, *Insidious changes in stromal matrix fuel cancer progression.* Mol Cancer Res, 2014. **12**(3): p. 297-312.
53. Oskarsson, T., et al., *Breast cancer cells produce tenascin C as a metastatic niche component to colonize the lungs.* Nat Med, 2011. **17**(7): p. 867-74.
54. Grum-Schwensen, B., et al., *Suppression of tumor development and metastasis formation in mice lacking the S100A4(mts1) gene.* Cancer Res, 2005. **65**(9): p. 3772-80.
55. Kennel, K.B., et al., *Cancer-Associated Fibroblasts in Inflammation and Antitumor Immunity.* Clinical Cancer Research, 2023. **29**(6): p. 1009-1016.
56. Barrett, R.L. and E. Puré, *Cancer-associated fibroblasts and their influence on tumor immunity and immunotherapy.* Elife, 2020. **9**.
57. Cohen, N., et al., *Fibroblasts drive an immunosuppressive and growth-promoting microenvironment in breast cancer via secretion of Chitinase 3-like 1.* Oncogene, 2017. **36**(31): p. 4457-4468.
58. Augsten, M., et al., *Cancer-associated fibroblasts expressing CXCL14 rely upon NOS1-derived nitric oxide signaling for their tumor-supporting properties.* Cancer Res, 2014. **74**(11): p. 2999-3010.
59. Ren, G., et al., *CCR2-dependent recruitment of macrophages by tumor-educated mesenchymal stromal cells promotes tumor development and is mimicked by TNFalpha.* Cell Stem Cell, 2012. **11**(6): p. 812-24.
60. Yu, P.F., et al., *TNFalpha-activated mesenchymal stromal cells promote breast cancer metastasis by recruiting CXCR2(+) neutrophils.* Oncogene, 2017. **36**(4): p. 482-490.
61. Yang, X., et al., *FAP Promotes Immunosuppression by Cancer-Associated Fibroblasts in the Tumor Microenvironment via STAT3-CCL2 Signaling.* Cancer Res, 2016. **76**(14): p. 4124-35.
62. Monteran, L. and N. Erez, *The Dark Side of Fibroblasts: Cancer-Associated Fibroblasts as Mediators of Immunosuppression in the Tumor Microenvironment.* Front Immunol, 2019. **10**: p. 1835.
63. Khalili, J.S., et al., *Oncogenic BRAF(V600E) promotes stromal cell-mediated immunosuppression via induction of interleukin-1 in melanoma.* Clin Cancer Res, 2012. **18**(19): p. 5329-40.

64. de Lourdes Mora-Garcia, M., et al., *Mesenchymal stromal cells derived from cervical cancer produce high amounts of adenosine to suppress cytotoxic T lymphocyte functions.* J Transl Med, 2016. **14**(1): p. 302.
65. Martinez-Zubiaurre, I., A.J. Chalmers, and T. Hellevik, *Radiation-Induced Transformation of Immunoregulatory Networks in the Tumor Stroma.* Front Immunol, 2018. **9**: p. 1679.
66. Tran, J.H., et al., *Outcomes Following SBRT vs. IMRT and 3DCRT for Older Patients with Stage IIA Node-Negative Non-Small Cell Lung Cancer > 5 cm.* Clin Lung Cancer, 2023. **24**(1): p. e9-e18.
67. Schneider, C.S., et al., *Nonoperative Treatment of Large (5–7 cm), Node-Negative Non–Small Cell Lung Cancer Commonly Deviates From NCCN Guidelines.* Journal of the National Comprehensive Cancer Network, 2021. **20**(4): p. 371-377. e5.
68. Barker, H.E., et al., *The tumour microenvironment after radiotherapy: mechanisms of resistance and recurrence.* Nat Rev Cancer, 2015. **15**(7): p. 409-25.
69. Citrin, D.E., *Recent Developments in Radiotherapy.* N Engl J Med, 2017. **377**(11): p. 1065-1075.
70. Shaltiel, I.A., et al., *The same, only different–DNA damage checkpoints and their reversal throughout the cell cycle.* Journal of cell science, 2015. **128**(4): p. 607-620.
71. Eriksson, D. and T. Stigbrand, *Radiation-induced cell death mechanisms.* Tumour Biol, 2010. **31**(4): p. 363-72.
72. Patel, N.H., et al., *The Roles of Autophagy and Senescence in the Tumor Cell Response to Radiation.* Radiat Res, 2020. **194**(2): p. 103-115.
73. Kumari, S., et al., *Immunomodulatory Effects of Radiotherapy.* Int J Mol Sci, 2020. **21**(21).
74. Meyer, K.K., *Radiation-induced lymphocyte-immune deficiency. A factor in the increased visceral metastases and decreased hormonal responsiveness of breast cancer.* Arch Surg, 1970. **101**(2): p. 114-21.
75. Raben, M., et al., *The effect of radiation therapy on lymphocyte subpopulations in cancer patients.* Cancer, 1976. **37**(3): p. 1417-21.
76. Ehlers, G. and M. Fridman, *Abscopal effect of radiation in papillary adenocarcinoma.* Br J Radiol, 1973. **46**(543): p. 220-2.
77. Rees, G.J. and C.M. Ross, *Abscopal regression following radiotherapy for adenocarcinoma.* Br J Radiol, 1983. **56**(661): p. 63-6.
78. Demaria, S., et al., *Ionizing radiation inhibition of distant untreated tumors (abscopal effect) is immune mediated.* Int J Radiat Oncol Biol Phys, 2004. **58**(3): p. 862-70.
79. Wennerberg, E., et al., *Barriers to Radiation-Induced In Situ Tumor Vaccination.* Front Immunol, 2017. **8**: p. 229.
80. Galluzzi, L., O. Kepp, and G. Kroemer, *Immunogenic cell death in radiation therapy.* Oncoimmunology, 2013. **2**(10): p. e26536.
81. Chen, D.S. and I. Mellman, *Oncology meets immunology: the cancer-immunity cycle.* Immunity, 2013. **39**(1): p. 1-10.
82. Golden, E.B., et al., *The convergence of radiation and immunogenic cell death signaling pathways.* Front Oncol, 2012. **2**: p. 88.
83. Naimi, A., et al., *Tumor immunotherapies by immune checkpoint inhibitors (ICIs); the pros and cons.* Cell Communication and Signaling, 2022. **20**(1): p. 44.
84. Bruni, D., H.K. Angell, and J. Galon, *The immune contexture and Immunoscore in cancer prognosis and therapeutic efficacy.* Nat Rev Cancer, 2020. **20**(11): p. 662-680.
85. Hegde, P.S. and D.S. Chen, *Top 10 Challenges in Cancer Immunotherapy.* Immunity, 2020. **52**(1): p. 17-35.

86. Hegde, P.S., V. Karanikas, and S. Evers, *The Where, the When, and the How of Immune Monitoring for Cancer Immunotherapies in the Era of Checkpoint Inhibition.* Clin Cancer Res, 2016. **22**(8): p. 1865-74.
87. Sevenich, L., *Turning "Cold" Into "Hot" Tumors-Opportunities and Challenges for Radio-Immunotherapy Against Primary and Metastatic Brain Cancers.* Front Oncol, 2019. **9**: p. 163.
88. Barcellos-Hoff, M., *The potential influence of radiation-induced microenvironments in neoplastic progression.* Journal of mammary gland biology and neoplasia, 1998. **3**(2): p. 165.
89. McBride, W.H., et al., *A sense of danger from radiation.* Radiation research, 2004. **162**(1): p. 1-19.
90. Calvo, F., et al., *Mechanotransduction and YAP-dependent matrix remodelling is required for the generation and maintenance of cancer-associated fibroblasts.* Nature cell biology, 2013. **15**(6): p. 637-646.
91. Tsai, K.K., et al., *Cellular mechanisms for low-dose ionizing radiation-induced perturbation of the breast tissue microenvironment.* Cancer Res, 2005. **65**(15): p. 6734-44.
92. Martinez-Zubiaurre, I., et al., *Tumorigenic responses of cancer-associated stromal fibroblasts after ablative radiotherapy: a transcriptome-profiling study.* 2013.
93. Rodier, F., et al., *Persistent DNA damage signalling triggers senescence-associated inflammatory cytokine secretion.* Nat Cell Biol, 2009. **11**(8): p. 973-9.
94. Gorchs, L., et al., *Cancer-associated fibroblasts from lung tumors maintain their immunosuppressive abilities after high-dose irradiation.* Front Oncol, 2015. **5**: p. 87.
95. Berzaghi, R., et al., *Ionizing Radiation Curtails Immunosuppressive Effects From Cancer-Associated Fibroblasts on Dendritic Cells.* Front Immunol, 2021. **12**: p. 662594.
96. Yang, N., et al., *Irradiated Tumor Fibroblasts Avoid Immune Recognition and Retain Immunosuppressive Functions Over Natural Killer Cells.* Front Immunol, 2020. **11**: p. 602530.
97. Berzaghi, R., et al., *Fibroblast-Mediated Immunoregulation of Macrophage Function Is Maintained after Irradiation.* Cancers (Basel), 2019. **11**(5).
98. Fredholm, B.B., et al., *International Union of Pharmacology. XXV. Nomenclature and classification of adenosine receptors.* Pharmacol Rev, 2001. **53**(4): p. 527-52.
99. Alvarez, C.L., M.F. Troncoso, and M.V. Espelt, *Extracellular ATP and adenosine in tumor microenvironment: Roles in epithelial-mesenchymal transition, cell migration, and invasion.* J Cell Physiol, 2022. **237**(1): p. 389-400.
100. Layland, J., et al., *Adenosine: physiology, pharmacology, and clinical applications.* JACC: Cardiovascular Interventions, 2014. **7**(6): p. 581-591.
101. Yegutkin, G.G., et al., *The evidence for two opposite, ATP-generating and ATP-consuming, extracellular pathways on endothelial and lymphoid cells.* Biochemical Journal, 2002. **367**(1): p. 121-128.
102. Horenstein, A.L., et al., *A CD38/CD203a/CD73 ectoenzymatic pathway independent of CD39 drives a novel adenosinergic loop in human T lymphocytes.* Oncoimmunology, 2013. **2**(9): p. e26246.
103. Jiang, X., et al., *The ectonucleotidases CD39 and CD73 on T cells: The new pillar of hematological malignancy.* Front Immunol, 2023. **14**: p. 1110325.
104. Karmouty-Quintana, H., Y. Xia, and M.R. Blackburn, *Adenosine signaling during acute and chronic disease states.* Journal of molecular medicine, 2013. **91**: p. 173-181.
105. Di Virgilio, F., et al., *Extracellular ATP and P2 purinergic signalling in the tumour microenvironment.* Nature Reviews Cancer, 2018. **18**(10): p. 601-618.

106. Kroemer, G., et al., *Immunogenic cell death in cancer therapy.* Annual review of immunology, 2013. **31**: p. 51-72.
107. Vultaggio-Poma, V., A.C. Sarti, and F. Di Virgilio, *Extracellular ATP: A Feasible Target for Cancer Therapy.* Cells, 2020. **9**(11).
108. Galluzzi, L., et al., *Immunogenic cell death in cancer and infectious disease.* Nat Rev Immunol, 2017. **17**(2): p. 97-111.
109. Allard, B., et al., *Immunosuppressive activities of adenosine in cancer.* Current opinion in pharmacology, 2016. **29**: p. 7-16.
110. Spychala, J. and J. Kitajewski, *Wnt and β-catenin signaling target the expression of ecto-5′-nucleotidase and increase extracellular adenosine generation.* Experimental cell research, 2004. **296**(2): p. 99-108.
111. Inoue, Y., et al., *Prognostic impact of CD73 and A2A adenosine receptor expression in non-small-cell lung cancer.* Oncotarget, 2017. **8**(5): p. 8738-8751.
112. Zhu, J., et al., *CD73/NT5E is a target of miR-30a-5p and plays an important role in the pathogenesis of non-small cell lung cancer.* Molecular cancer, 2017. **16**(1): p. 1-15.
113. Chalmin, F., et al., *Stat3 and Gfi-1 transcription factors control Th17 cell immunosuppressive activity via the regulation of ectonucleotidase expression.* Immunity, 2012. **36**(3): p. 362-373.
114. Sitkovsky, M.V., et al., *Physiological control of immune response and inflammatory tissue damage by hypoxia-inducible factors and adenosine A2A receptors.* Annu. Rev. Immunol., 2004. **22**: p. 657-682.
115. Wang, L., et al., *CD73 has distinct roles in nonhematopoietic and hematopoietic cells to promote tumor growth in mice.* The Journal of clinical investigation, 2011. **121**(6): p. 2371-2382.
116. Ohta, A., et al., *The development and immunosuppressive functions of CD4+ CD25+ FoxP3+ regulatory T cells are under influence of the adenosine-A2A adenosine receptor pathway.* Frontiers in immunology, 2012. **3**: p. 190.
117. Chambers, A.M., et al., *Adenosinergic signaling alters natural killer cell functional responses.* Frontiers in Immunology, 2018. **9**: p. 2533.
118. Zanin, R.F., et al., *Differential macrophage activation alters the expression profile of NTPDase and ecto-5′-nucleotidase.* PLoS One, 2012. **7**(2): p. e31205.
119. Montalbán del Barrio, I., et al., *Adenosine-generating ovarian cancer cells attract myeloid cells which differentiate into adenosine-generating tumor associated macrophages–a self-amplifying, CD39-and CD73-dependent mechanism for tumor immune escape.* Journal for immunotherapy of cancer, 2016. **4**: p. 1-16.
120. Esparza-Lopez, J., J.F. Martinez-Aguilar, and M.J. Ibarra-Sanchez, *Deriving Primary Cancer Cell Cultures for Personalized Therapy.* Rev Invest Clin, 2019. **71**(6): p. 369-380.
121. Ali, M.M., et al., *Cell-surface sensors: lighting the cellular environment.* Wiley Interdiscip Rev Nanomed Nanobiotechnol, 2012. **4**(5): p. 547-61.
122. Adan, A., et al., *Flow cytometry: basic principles and applications.* Crit Rev Biotechnol, 2017. **37**(2): p. 163-176.
123. Mahmood, T. and P.C. Yang, *Western blot: technique, theory, and trouble shooting.* N Am J Med Sci, 2012. **4**(9): p. 429-34.
124. Bradford, M.M., *A rapid and sensitive method for the quantitation of microgram quantities of protein utilizing the principle of protein-dye binding.* Analytical Biochemistry, 1976. **72**(1): p. 248-254.
125. Jiao, J., et al., *Comparison of two commonly used methods for stimulating T cells.* Biotechnology Letters, 2019. **41**(12): p. 1361-1371.

126. Parish, C.R., et al., *Use of the intracellular fluorescent dye CFSE to monitor lymphocyte migration and proliferation.* Curr Protoc Immunol, 2009. **Chapter 4**: p. Unit4 9.
127. McCoy, J.P., Jr., *Basic principles of flow cytometry.* Hematol Oncol Clin North Am, 2002. **16**(2): p. 229-43.
128. Faraoni, E.Y., et al., *Radiofrequency ablation in combination with CD73 inhibitor AB680 reduces tumor growth and enhances anti-tumor immunity in a syngeneic model of pancreatic ductal adenocarcinoma.* Front Oncol, 2022. **12**: p. 995027.
129. Cremasco, V., et al., *FAP Delineates Heterogeneous and Functionally Divergent Stromal Cells in Immune-Excluded Breast Tumors.* Cancer Immunol Res, 2018. **6**(12): p. 1472-1485.
130. Chen, X. and E. Song, *Turning foes to friends: targeting cancer-associated fibroblasts.* Nat Rev Drug Discov, 2019. **18**(2): p. 99-115.
131. Erez, N., et al., *Cancer-Associated Fibroblasts Are Activated in Incipient Neoplasia to Orchestrate Tumor-Promoting Inflammation in an NF-kappaB-Dependent Manner.* Cancer Cell, 2010. **17**(2): p. 135-47.
132. Liu, T., et al., *Cancer-Associated Fibroblasts Build and Secure the Tumor Microenvironment.* Front Cell Dev Biol, 2019. **7**: p. 60.
133. Su, S., et al., *CD10(+)GPR77(+) Cancer-Associated Fibroblasts Promote Cancer Formation and Chemoresistance by Sustaining Cancer Stemness.* Cell, 2018. **172**(4): p. 841-856 e16.
134. Helms, E., M.K. Onate, and M.H. Sherman, *Fibroblast Heterogeneity in the Pancreatic Tumor Microenvironment.* Cancer Discov, 2020. **10**(5): p. 648-656.
135. Özdemir, B.C., et al., *Depletion of carcinoma-associated fibroblasts and fibrosis induces immunosuppression and accelerates pancreas cancer with reduced survival.* Cancer Cell, 2014. **25**(6): p. 719-34.
136. McAndrews, K.M., et al., *αSMA(+) fibroblasts suppress Lgr5(+) cancer stem cells and restrain colorectal cancer progression.* Oncogene, 2021. **40**(26): p. 4440-4452.
137. Chuaysri, C., et al., *Alpha-smooth muscle actin-positive fibroblasts promote biliary cell proliferation and correlate with poor survival in cholangiocarcinoma.* Oncol Rep, 2009. **21**(4): p. 957-69.
138. Schliekelman, M.J., et al., *Thy-1(+) Cancer-associated Fibroblasts Adversely Impact Lung Cancer Prognosis.* Sci Rep, 2017. **7**(1): p. 6478.
139. Zhao, X., et al., *Diminished CD68(+) Cancer-Associated Fibroblast Subset Induces Regulatory T-Cell (Treg) Infiltration and Predicts Poor Prognosis of Oral Squamous Cell Carcinoma Patients.* Am J Pathol, 2020. **190**(4): p. 886-899.
140. Servais, C. and N. Erez, *From sentinel cells to inflammatory culprits: cancer-associated fibroblasts in tumour-related inflammation.* J Pathol, 2013. **229**(2): p. 198-207.
141. Barrett, R. and E. Puré, *Cancer-associated fibroblasts: key determinants of tumor immunity and immunotherapy.* Curr Opin Immunol, 2020. **64**: p. 80-87.
142. Allard, B., et al., *The ectonucleotidases CD39 and CD73: Novel checkpoint inhibitor targets.* Immunol Rev, 2017. **276**(1): p. 121-144.
143. Allard, B., et al., *Publisher Correction: The adenosine pathway in immuno-oncology.* Nat Rev Clin Oncol, 2020. **17**(10): p. 650.
144. LeBleu, V.S. and R. Kalluri, *A peek into cancer-associated fibroblasts: origins, functions and translational impact.* Dis Model Mech, 2018. **11**(4).
145. Grinde, M.T., et al., *Ionizing radiation abrogates the pro-tumorigenic capacity of cancer-associated fibroblasts co-implanted in xenografts.* Scientific Reports, 2017. **7**(1): p. 46714.

146. Papadopoulou, A. and D. Kletsas, *Human lung fibroblasts prematurely senescent after exposure to ionizing radiation enhance the growth of malignant lung epithelial cells in vitro and in vivo.* Int J Oncol, 2011. **39**(4): p. 989-99.
147. Hellevik, T., et al., *Cancer-associated fibroblasts from human NSCLC survive ablative doses of radiation but their invasive capacity is reduced.* Radiat Oncol, 2012. **7**: p. 59.
148. Lupia, M., et al., *CD73 Regulates Stemness and Epithelial-Mesenchymal Transition in Ovarian Cancer-Initiating Cells.* Stem cell reports, 2018. **10**(4): p. 1412-1425.
149. Reinhardt, J., et al., *MAPK Signaling and Inflammation Link Melanoma Phenotype Switching to Induction of CD73 during Immunotherapy.* Cancer Res, 2017. **77**(17): p. 4697-4709.
150. Samanta, D., et al., *Chemotherapy induces enrichment of CD47(+)/CD73(+)/PDL1(+) immune evasive triple-negative breast cancer cells.* Proc Natl Acad Sci U S A, 2018. **115**(6): p. E1239-e1248.
151. Allard, D., et al., *Targeting the CD73-adenosine axis in immuno-oncology.* Immunol Lett, 2019. **205**: p. 31-39.
152. Biswas, S.K., *Metabolic Reprogramming of Immune Cells in Cancer Progression.* Immunity, 2015. **43**(3): p. 435-49.
153. Mittal, D.K., et al., *Adenosine 2B Receptor Expression on Cancer Cells Promotes Metastasis.* Cancer research, 2016. **76 15**: p. 4372-82.
154. Loi, S., et al., *CD73 promotes anthracycline resistance and poor prognosis in triple negative breast cancer.* Proc Natl Acad Sci U S A, 2013. **110**(27): p. 11091-6.
155. Turcotte, M., et al., *CD73 is associated with poor prognosis in high-grade serous ovarian cancer.* Cancer Res, 2015. **75**(21): p. 4494-503.
156. Costa, A., et al., *Fibroblast Heterogeneity and Immunosuppressive Environment in Human Breast Cancer.* Cancer Cell, 2018. **33**(3): p. 463-479.e10.
157. Yu, M., et al., *CD73 on cancer-associated fibroblasts enhanced by the A2B-mediated feedforward circuit enforces an immune checkpoint.* Nature Communications, 2020. **11**(1): p. 515.
158. Mediavilla-Varela, M., et al., *Antagonism of adenosine A2A receptor expressed by lung adenocarcinoma tumor cells and cancer associated fibroblasts inhibits their growth.* Cancer Biol Ther, 2013. **14**(9): p. 860-8.
159. Giatromanolaki, A., et al., *Ectonucleotidase CD73 and CD39 expression in non-small cell lung cancer relates to hypoxia and immunosuppressive pathways.* Life Sci, 2020. **259**: p. 118389.
160. Boison, D. and G.G. Yegutkin, *Adenosine Metabolism: Emerging Concepts for Cancer Therapy.* Cancer Cell, 2019. **36**(6): p. 582-596.
161. Zimmermann, H., *5'-Nucleotidase: molecular structure and functional aspects.* Biochemical Journal, 1992. **285**(Pt 2): p. 345.
162. Deterre, P., et al., *Coordinated regulation in human T cells of nucleotide-hydrolyzing ecto-enzymatic activities, including CD38 and PC-1. Possible role in the recycling of nicotinamide adenine dinucleotide metabolites.* Journal of immunology (Baltimore, Md.: 1950), 1996. **157**(4): p. 1381-1388.
163. Cekic, C. and J. Linden, *Purinergic regulation of the immune system.* Nature Reviews Immunology, 2016. **16**(3): p. 177-192.
164. Kepp, O., et al., *Immunogenic cell death modalities and their impact on cancer treatment.* Apoptosis, 2009. **14**(4): p. 364-75.
165. Frey, B., et al., *Modulation of inflammation by low and high doses of ionizing radiation: Implications for benign and malign diseases.* Cancer Lett, 2015. **368**(2): p. 230-7.

166. Tofilon, P.J. and K. Camphausen, *Increasing the therapeutic ratio of radiotherapy*. 2017, Springer.
167. Zhang, H., et al., *CAF-secreted CXCL1 conferred radioresistance by regulating DNA damage response in a ROS-dependent manner in esophageal squamous cell carcinoma.* Cell Death Dis, 2017. **8**(5): p. e2790.
168. Li, D., et al., *Radiation promotes epithelial-to-mesenchymal transition and invasion of pancreatic cancer cell by activating carcinoma-associated fibroblasts.* Am J Cancer Res, 2016. **6**(10): p. 2192-2206.
169. Papadopoulou, A. and D. Kletsas, *Human lung fibroblasts prematurely senescent after exposure to ionizing radiation enhance the growth of malignant lung epithelial cells in vitro and in vivo.* International journal of oncology, 2011. **39**(4): p. 989-999.
170. de Leve, S., F. Wirsdörfer, and V. Jendrossek, *Targeting the Immunomodulatory CD73/Adenosine System to Improve the Therapeutic Gain of Radiotherapy.* Front Immunol, 2019. **10**: p. 698.
171. de Leve, S., et al., *Loss of CD73 prevents accumulation of alternatively activated macrophages and the formation of prefibrotic macrophage clusters in irradiated lungs.* The FASEB Journal, 2017. **31**(7): p. 2869.
172. Allard, D., et al., *Targeting the CD73-adenosine axis in immuno-oncology.* Immunology letters, 2019. **205**: p. 31-39.
173. Wennerberg, E., et al., *CD73 Blockade Promotes Dendritic Cell Infiltration of Irradiated Tumors and Tumor Rejection.* Cancer Immunol Res, 2020. **8**(4): p. 465-478.
174. Gaudreau, P.-O., et al., *CD73-adenosine reduces immune responses and survival in ovarian cancer patients.* Oncoimmunology, 2016. **5**(5): p. e1127496.
175. Koivisto, M.K., et al., *Cell-type-specific CD73 expression is an independent prognostic factor in bladder cancer.* Carcinogenesis, 2019. **40**(1): p. 84-92.
176. Li, J., et al., *CD39/CD73 upregulation on myeloid-derived suppressor cells via TGF-β-mTOR-HIF-1 signaling in patients with non-small cell lung cancer.* Oncoimmunology, 2017. **6**(6): p. e1320011.
177. Ziani, L., et al., *Hypoxia increases melanoma-associated fibroblasts immunosuppressive potential and inhibitory effect on T cell-mediated cytotoxicity.* Oncoimmunology, 2021. **10**(1): p. 1950953.
178. Tsukui, H., et al., *CD73 blockade enhances the local and abscopal effects of radiotherapy in a murine rectal cancer model.* BMC cancer, 2020. **20**: p. 411.
179. Chen, L., et al., *CD38-mediated immunosuppression as a mechanism of tumor cell escape from PD-1/PD-L1 blockade.* Cancer discovery, 2018. **8**(9): p. 1156-1175.
180. Lewis, J.E., et al., *Targeting NAD(+) Metabolism to Enhance Radiation Therapy Responses.* Semin Radiat Oncol, 2019. **29**(1): p. 6-15.
181. Müller, G.A., *The release of glycosylphosphatidylinositol-anchored proteins from the cell surface.* Arch Biochem Biophys, 2018. **656**: p. 1-18.
182. Vieira, C., et al., *Feed-forward inhibition of CD73 and upregulation of adenosine deaminase contribute to the loss of adenosine neuromodulation in postinflammatory ileitis.* Mediators Inflamm, 2014. **2014**: p. 254640.
183. Camici, M., M. Garcia-Gil, and M.G. Tozzi, *The Inside Story of Adenosine.* Int J Mol Sci, 2018. **19**(3).
184. Cao, X., et al., *CD73 is a hypoxia-responsive gene and promotes the Warburg effect of human gastric cancer cells dependent on its enzyme activity.* J Cancer, 2021. **12**(21): p. 6372-6382.
185. DePeaux, K. and G.M. Delgoffe, *Metabolic barriers to cancer immunotherapy.* Nat Rev Immunol, 2021. **21**(12): p. 785-797.

186. Bao, C.-H., et al., *Irradiated fibroblasts promote epithelial–mesenchymal transition and HDGF expression of esophageal squamous cell carcinoma.* Biochemical and Biophysical Research Communications, 2015. **458**(2): p. 441-447.
187. Morello, S., et al., *Soluble CD73 as biomarker in patients with metastatic melanoma patients treated with nivolumab.* Journal of translational medicine, 2017. **15**: p. 1-9.
188. Pinchuk, I.V., et al., *PD-1 ligand expression by human colonic myofibroblasts/fibroblasts regulates CD4+ T-cell activity.* Gastroenterology, 2008. **135**(4): p. 1228-1237, 1237.e1-2.
189. *Blocking CD73 Can Shrink Pancreatic Tumors.* Cancer Discov, 2021. **11**(5): p. Of4.
190. Golden, E.B., et al., *Radiation fosters dose-dependent and chemotherapy-induced immunogenic cell death.* Oncoimmunology, 2014. **3**: p. e28518.
191. Jones, B., et al., *The role of biologically effective dose (BED) in clinical oncology.* Clin Oncol (R Coll Radiol), 2001. **13**(2): p. 71-81.
192. Apetoh, L., et al., *Toll-like receptor 4-dependent contribution of the immune system to anticancer chemotherapy and radiotherapy.* Nat Med, 2007. **13**(9): p. 1050-9.
193. Gupta, A., et al., *Radiotherapy promotes tumor-specific effector CD8+ T cells via dendritic cell activation.* J Immunol, 2012. **189**(2): p. 558-66.
194. Tommelein, J., et al., *Radiotherapy-Activated Cancer-Associated Fibroblasts Promote Tumor Progression through Paracrine IGF1R Activation.* Cancer Res, 2018. **78**(3): p. 659-670.
195. Mishra, P., et al., *Application of student's t-test, analysis of variance, and covariance.* Ann Card Anaesth, 2019. **22**(4): p. 407-411.

Appendix

A. Additional materials

A.1 Reagents For Cell Culture

	Catalog number	Supplier	Origin of the product
Cell detachment			
Enzyme-free cell dissociation solution (PBS based)	S-014-B	EMDMillipore	Great Britain
Trypsin-EDTA	T4049	Sigma Aldrich	USA
Cell freezing			
Dimethyl Sulfoxide (DMSO)	20385.01	Serva	Germany
Cell washing			
Phosphate Buffer Saline (PBS)	D8537	Sigma Aldrich	USA
Lysis reagent			
Halt ™ Protease and Phosphatase	78442	Thermo Scientific	Denmark
PBMC Isolation			
Lymphoprep™	1114544	Axis-Shield	Norway
Mitogenic Reagent			
Phytohaemagglutinin-L (PHA-L)	1249738	Roche	Germany

A.2 Dyes and Stains

	Catalog number	Supplier	Origin of the product
Cell TraceTM CarboxyFluorescein Succimidyl Ester (CFSE)	C34554 Molecular Probes USA	Molecular Probes	USA
Vio blue 405/452 Fixable dye	130-109-816	Miltenyi Biotec	Germany
Propidium Iodide	130-093-233	Miltenyi Biotec	Germany

A.3 FACs Flow Products

	Catalog number	Supplier	Origin of the product
Reagents			
autoMACS Rinsing Solution	130-091-222	Miltenyi Biotec	Germany
MACS BSA slock solution	130-091-376	Miltenyi Biotec	Germany
FACs flow tube			
Falcon™ Round-Bottom Polystyrene Tubes (5ml)	352054	Corning	USA

A.4 Cell lysate reagents

	Catalog Number	Supplier	Origin
Radio-Immunoprecipitation Assay (RIPA) Buffer	156034	Abcam	UK
Halt™ Protease and Phosphatase Inhibitor Single-Use Cocktail (100X)	78442	ThermoScintific	Denmark
Red blood cell lysis buffer	11814389001	Roshe	Germany

A.5 Bradford assay reagents

	Catalog number	Supplier	Origin
Bovine Serum Albumin(BSA)	422371X	VWR	UK
Bradford reagent	23246	ThermoScientific	Denmark

A.6 Gel Electrophoresis and Western Blotting Reagents

	Catalog number	Supplier	Origin
Gel			
NuPAGE gel	NP0335BOX	Invitrogen	USA
Buffers and other reagents			
4x NuPAGE®LDS Sample Buffer	NP0007	Invitrogen	USA
10x NuPAGE®LDS Sample Reducing Buffer	NP0009	Invitrogen	USA
20x NUPAGE® Transfer Buffer	NP0006	Invitrogen	USA
MagicMark™ Xp Western Protein Standard	LC5602	Invitrogen	USA
PVDF transfer membrane, 0.45 µm	88518	Invitrogen	USA
Ponceau S Staining Solution	A40000279	ThermoScientific	Denmark
Blocking Buffer	37535	ThermoScientific	USA
96% Methanol	20864.320	VWR	UK
Super Signal West Pico Chemiluminescent Substrate	SC-2048	ImmunoCruz™	USA

A.7 Software

	Supplier	Origin
Flow cytometry Software		
CellQuestTMPro Software	BD Bioscience	USA
Flow Jo Office V10	Tree star	USA
Statistics Software		
Excel® 365	Microsoft	USA
GraphPad Prism 9.4.1	GraphPad	USA
Image analysis software		
ImageJ V 1.53t	Wayne Rasband	USA
Image creating software		
BioRender	BioRender	Canada

A.8 Instruments

	Supplier	Origin
Flow Cytometry		
BD FACSAria III	BD Bioscience	USA
BD LSRFortessa™ Cell Analyzer	BD Bioscience	USA
Bioluminescent image analyser		
Image Quant LAS 4000	GE HealthCare	Germany
Centrifuges		
Heraeus Sepatech Biofuge 13	Heraeus Sepatech GmbH	Germany
Multifuge X3R	ThermoScientific	Germany
Centrifugal Vacuum Concentrator (Rotavapor)	Eppendorf /lifescience	Germany
Incubators		
HERA cell 150 (37ºC Incubator)	Termaks AS	Norway
HERAcell 240i (CO2 cell culture incubator)	ThermoScientific	Germany
HERAcell 150i (CO2 cell culture incubator)	ThermoScientific	Germany
Microplate Readers		
Luminometer	Labsystems Luminoskan	USA
Bio-Plex® 200 systems	BIO-RAD	USA
EMax®	Molecular Devices	USA
Microscope		
Inverted Microscope ECLIPSE TS100-F	Nikon	Japan
Protein measurements		
NanoDrop® Spectrophotometer	Saveen Werner life science	USA

B. Protocols

B.1 Protocol for Human CD73 ELISA kit

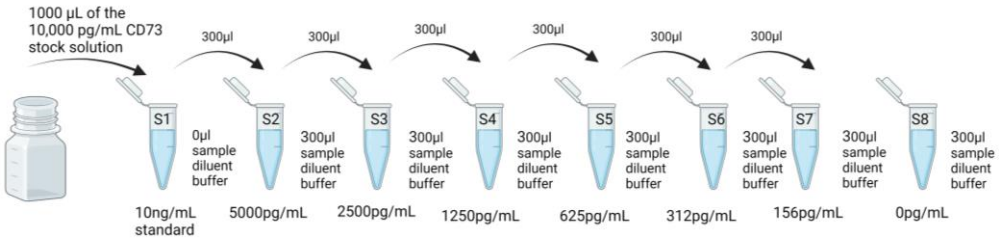

- Prepared standards according to the manufacturer's instructions.
- Prepared blank with 10% DMEM and sample dilution buffer at a dilution of 1:1.

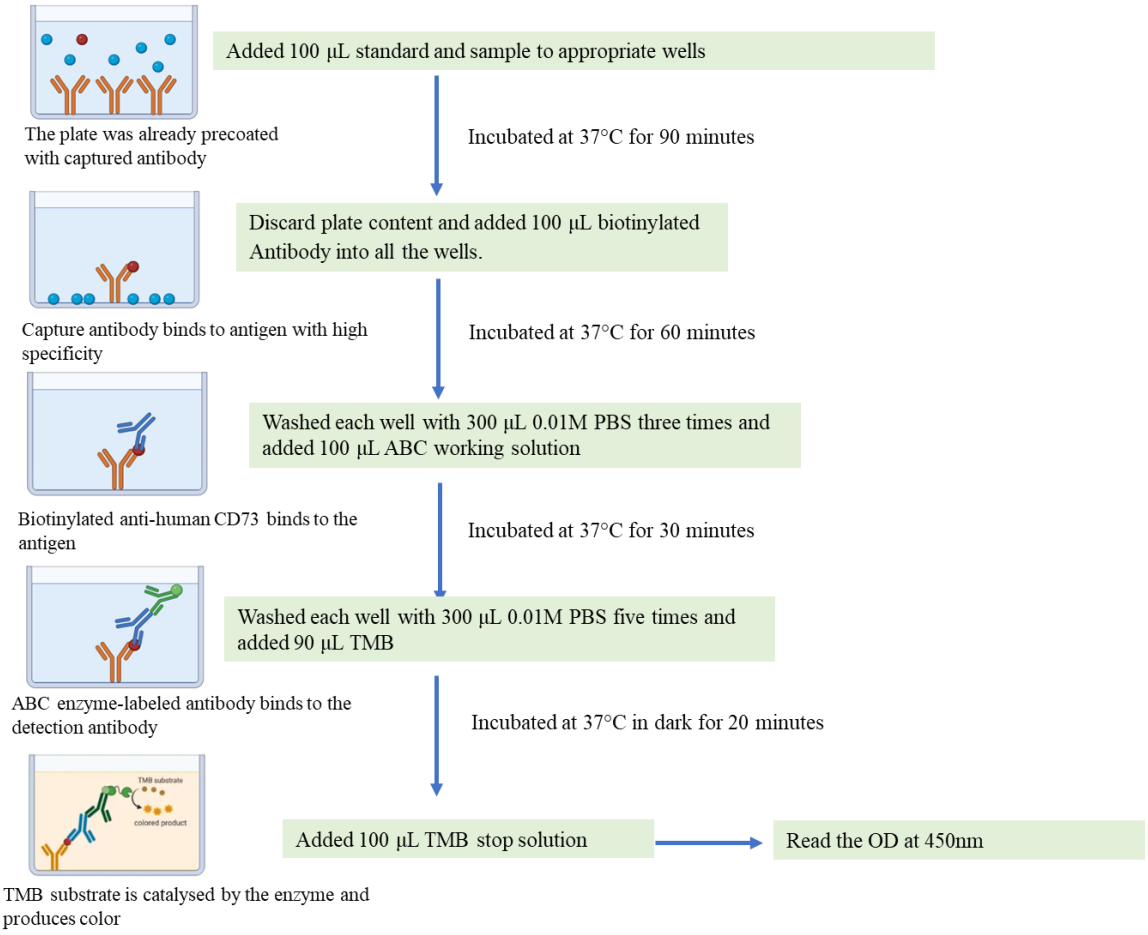

Protocol adapted from Human CD73 ELISA Kit(abcam),

The Figure was made with Biorander.com

B.2 Protocol for adenosine assay

a. Adenosine assay principle

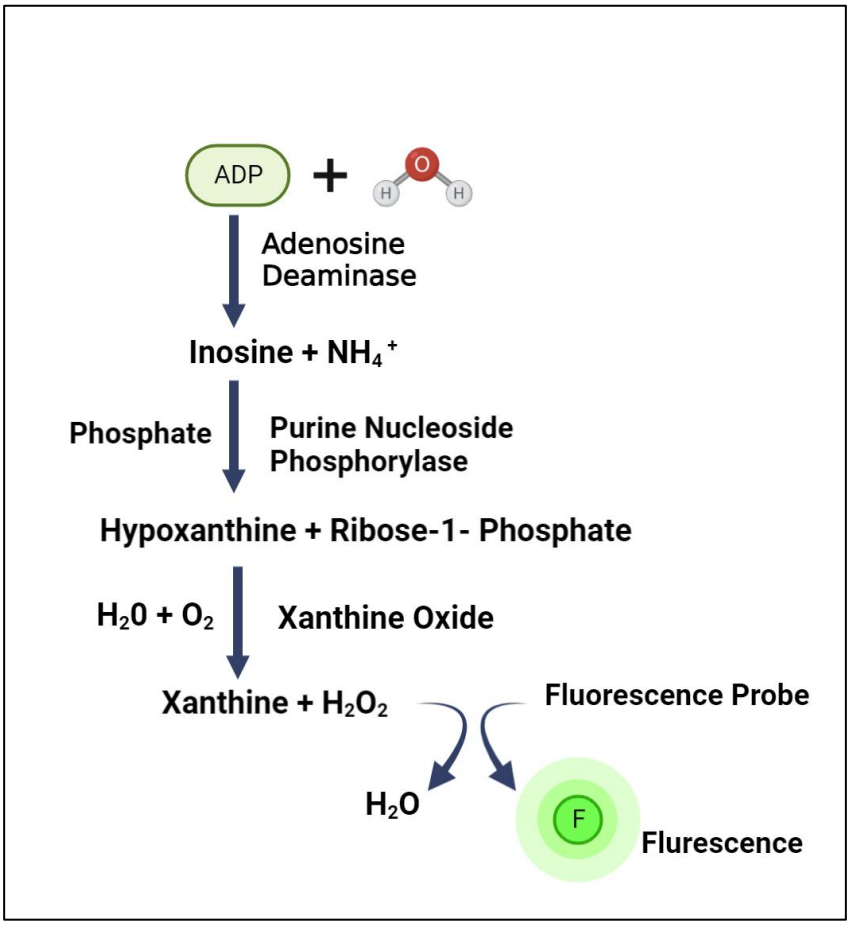

Protocol adapted from Adenosine Assay Kit(Cell Biolabs)

b. Preparation of Reagents

• 1X Assay Buffer: Prepared 1X Assay Buffer by diluting the stock 10X Assay Buffer with deionized water in a 1:10 ratio.

• Reaction Mix: Prepared a Reaction Mix by diluting several enzymes and a fluorometric probe in 1X Assay Buffer. Diluted Fluorometric Probe 1:100, HRP 1:500, Adenosine Deaminase 1:500, Purine Nucleoside Phosphorylase 1:10, and Xanthine Oxidase 1:50 in 1X Assay Buffer.

• Control Mix: Prepared a Control Mix by preparing a Reaction Mix without Adenosine Deaminase. Diluted Fluorometric Probe 1:100, HRP 1:500, Purine Nucleoside Phosphorylase 1:10, and Xanthine Oxidase 1:50 in 1X Assay Buffer.

c. Preparation of standard

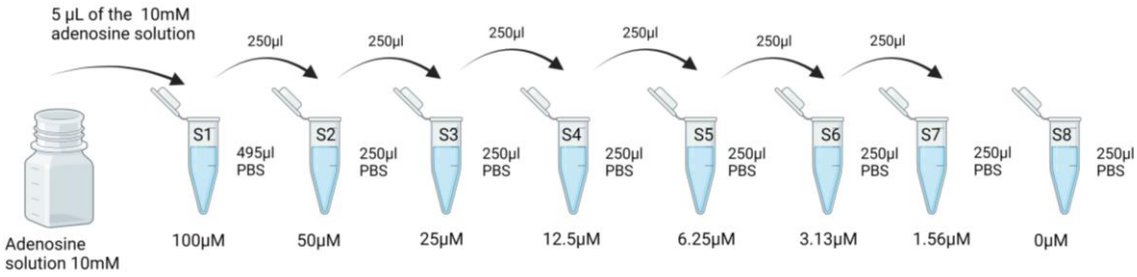

d. Assay protocol

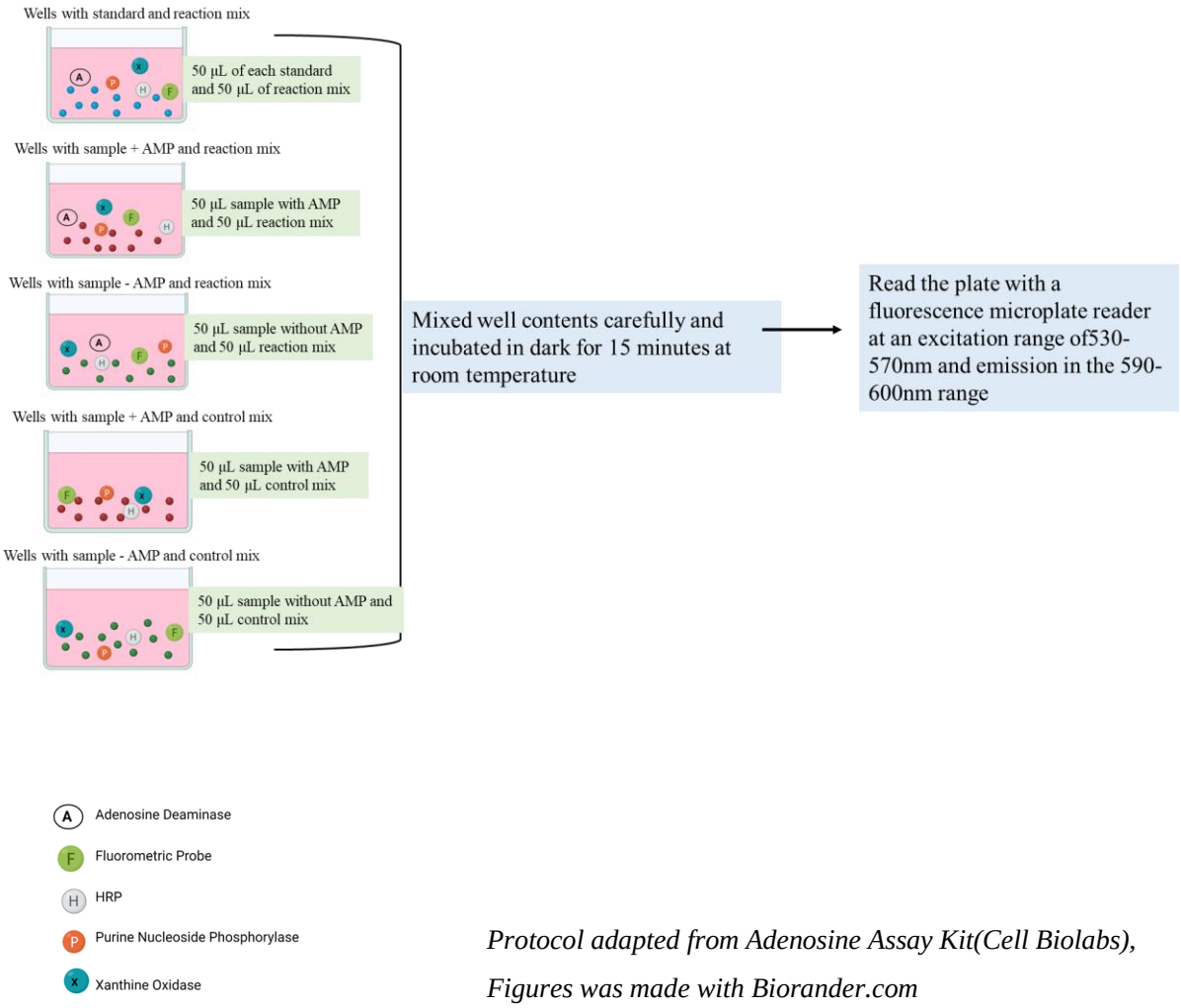

Protocol adapted from Adenosine Assay Kit(Cell Biolabs), Figures was made with Biorander.com

C. Workflow for different methods

C.1 Workflow for flow cytometry

Methods

1. **Flow Cytometry:** Surface expression of (ADO conversion enzymes) – CD73 - CD39 - CD38 - on
- Control CAFs
- Irradiated CAFs (1x6Gy and 1x18Gy)
- Tumor cells (A549)

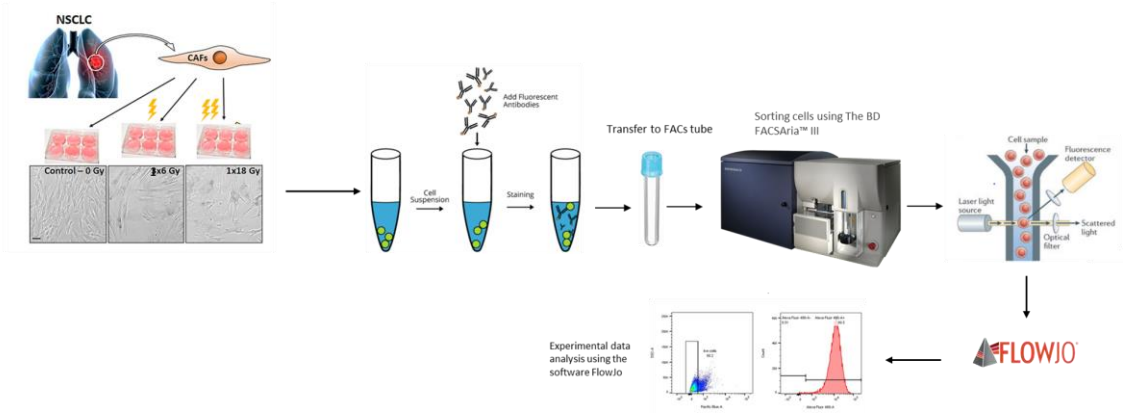

C.2 Workflow for western blot

Method

2. **Western blot:** Total protein content of CD39, CD73, CD38
- Control CAFs.
- Irradiated CAFs (1x6Gy and 1x18Gy)
- Tumor cells (A549)

Western blot general workflow

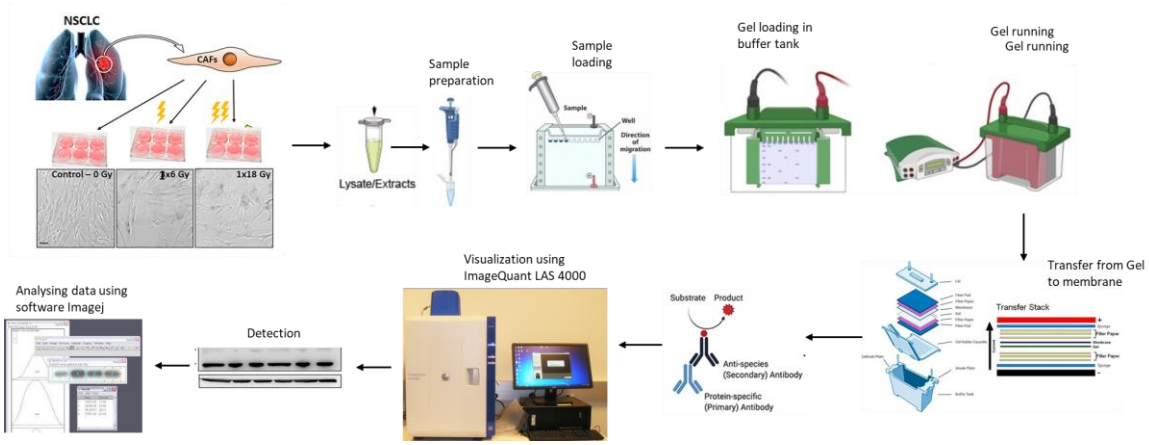

C.3 Workflow for lymphocyte proliferation assay

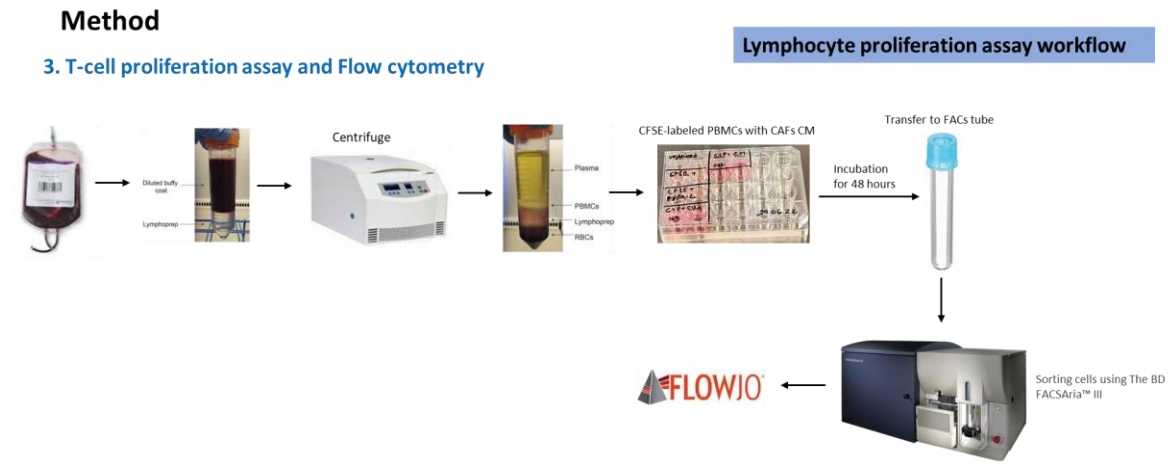

All the workflows were made with Biorander.com and Microsoft powerpoint

D. Additional results

D.1 Expression of CD38 was not detectable in both non-radiated and irradiated CAFs cell lysate

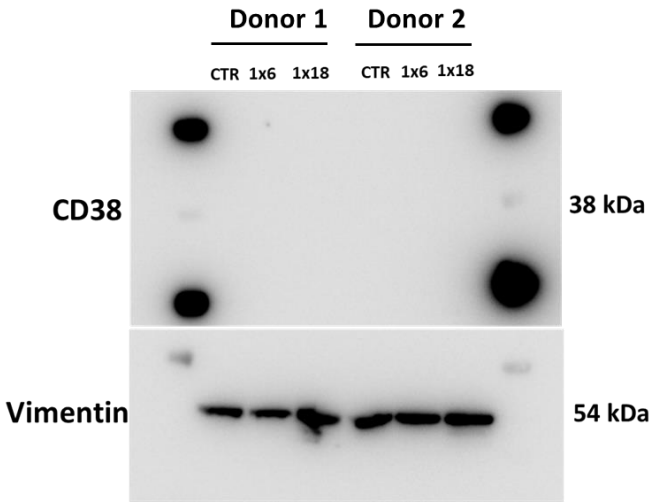

Additional figure: Effect of radiation on CD38 expression by non-radiated and irradiated CAFs (n=2) whole cell*. Cells were irradiated with a single dose of 6xGy and 18xGy. Overall expression of CD38 was undetectable by Western blotting.*